DRAMATIC MGCMを用いた現在の火星環境における水循環のシミュレーション

黒田 剛史 [1]
[1] NICT

Simulation of the water cycle on the present Martian environment using DRAMATIC MGCM

Takeshi Kuroda[1]
[1] NICT

The spacecrafts on the Mars orbit, such as Mars Global Surveyor, Mars Odyssey, Mars Express and Mars Reconnaisance Orbiter, have continuously observed the global distributions of water vapor and water ice clouds for these 17 years. Simulating the water cycle on Mars consistently with those observations using Martian General Circulation Models (MGCMs) is a challenging topic, as the required physical processes are not well known.

First simulations of the Martian water cycle which incorporated the observations were made by Richardson and Wilson [2002, JGR] and Richardson et al. [2002, JGR], assuming the prescribed ice cloud radius of 2 um to determine the sedimentation velocity. Montmessin et al. [2004, JGR] first introduced the cloud microphysics which was substantially important for the reproduction of the realistic seasonal and latitudinal variances of the water ice opacity. In those studies the radiative effects of water ice clouds were missing, but later Wilson et al. [2008, GRL] first showed the importance of them on the temperature fields. The development of a model which consistently reproduces the water cycle with radiatively-active water ice clouds has been difficult [e.g. Haberle et al., 2011, Paris workshop], although Navarro et al. [2014, JGR] indicated that the scavenging of dust particles due to the condensation ice also plays a significant role.

In this context, we are also starting to simulate the water cycle of the present Martian environment using the DRAMATIC (Dynamics, RAdiation, MAterial Transport and their mutual InteraCtions) MGCM whose dynamical core is based on the CCSR/NIES/FRCGC MIROC model, for the further investigations of the water cycle system and related material transport on Mars. The model has a spectral solver for the three-dimensional primitive equations, with the horizontal resolution of T21 (about 5.6^ox5.6^o, ˜333 km at equator) and vertical 59 sigma-levels up to ˜100 km. Realistic topography, albedo, thermal inertia and roughness data for the Mars surface are introduced. Radiative effects of CO_2 gas (considering only LTE) and dust are taken into account, and radiative effects of water ice clouds can also be included. The standard seasonal and latitudinal changes of dust opacity are defined externally, with the vertical distribution of so-called 'Conrath profile' [Conrath, 1975]. In the formation of water ice clouds, the cloud microphysics process following Montmessin et al. [2004] is implemented, setting a part of airborne dust as nuclei. In the cloud formation scheme, the water ice cloud radius inside each grid and layer is set to be constant. The sedimentation of water ice clouds, accumulation on the surface and sublimation of water ice from the surface are implemented.

Our results show the consistent seasonal and latitudinal changes of zonal-mean water vapor column density and ice opacity with observations in the run without the radiative effects of water ice clouds and adjusting the number of nuclei to be 5-10 um of the ice cloud radius in maximum at the equatorial cloud belt in northern summer. With the radiative effects of water ice clouds, the altitude of equatorial cloud belt becomes ˜20 km higher and the ice opacity there becomes much smaller. Also the radiatively-active water ice clouds largely change the temperature fields, increasing up to ˜50 K at equatorial cloud belt and ˜30 K in winter polar regions. Then, our results indicate that taking interactive dust transport including scavenging into consideration would be important for the consistent simulations with the radiatively-active water ice clouds.

The isotopic fractionations for HDO and H_2O are already implemented into our model [Kuroda et al., 2012, NASA workshop], and further developments for the water cycle would contribute to support the future missions such as ExoMars Trace Gas Orbiter which targets to observe the isotopic ratios of water vapor.

火星探査機MAVENの観測データを使用した誘導磁気圏界面とイオン成分境界についての統計解析研究

松永 和成 [1]; 関 華奈子 [2]; Brain David A.[3]; 原 拓也 [4]; McFadden James P.[4]; Halekas Jasper S.[5]; Mitchell David L.[4]; Mazelle Christian[6]; Espley Jared R.[7]; Jakosky Bruce M.[8]
[1] 名大 ISEE; [2] 東大理・地球惑星科学専攻; [3] LASP, Univ. of Colorado at Boulder, USA; [4] SSL, UC Berkeley; [5] Dept. Phys. & Astron., Univ. Iowa; [6] CNRS,IRAP; [7] NASA GSFC; [8] LASP, CU Boulder

Statistical study of relation between the magnetic pileup boundary and ion composition boundary around Mars observed by MAVEN

Kazunari Matsunaga[1]; Kanako Seki[2]; David A. Brain[3]; Takuya Hara[4]; James P. McFadden[4]; Jasper S. Halekas[5]; David L. Mitchell[4]; Christian Mazelle[6]; Jared R. Espley[7]; Bruce M. Jakosky[8]
[1] ISEE, Nagoya Univ.; [2] Dept. Earth & Planetary Sci., Science, Univ. Tokyo; [3] LASP, Univ. of Colorado at Boulder, USA; [4] SSL, UC Berkeley; [5] Dept. Phys. & Astron., Univ. Iowa; [6] CNRS,IRAP; [7] NASA GSFC; [8] LASP, CU Boulder

Direct interaction between the solar wind and the Martian upper atmosphere forms a characteristic transition region, so-called the magnetic pileup region, between the shocked solar wind (magnetosheath) and the Martian ionosphere. In this transition region, the solar wind is decelerated due to increasing mass loading by heavy ions, which are produced from the ionization of extended Martian neutral atmosphere. Since the interplanetary magnetic field (IMF) frozen-in the solar wind plasma, the solar wind deceleration make IMF to pile up and drape around the planet. After Mars Global Surveyor observations, the outer boundary of the magnetic pile up region is called as the magnetic pileup boundary (MPB). Previous observations by Phobos 2 and Mars Express, on one hand, showed existence of a boundary that separates the solar wind protons dominant region from the planetary heavy ions dominant one, which is referred to the ion composition boundary (ICB). However, due to the lack of continuous simultaneous measurements of the magnetic field and ion composition before Mars Atmosphere and Volatile EvolutioN (MAVEN), relation between MPB and ICB are far from understood.

In this study, we investigate relative locations of MPB and ICB, as well as their dependence on solar wind parameters by using MAVEN ion, electron, and magnetic field data. We conducted a statistical analysis for two periods from November 2014 to March 2015 and from June 2015 to October 2015, when MAVEN orbital configuration allows direct measurements of the solar wind near its apoapsis. We developed an automated algorithm to identify MPB and ICB. We identified MPB with criteria combining the time derivative of electron flux, strength of the high-frequency (>0.1Hz) magnetic field fluctuation, and plasma beta. As for ICB identification, we used the density ratio between the planetary heavy ions and the solar wind protons. Results show there is a north-south asymmetry in locations of MPB and ICB in MSO coordinates. Observations indicated that the southern crustal magnetic fields seem to play an important a role of the north-south asymmetry. Observations also indicate that locations of MPB and ICB depend on the solar wind dynamic pressure and the IMF direction. Based on the results, we will discuss relation between MPB and ICB, and formation processes of these boundaries.

火星探査機MAVENの観測に基づいた火星上層大気への降下SEP電子の特性の研究

関 華奈子 [1]; 原 拓也 [2]; Brain David A.[3]; Lillis Robert J.[2]; 松永 和成 [4]; 益永 圭 [5]; 寺田 直樹 [6]; Larson Davin E.[2]; Mitchell David L.[2]; Espley Jared R.[7]; Connerney John E. P.[7]; Luhmann Janet G.[2]; Jakosky Bruce M.[8]
[1] 東大理・地球惑星科学専攻; [2] SSL, UC Berkeley; [3] LASP, Univ. of Colorado at Boulder, USA; [4] 名大 ISEE; [5] 東大・理
; [6] 東北大・理・地物; [7] NASA GSFC; [8] LASP, CU Boulder

Characteristics of penetrating SEP electrons into Martian upper atmosphere observed by MAVEN

Kanako Seki[1]; Takuya Hara[2]; David A. Brain[3]; Robert J. Lillis[2]; Kazunari Matsunaga[4]; Kei Masunaga[5]; Naoki Terada[6]; Davin E. Larson[2]; David L. Mitchell[2]; Jared R. Espley[7]; John E. P. Connerney[7]; Janet G. Luhmann[2]; Bruce M. Jakosky[8]
[1] Dept. Earth & Planetary Sci., Science, Univ. Tokyo; [2] SSL, UC Berkeley; [3] LASP, Univ. of Colorado at Boulder, USA; [4] ISEE, Nagoya Univ.; [5] Univ. Tokyo; [6] Dept. Geophys., Grad. Sch. Sci., Tohoku Univ.; [7] NASA GSFC; [8] LASP, CU Boulder

Recent discovery of new diffuse aurora at Mars caused by the SEP (solar energetic particle) electrons [Schneider et al., 2015] sheds a new light on the high-energy particle environment at Mars. In contrast to Earth, Mars posses no global intrinsic magnetic field and the solar wind interacts directly with Martian upper atmosphere. The diffuse aurora observation in the northern hemisphere at Mars, where the crustal field is absent, indicates penetration of the high-energy electrons of ~100 keV down to the altitudes around 70 km along the draped interplanetary magnetic field around the planet. However, to what extent the draped magnetic field configuration around Mars controls the SEP electron penetration to the atmosphere is far from understood.

In this study, we investigate pitch angle distributions of the high-energy (30-210 keV) electrons observed in the Martian ionosphere based on the MAVEN observations during strong SEP events. In order to achieve a good coverage in the 2-D (pitch angle-energy) phase space, data obtained during a SEP event is accumulated and binned. The obtained pitch angle distributions in the ionosphere are compared with the distributions of the source electrons in the solar wind. The results show that the field-aligned electrons are dominant in the ionosphere. While the low-energy (<~100 keV) electrons are more unidirectional, high-energy electrons tend to have bi-directional distributions. We will discuss possible cause of the energy-dependent pitch angle distributions and their relation to the magnetic field configuration around the planet.

火星磁気シースへ入射する酸素ピックアップイオンの反射率の導出とその太陽風依存性

益永 圭 [1]; 関 華奈子 [2]; Brain David A.[3]; Fang Xiaohua[4]; Dong Yaxue[4]; Jakosky Bruce M.[4]; McFadden James P.[5]; Halekas Jasper S.[6]; Connerney John E. P.[7]
[1] 東大・理
; [2] 東大理・地球惑星科学専攻; [3] LASP, Univ. of Colorado at Boulder, USA; [4] LASP, CU Boulder; [5] SSL, UC Berkeley; [6] Dept. Phys. & Astron., Univ. Iowa; [7] NASA GSFC

Statistical analysis of reflection of incident O+ pickup ions at Mars: Reflection ratios and solar wind dependences

Kei Masunaga[1]; Kanako Seki[2]; David A. Brain[3]; Xiaohua Fang[4]; Yaxue Dong[4]; Bruce M. Jakosky[4]; James P. McFadden[5]; Jasper S. Halekas[6]; John E. P. Connerney[7]
[1] Univ. Tokyo; [2] Dept. Earth & Planetary Sci., Science, Univ. Tokyo; [3] LASP, Univ. of Colorado at Boulder, USA; [4] LASP, CU Boulder; [5] SSL, UC Berkeley; [6] Dept. Phys. & Astron., Univ. Iowa; [7] NASA GSFC

Analyzing ~1.3 year dataset (November 2014 to February 2016) of O+ ion velocity distribution functions obtained from the Suprathermal and Thermal Ion Composition (STATIC) instrument on the Mars Atmosphere and Volatile Evolution (MAVEN) spacecraft, we statistically investigate reflections of incident O+ pickup ions (>10 keV) from the Martian dayside magnetosheath. To quantitatively evaluate importance of the O+ pickup ion reflection, we estimate a reflection ratio by calculating average inward and outward O+ ion fluxes above the Martian bow shock. Our result shows that ~14 % of incident O+ pickup ions is reflected. We also investigate dependences of the reflection ratio on the solar wind. We find that the reflection ratio strongly depends on the magnitude of the interplanetary magnetic field (IMF): ~6 % for the weak IMF case and ~18 % for the strong magnetic field case. We suggest that this dependence is caused by differences of O+ gyroradii. Since the magnetic field in the magnetosheath also becomes strong for the strong IMF case, O+ ion gyroradii become small and thus more incident O+ pickup ions can experience partial gyrations in the magnetosheath to go back to the solar wind compared to the weak IMF case. Since the incident O+ pickup ions are a major source of atmospheric sputtering escape from Mars, this result suggests that ion reflections might have a role to reduce the sputtering escape from ancient Mars if the young sun had a stronger IMF than that of the current sun.

Electron energetics in the Martian dayside ionosphere: Model comparisons with MAVEN data

Shotaro Sakai[1]; Laila Andersson[2]; Thomas E. Cravens[1]; David L. Mitchell[3]; Christian Mazelle[4]; Ali Rahmati[3]; Christopher M. Fowler[2]; Stephen W. Bougher[5]; Edward M. B. Thiemann[2]; Francis G. Eparvier[2]; Juan M. Fontenla[6]; Paul R. Mahaffy[7]; John E. P. Connerney[7]; Bruce M. Jakosky[2]

[1] U. Kansas; [2] LASP, CU Boulder; [3] SSL, UC Berkeley; [4] CNRS,IRAP; [5] U. Michigan; [6] NWRA; [7] NASA GSFC

The goal of the Mars Atmosphere and Volatile EvolutioN (MAVEN) mission is to characterize the loss of atmospheric gas to space and how this has affected the Martian climate through. Atomic oxygen is a key species in atmospheric loss at Mars and the current key path for photochemical loss of neutral oxygen is the dissociative recombination of ionospheric O_2^+, which is associated with the electron temperature in the ionosphere. We present a study of the energetics of the dayside ionosphere of Mars using models and data from several instruments onboard the MAVEN spacecraft. In particular, calculated photoelectron fluxes are compared with suprathermal electron fluxes measured by the Solar Wind Electron Analyzer (SWEA), and calculated electron temperatures are compared with temperatures measured by the Langmuir Probe and Waves (LPW) experiment. The major heat source for the thermal electrons is Coulomb heating from the suprathermal electron population, and cooling due to collisional rotational and vibrational CO_2 dominates the energy loss. The models used in this study were largely able to reproduce the observed high topside ionosphere electron temperatures (e.g., 3000 K at 300 km altitude) without using a topside heat flux when magnetic field topologies consistent with the measured magnetic field were adopted. Magnetic topology affects both suprathermal electron transport and thermal electron heat conduction. The electron temperature is shown to affect the O_2^+ dissociative recombination rate coefficient, which in turn affects photochemical escape of oxygen from Mars.

Change in radial distribution of Io plasma torus and Jupiter's aurora activity during Io's volcanic active period in 2015

Fuminori Tsuchiya[1]; Masato Kagitani[2]; Mizuki Yoneda[3]; Tomoki Kimura[4]; Kazuo Yoshioka[5]; Go Murakami[6]; Chihiro Tao[7]; Hiroaki Misawa[8]; Atsushi Yamazaki[9]; Ichiro Yoshikawa[10]; Yasumasa Kasaba[11]; Takeshi Sakanoi[12]
[1] Planet. Plasma Atmos. Res. Cent., Tohoku Univ.; [2] PPARC, Tohoku Univ; [3] none; [4] RIKEN; [5] The Univ. of Tokyo; [6] ISAS/JAXA; [7] NICT; [8] PPARC, Tohoku Univ.; [9] ISAS/JAXA; [10] EPS, Univ. of Tokyo; [11] Tohoku Univ.; [12] Grad. School of Science, Tohoku Univ.

Long term and continuous observations of Io plasma torus in the spring of 2015 with HISAKI have revealed responses of the plasma torus to volcanic activity change at the satellite Io. The HISAKI observation shows that brightness of singly ionized sulfur and oxygen due to electron impact excitation increased from DOY 20 to 40 in 2015. Doubly ionized sulfur began to increase several days after the singly ionized ion and reached a maximum around DOY 60. The intensities of these ions kept intense until DOY 70. The singly charged sulfur showed two-step decreased on DOY 70 and 90. The singly ionized oxygen and doubly ionized sulfur begins to decrease on DOY 90. The ion intensities returned to the usual level by DOY 120. These behaviors show response of the plasma torus to the change in neutral source from Io. To evaluate mass supply rate from inner to middle magnetospheres, radial gradient of emission intensity was derived from spatially resolved HISAKI data set. It is proportional to radial gradient of ion flux tube content and could be a qualitative proxy of the mass supply rate. The radial gradient at 8.5 Jovian radii from Jupiter suggested that the mass loading rate increased from DOY 40 to 80. During this period unusually strong transient enhancements of Jovian aurora were observed by HISAKI. Time interval between enhancements was a few days, which is consistent with quasi-periodic substom-like event identified by the Galileo spacecraft. Several hours after the aurora enhancement, short-live brightening was also identified in the Io plasma torus. After DOY 90 when the radial gradient almost returned to the value before the volcanic enhancement, the sporadic aurora events were still observed until DOY 110 but they did not accompany the plasma torus brightening. Transport of hot electron population to the inner magnetosphere with density depleted interchange flux tube is one of possible mechanisms to explain the HISAKI observation.

木星ナトリウム雲に見るイオの火山活動

米田 瑞生 [1]; 土屋 史紀 [2]; 鍵谷 将人 [3]; 坂野井 健 [4]; 古賀 亮一 [5]
[1] なし; [2] 東北大・理・惑星プラズマ大気; [3] 東北大・理・惑星プラズマ大気研究センター; [4] 東北大・理; [5] 東北大・理・地物

Jupiter’s extended sodium nebula as an index of Io’s volcanic activity

Mizuki Yoneda[1]; Fuminori Tsuchiya[2]; Masato Kagitani[3]; Takeshi Sakanoi[4]; Ryoichi Koga[5]
[1] none; [2] Planet. Plasma Atmos. Res. Cent., Tohoku Univ.; [3] PPARC, Tohoku Univ; [4] Grad. School of Science, Tohoku Univ.; [5] Geophysics, Tohoku Univ.

Io, which has the innermost orbit among the Gelilean moon, is the most volcanically active body in the Solar System. This volcanic atmosphere is ionized, becomes plaema and escapes into Jupiter’s inner magnetosphere due to the interaction with Jupiter’s co-rotating magnetic fields. This plasma forms a structure called Io plasma torus. This torus is mostly occupied by sulfur and oxygen ions, and most of these ions have emissions lines at UV wavelengths. Although this is a minor constituent, the torus includes NaCl+ ions that are originated in Io’s volcanic gas. Pick-up of these NaCl+ ions from Io’s ionosphere and their subsequent destruction in the plasma torus produces fast from of neutral sodium atoms, then Jupiter’s sodium nebula is formed. The sodium

nebula has an extent of 1,000 Jupiter’s radii. We have been making observations of this sodium nebula from the ground. The sodium nebula is showing variations in its sodium D-line brightness which are attributed variations in Io’s volcanism. On the other hand, ground-based observations Io’s volcanic activity can be made by measuring thermal near infrared emissions from volcanic hotspot. In this presentation, comparison among data of Jupiter’s sodium nebula, Io’s volcanic infrared emissions and plasma emissions in the torus obtained by the Hisaki-sapcecraft will be shown.

ひさき衛星を用いたイオ周辺の130.4nm酸素原子発光の時間変動解析

古賀 亮一 [1]; 坂野井 健 [2]; 鍵谷 将人 [3]; 土屋 史紀 [4]; 米田 瑞生 [5]; 吉川 一朗 [6]; 吉岡 和夫 [7]; 村上 豪 [8]; 山崎 敦 [9]; 木村 智樹 [10]
[1] 東北大・理・地物; [2] 東北大・理; [3] 東北大・理・惑星プラズマ大気研究センター; [4] 東北大・理・惑星プラズマ大気; [5] なし; [6] 東大・理・地惑; [7] 東大・理; [8] ISAS/JAXA; [9] JAXA・宇宙研; [10] 理研

Time variation of 130.4nm atomic oxygen emission near Io observed by Hisaki/EXCEED

Ryoichi Koga[1]; Takeshi Sakanoi[2]; Masato Kagitani[3]; Fuminori Tsuchiya[4]; Mizuki Yoneda[5]; Ichiro Yoshikawa[6]; Kazuo Yoshioka[7]; Go Murakami[8]; Atsushi Yamazaki[9]; Tomoki Kimura[10]
[1] Geophysics, Tohoku Univ.; [2] Grad. School of Science, Tohoku Univ.; [3] PPARC, Tohoku Univ; [4] Planet. Plasma Atmos. Res. Cent., Tohoku Univ.; [5] none; [6] EPS, Univ. of Tokyo; [7] The Univ. of Tokyo; [8] ISAS/JAXA; [9] ISAS/JAXA; [10] RIKEN

The brightening event of the Io's extended sodium nebula was reported by the ground imaging observation from December 2014 to May 2015 (Yondeda et al., 2015). This event shows Io's volcanism was active in the spring of 2015. Variation of main components of gaseous plume (sulfur dioxide which is subsequently dissociated to atomic oxygen and sulfur) has not been investigated yet. We present the result of time variation of 130.4nm atomic oxygen emission around Io observed by Hisaki/EXCEED during the volcanic event in the spring of 2015, and compare it with the extended sodium nebula.

We selected observed data when Io was in the dawn side (Io's phase angele of 45˜135 degrees) and in the dusk side (225˜315 degrees), and overlapped the data whose center correspond to Io to obtain the averaged image. It is found that the brightness of the atomic oxygen emission started to increase in the middle January and showed the maximum in the middle of February. Afterward, it decreased toward the end of May and finally returned the normal brightness level. Both the solar resonant scattering and electron impact excitation can contribute to 130.4nm atomic oxygen emission. We adopt two Maxwellian-distributed electron populations to evaluate which process is duminant to produce the emission. For the cases that thermal electron density and temperature are 2000/cc and 5eV, and hot electron temperature and fraction are 50eV and 2 percent, respectively. We confirmed that the contribution of electron impact excitation was several hundred times higher than that of solar scattering.

The time variation of atomic oxygen emission is well correlated with that of sodium emission in increasing phase, but decline time scale of atomic oxygen emission is about 30 days longer than that of sodium emission. there are two candidates which cloud explain the difference. First is time variation of electron density and temperature in the Io plasma torus. If electron density or hot electron fraction increases after the peak of time variation of 130.4nm emission, 130.4nm atomic oxygen emission decline speed goes slow compared to the sodium emission. Second is the difference of source regions between sodium chloride and sulfur emission. Gaseous sodium chloride is emitted only by hot spot, but sulfur dioxide may be emitted not only by the hot spot but wide lava lake because of its low sublimation point.

イオ起源の木星磁気圏全体に広がるナトリウム雲の発光の増大が2014年11月～2015年5月の間で観測された(Yoneda et al., 2015)。このイベントは2015年春にイオの火山活動が活発になったことを示している。火山ガスの主成分(二酸化硫黄やのちに解離して酸素原子や硫黄原子)の時間変動はいまだに明らかにされていない。そこで、私たちは今回ひさき衛星で観測されたイオ周辺の130.4nmの酸素原子発光の時間変動を示し、その結果と広域ナトリウム雲の発光変動を比較する。

私たちは観測されたデータの内、イオがdawn側にいるとき(位相角45˜135度)とdusk側にいるとき(225˜315度)のデータを選択し、イオを中心に画像を重ね合わせて前後20秒角の範囲の明るさの平均を解析した。その結果、酸素原子発光は1月中旬から強度を増大させ始め、2月の中旬にピークを迎え、その後、3月の終わりまで減少し元の明るさに戻った。130.4nm酸素原子発光の発光機構として共鳴散乱と電子衝突励起の両方がありえるので、どちらが支配的か明らかにする必要がある。私たちは電子密度にマクスウェル分布を仮定して共鳴散乱と電子衝突励起の発光の寄与を定量的に調べた。低温電子の密度と温度を2000/ccと5eV、高温電子の温度と割合を40eVと2％と仮定した。その結果、共鳴散乱より電子衝突励起の方が数百倍寄与していることが明らかになった。

増光フェーズでは酸素原子発光の時間変動はナトリウムの発光とよい相関があるが、その一方ピークから減光する時間スケールは酸素原子の方がナトリウムより30日程度長い。この減光時間スケールの違いを説明できる候補は二つある。ひとつはイオトーラス中の電子密度や温度の時間変化である。もし酸素原子発光変動のピーク後に電子密度や高温電子の割合が増大すれば、ナトリウムに比べて酸素の減光スピードが緩やかになる。二つ目は、塩化ナトリウムと二酸化硫黄の供給源の違いである。気体の塩化ナトリウムは高温の火口からしか排出されないが、二酸化硫黄は昇華点の低さから高温の火口からだけでなく溶岩が表面を溶かすことによっても排出されることが考えられる。

The plasma dynamics of the Io plasma torus observed by the Hisaki

Kazuo Yoshioka[1]; Fuminori Tsuchiya[2]; Tomoki Kimura[3]; Masato Kagitani[4]; Go Murakami[5]; Atsushi Yamazaki[6]; Masaki Kuwabara[7]; Reina Hikida[8]; Fumiharu Suzuki[9]; Ichiro Yoshikawa[10]; Masaki Fujimoto[11]
[1] The Univ. of Tokyo; [2] Planet. Plasma Atmos. Res. Cent., Tohoku Univ.; [3] RIKEN; [4] PPARC, Tohoku Univ; [5] ISAS/JAXA; [6] ISAS/JAXA; [7] The Univ. of Tokyo; [8] Frontier Sciences, Tokyo Univ.; [9] Earth and planetary science, Univ.Tokyo; [10] EPS, Univ. of Tokyo; [11] ISAS, JAXA

The Io plasma torus situated in the Jovian inner magnetosphere is filled with heavy ions and electrons, a large part of which is derived from Io’s volcanos. Being the key area connecting the radiation belt, where energetic electrons are created, with the mid-magnetosphere, where highly dynamic phenomena are taking place, revealing the plasma behavior of the torus has been among the key factors in elucidating Jovian magnetospheric dynamics. A global picture of the Io plasma torus can be obtained via spectral diagnosis of remotely-sensed ion emissions generated via electron impact excitation. Hisaki, an earth orbiting spacecraft equipped with an extreme ultraviolet spectroscope EXCEED, has observed the torus with a high spectral resolution and the data has been submitted to a spectral diagnosis analysis and a chemical balance modeling under the assumption of axial symmetry. Outputs from the investigation are radial profiles of various parameters including electron density and temperature as well as ion densities. This presentation shows the deduced timescales of inward and outward transportation of plasma. The ratio may represents the occurrence rate of depleted inward flux tubes seen in in-situ observation by Galileo. The possible future collaboration with Juno’s microscopic observation on this topic will also be discussed.

ひさき衛星によるオーロラとプラズマ供給率の連続監視で明らかにする木星サブストームライクイベントの動力学

木村 智樹 [1]; 吉岡 和夫 [2]; 土屋 史紀 [3]; 平木 康隆 [4]; 垰 千尋 [5]; 北 元 [6]; 村上 豪 [7]; 山崎 敦 [8]; 藤本 正樹 [9]
[1] RIKEN; [2] 東大・理; [3] 東北大・理・惑星プラズマ大気; [4] 電通大; [5] NICT; [6] 東北大・理・惑星プラズマ大気; [7] ISAS/JAXA; [8] JAXA・宇宙研; [9] 宇宙研

Dynamics of Jupiter’s substorm-like event explored by monitoring of aurora and plasma mass loading with the Hisaki satellite

Tomoki Kimura[1]; Kazuo Yoshioka[2]; Fuminori Tsuchiya[3]; Yasutaka Hiraki[4]; Chihiro Tao[5]; Hajime Kita[6]; Go Murakami[7]; Atsushi Yamazaki[8]; Masaki Fujimoto[9]
[1] RIKEN; [2] The Univ. of Tokyo; [3] Planet. Plasma Atmos. Res. Cent., Tohoku Univ.; [4] UEC; [5] NICT; [6] Tohoku Univ.; [7] ISAS/JAXA; [8] ISAS/JAXA; [9] ISAS, JAXA

Plasma production and transfer processes in the planetary and stellar magnetospheres are essential for understanding the space environments around these bodies. It is hypothesized that the mass of plasma loaded from Io’s volcano to Jupiter’s rotating magnetosphere is recurrently ejected as blobs from the distant tail region of the magnetosphere. The plasma ejections are likely triggered by the magnetic reconnections, which are followed by the particle energization, bursty planetward plasma flow, and resultant auroral emissions. They are referred to as the ’substorm-like events’. However, there has not been no evidence that the plasma mass loading actually causes the substorm-like events because of lack of the simultaneous observation for them. This study presents that the recurrent transient auroras, which are representative for the substorm-like events, are caused by the mass loading. Continuous monitoring of the aurora and Io plasma torus indicates onset of the recurrent auroras when accumulation of the loaded plasma mass reaches the canonical total mass of the magnetosphere. This onset condition implies that the plasma mass overflows from the fully filled magnetosphere accompanying the substorm-like events.

Jupiter’s auroral energy input and its modulations by Io’s volcanic activity observed by Hisaki/EXCEED

Chihiro Tao[1]; Tomoki Kimura[2]; Fuminori Tsuchiya[3]; Go Murakami[4]; Kazuo Yoshioka[5]; Hajime Kita[6]; Atsushi Yamazaki[7]; Yasumasa Kasaba[8]; Ichiro Yoshikawa[9]; Masaki Fujimoto[10]

[1] NICT; [2] RIKEN; [3] Planet. Plasma Atmos. Res. Cent., Tohoku Univ.; [4] ISAS/JAXA; [5] The Univ. of Tokyo; [6] Tohoku Univ.; [7] ISAS/JAXA; [8] Tohoku Univ.; [9] EPS, Univ. of Tokyo; [10] ISAS, JAXA

Aurora is an important indicator representing the momentum transfer from the fast-rotating outer planet to the magnetosphere and the energy input into the atmosphere through the magnetosphere-ionosphere coupling. Long-term monitoring of Jupiter’s northern aurora is achieved by the Extreme Ultraviolet (EUV) spectrometer called EXCEED (Extreme Ultraviolet Spectroscope for Exospheric Dynamics) onboard JAXA’s Earth-orbiting planetary space telescope Hisaki until today after its launch in September 2013. We have proceeded the statistical survey of the Jupiter’s auroral energy input into the upper atmosphere. The auroral electron energy is estimated using a hydrocarbon color ratio (CR) adopted for the wavelength range of EXCEED. The emission power in the long wavelength range 138.5-144.8 nm is used to derive the total emitted power before hydrocarbon absorption which is a good indicator for the total energy input into the atmosphere. Long-term observation provides us a "typical" occurrence ratio profile of the input energy following a log-normal distribution with the highest occurrence at 1.12 TW. In addition, temporal dynamic variation of the auroral intensity was detected when Io’s volcanic activity and thus EUV emission from the Io plasma torus are enhanced in the early 2015. Average of the total input power over 80 days increases by ˜10% with sometimes sporadically more than a factor of 3 upto 7, while the CR indicates the auroral electron energy decreases by ˜20% during the volcanic event compared to the other period. This indicates much more increase in the current system and Joule heating which contributes heating of the upper atmosphere. We will discuss the impact of this event on the upper atmosphere and ionosphere.

Statistical study of solar wind control on Jovian UV auroral activity obtained from long-term Hisaki EXCEED observations

Hajime Kita[1]; Tomoki Kimura[2]; Chihiro Tao[3]; Fuminori Tsuchiya[4]; Atsushi Yamazaki[5]; Go Murakami[6]; Kazuo Yoshioka[7]; Hiroaki Misawa[8]; Takeshi Sakanoi[9]; Yasumasa Kasaba[10]; Ichiro Yoshikawa[11]; Masaki Fujimoto[12]
[1] Tohoku Univ.; [2] RIKEN; [3] NICT; [4] Planet. Plasma Atmos. Res. Cent., Tohoku Univ.; [5] ISAS/JAXA; [6] ISAS/JAXA; [7] The Univ. of Tokyo; [8] PPARC, Tohoku Univ.; [9] Grad. School of Science, Tohoku Univ.; [10] Tohoku Univ.; [11] EPS, Univ. of Tokyo; [12] ISAS, JAXA

While the Jovian magnetosphere is known to have the internal source for its activity, it also has the influence from the solar wind. In a theoretical model, the ultraviolet (UV) aurora and solar wind dynamic pressure are anti-correlated. On the other hand, previous observations such as those by the Hubble Space Telescope showed a positive correlation between them. We made a statistical analysis for the total power variation of Jovian UV aurora obtained by the spectrometer EXCEED (Extreme Ultraviolet Spectroscope for Exospheric Dynamics) on board the Hisaki satellite. The data set was obtained from Dec. 2013 to Feb. 2014 and from Dec. 2014 to Feb. 2015. We compared the total UV auroral power in 900-1480 A with solar wind dynamic pressure at Jupiter estimated from the observation at 1 AU with a one-dimensional MHD model.

Superposed epoch analysis supports the positive correlation as the previous observation: Auroral total power increases when solar wind dynamic pressure enhanced around Jupiter. Furthermore, the auroral total power shows a positive correlation to the duration of a quiescent interval of the solar wind before the enhancements of the dynamic pressure with the correlation coefficient of 0.86. It is more than the correlation to the amplitude of dynamic pressure enhancement with the correlation coefficient of 0.44. A similar trend was observed in the auroral field-aligned currents which are inferred from the color ratio between the two bands of the Hisaki spectrum data. These statistical characteristics define the next step to unveil the physical mechanism of the solar wind control on the Jovian magnetospheric dynamics.

One possible scenario to explain the results is that the magnetospheric plasma content controls the aurora response to the solar wind variation. A long quiescent interval would mean that more plasma supplied from Io is accumulated in the magnetosphere. The solar wind compression causes adiabatic acceleration of the plasma and then the aurora increases. However, it is still unclear how the angular velocity distribution of magnetospheric plasma and auroral brightness distribution vary during the solar wind compression. Observationally, the next step for this study is to accompany an imaging observation to inspect morphological changes upon a hit by a solar wind shock. We will also discuss the possible mechanism from the initial result of the ground-based infrared observations in 2016.

LWA1モジュレーションレーンデータにより測定したIo-CとIo-Bの木星デカメートル波電波源のパラメータについて

今井 一雅 [1]; Higgins Charles A.[2]; 今井 雅文 [3]; Clarke Tracy[4]
[1] 高知高専; [2] Middle Tennesee State University; [3] University of Iowa; [4] Naval Research Laboratory

Io-C and Io-B Source parameters of Jupiter's decametric emissions measured from LWA1 modulation lane data

Kazumasa Imai[1]; Charles A. Higgins[2]; Masafumi Imai[3]; Tracy Clarke[4]
[1] NIT, Kochi; [2] Middle Tennesee State University; [3] University of Iowa; [4] Naval Research Laboratory

The modulation lanes in Jupiter's decametric radiation, which were discovered by Riihimaa [1968], are groups of sloping parallel strips of alternately increasing and decreasing intensity in the dynamic spectra. The frequency-time slopes of the lanes can be either positive or negative depending on which of the Jovian sources are being observed. In the Imai et al. [1992a, 1992b, 1997] model for the production of modulation lanes, the lanes are assumed to be a manifestation of regularly spaced plasma density variations that exist in the Io plasma torus. The fringes are produced as a result of the passage of the multi-frequency radiation through an interference grating. By using our model, Jupiter's radio source locations and beam parameters can be measured precisely. This remote sensing tool is called the modulation lane method [Imai et al., 2002, 2006].

The Long Wavelength Array (LWA) is a low-frequency radio telescope designed to produce high-sensitivity, high-resolution spectra in the frequency range of 10-88 MHz. The Long Wavelength Array Station 1 (LWA1) is the first LWA station completed in April 2011, and is located near the VLA site in New Mexico, USA. LWA1 consists of a 256 element array operating as a single-station telescope. The sensitivity of the LWA1, combined with the low radio frequency interference environment, allows us to observe the fine structure of Jupiter's decametric modulation lanes. Using newly available wide band modulation lane data observed by LWA1, we measured source locations and beam parameters.

The results of LWA1 data analysis indicate that the radio emitting sources are located along a restricted range of Jupiter's System III longitude. We only receive one of the individual sources at a given time because the source has a very thin beam (probably less than few degrees). We show the measured locations of Io-related sources based on the modulation lanes observed by LWA1. In this analysis we identified the existence of two independent radio sources in the case of Io-C events, one from the northern hemisphere (right hand polarization; we named it as Io-C', Io-C-prime), and one from the southern hemisphere (left hand polarization, Io-C). Previously we considered that both of the right and left hand components were coming from the same hemisphere. However we have investigated four other cases to show that different modulation lane patterns exist between right and left hand components. Thus the right and left hand components are coming from different hemispheres.

We also identified the radio source of the early part of Io-B (we named it as Io-B', Io-B-prime). It is located between 50 to 100 degrees CML of System III longitude and is independent of the main part of Io-B between 100 to 180 degrees CML. The measured center of the source longitude range is about 110 degrees in the case of Io-B' and about 190 degrees in the case of the main part of Io-B. This 110 degrees source longitude corresponds to the brightness peak of the IFP (Io footprint) and when Io is close to the Io plasma torus center [Bonfond et al., 2013]. The 190 degrees source longitude is close to the center of the longitude range of the active magnetic flux tube for non-Io-related radio emissions [M.Imai et al., 2011].

投入一金星周年をむかえた金星探査機あかつき

あかつきプロジェクト 中村 正人 [1]
[1] -

Present status of Akatsuki one Venusian year after the Venus Orbit Insertion

Masato Nakamura Akatsuki Project[1]
[1] -

Venus orbiter Akatsuki arrived at Venus on 7th of December, 2015. 19th of July, 2016 was the first anniversary by the Venusian year of the Venus orbit insertion. The spacecraft has been operated carefully and all the subsystems and the science instruments are working almost normally. Its orbital period is about 10.7days and its apoapsis is 0.37million km. Venus observation is done by the onboard science instruments (4 cameras) every 2 hours except telecommunication time period of about 8 hours when the HGA is directed to the earth and cameras are not in good position to shoot Venus. When the spacecraft come to the closet point to Venus, rim observation, close up imaging, and radio science are sequentially done. Downloaded science data are stored in SIRIUS data system in ISAS and processed by data pipe-line which produces Level 1, 2, and 3 data sets. All the processed data will be delivered 1 year after the data acquisition.

２０１５年１２月７日に金星に到着した金星探査機あかつきは本年７月１９日に金星到着一（金星）周年を迎えた。各サブシステム、各観測機器は概ね順調に運用を続けている。現在の軌道周期は約１０．７日、遠金点高度は３７万 km である。地球との通信で探査機姿勢を HGA 地球指向にする時間以外は４つのカメラが２時間ごとに撮影を続けており、近金点付近ではリム観測、クローズアップ撮影、電波科学観測が行なわれている。取得されたデータは宇宙科学研究所のシリウスデータベースに一旦格納され、データ処理パイプラインを通してレベル１、２、３が作られていく。データの公開はデータ取得後１年間を目処に行われる。本講演では運用と観測の実態について報告する。

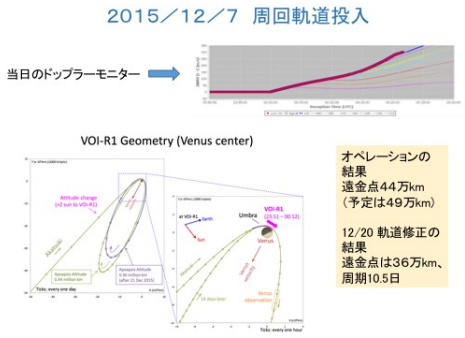

あかつき IR2 による金星昼面観測

佐藤 毅彦 [1]; 佐藤 隆雄 [2]; 中村 正人 [3]; 上野 宗孝 [4]; 鈴木 睦 [5]; はしもと じょーじ [6]; 榎本 孝之 [7]; 高見 康介 [8]; 中川 広務 [8]; 笠羽 康正 [9]
[1] 宇宙研; [2] 宇宙研; [3] 宇宙研; [4] 宇宙科学研究所; [5] JAXA・宇宙研; [6] 岡大・自然; [7] 総研大・物理・宇宙; [8] 東北大・理・地球物理; [9] 東北大・理

Observation of the Venus day-side disk with Akatsuki IR2

Takehiko Satoh[1]; Takao M. Sato[2]; Masato Nakamura[3]; Munetaka Ueno[4]; Makoto Suzuki[5]; George Hashimoto[6]; Takayuki Enomoto[7]; Kosuke Takami[8]; Hiromu Nakagawa[8]; Yasumasa Kasaba[9]
[1] ISAS, JAXA; [2] ISAS/JAXA; [3] ISAS; [4] ISAS, JAXA; [5] ISAS, JAXA; [6] Okayama Univ.; [7] Space and Astr., SOKENDAI; [8] Geophysics, Tohoku Univ.; [9] Tohoku Univ.

Observations of the Venus day-side disk with IR2 onboard Akatsuki are done through a filter centered at 2.02-um wavelength. This corresponds to a strong absorption band of CO_2, the primary molecule of the Venus atmosphere. As the sunlight is absorbed in both ways (to the cloud top and from the cloud top after reflection) with the absorption strength proportional to the path length, the 2.02-um images can visualize undulation of the cloud top. Such altimetry has been demonstrated in a different band with Venus Express/VIRTIS-M (Ignatiev, et al., 2009). However, the altimetry with high-resolution global images can, for the first time, be done with Akatsuki IR2.

We show an example image acquired on 6 May 2016 when Venus appears almost fully illuminated. To better visualize the fine structures, the limb-darkening is roughly removed and the high-pass filtering is applied. The high-latitude regions, in both hemispheres, are darker, indicating the cloud tops are lower in the atmosphere. This view is consistent with the previous studies. Many streaky features, parallel to the latitudinal bands, may be due to zonal winds. Turbulent clouds, suggesting active convections, in the afternoon to the evening, have correlation with features of “unknown absorber” seen in the UVI image. By accumulating such data, it may be expected to increase our knowledge about the vertical structure and dynamics, as well as the role of “unknown absorber” to them.

あかつき IR2 カメラの金星昼面観測は、中心波長 2.02um のフィルターを通して行われる。この波長は金星大気主成分である CO_2 の強い吸収帯に対応しており、金星雲頂の凹凸を明暗としてとらえることができる。入射太陽光が金星雲頂で反射され宇宙空間へ出るまでの光路長が長い（雲頂が低い）ほど吸収を強く受け、暗く観測されるという原理である。このような高度測定は、異なる吸収帯で、Venus Express/VIRTIS-M データを用いて行われた例がある（Ignatiev, et al., 2009）が、全球を高解像度スナップショットでとらえる測定は、IR2 によるものが最初である。

2016 年 5 月 6 日、ほぼ満月状の金星を波長 2.02um で観測した画像を図に示す。画像は周縁減光をおおまかに補正し、細かな模様を識別しやすくするためのハイパス処理を施している。これを見ると、南北ともに高緯度地方の雲頂が低い（暗く見える）ことが明らかであり、先行研究の結果と整合的である。緯度に平行な筋は東西流に伴う雲頂の凹凸を示すものと考えられる。また午後から夕方側に対流性を思わせる雲が多く見られるが、UVI 画像と比較すると「未知吸収物質による暗い模様」と対応しているものがある。こうしたデータを積み重ねてゆくことで、大気運動の垂直構造、未知吸収物質の役割の解明などにつながることが期待される。

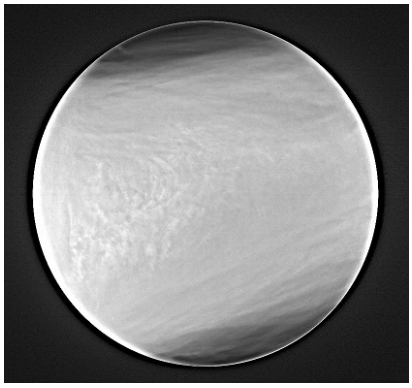

金星大気中に発見された巨大定在重力波

田口 真 [1]; 神山 徹 [2]; 今村 剛 [3]; 堀之内 武 [4]; 福原 哲哉 [5]; 二口 将彦 [6]; はしもと じょーじ [7]; 岩上 直幹 [8]; 村上 真也 [9]; 小郷原 一智 [10]; 佐藤 光輝 [11]; 佐藤 隆雄 [9]; 鈴木 睦 [12]; 高木 聖子 [13]; 上野 宗孝 [14]; 渡部 重十 [5]; 山田 学 [10]; 山崎 敦 [15]; 中村 正人 [16]
[1] 立教大・理・物理; [2] 産総研; [3] 東京大学; [4] 北大・地球環境; [5] 北大・理・宇宙; [6] 東邦大; [7] 岡大・自然; [8] なし; [9] 宇宙研; [10] 宇宙研; [11] 北大・理; [12] JAXA・宇宙研; [13] 東海大、TRIC; [14] 宇宙科学研究所; [15] JAXA・宇宙研; [16] 宇宙研

A huge stationary gravity wave found in the Venus atmosphere

Makoto Taguchi[1]; Toru Kouyama[2]; Takeshi Imamura[3]; Takeshi Horinouchi[4]; Tetsuya Fukuhara[5]; Masahiko Futaguchi[6]; George Hashimoto[7]; Naomoto Iwagami[8]; Shin-ya Murakami[9]; Kazunori Ogohara[10]; Mitsuteru SATO[11]; Takao M. Sato[9]; Makoto Suzuki[12]; Seiko Takagi[13]; Munetaka Ueno[14]; Shigeto Watanabe[5]; Manabu Yamada[10]; Atsushi Yamazaki[15]; Masato Nakamura[16]
[1] Rikkyo Univ.; [2] AIST; [3] The University of Tokyo; [4] Hokkaido University; [5] Cosmosciences, Hokkaido Univ.; [6] Toho Univ.; [7] Okayama Univ.; [8] none; [9] ISAS/JAXA; [10] JAXA/ISAS; [11] Hokkaido Univ.; [12] ISAS, JAXA; [13] Tokai Univ. TRIC; [14] ISAS, JAXA; [15] ISAS/JAXA; [16] ISAS

The Longwave Infrared Camera (LIR) onboard the Japanese Venus orbiter Akatsuki acquires a snap shot of Venus in the middle infrared region, and provides a brightness temperature distribution at the cloud-top altitudes of about 65 km. More than 800 of Venus images taken by LIR have been transferred to the ground since the successful Venus orbit insertion of Akatsuki on Dec. 7, 2015. Here we report that a bow-shaped thermal structure extending the northern high-latitudes to the southern high-latitudes with an end-to-end distance of longer than 10000 km was found in the brightness temperature map on Dec. 7, 2015 as shown in Figure. The bow-shaped structure lasted for four days at least, and stayed at an almost same geographical position. The bow-shaped structure looks symmetrical with the equator, and consists of a high temperature region in east or upstream of the background strong westward wind or the super rotation of the Venus atmosphere followed by a low temperature region in west with an amplitude of 5K. It appeared close to the evening terminator in the dayside, and seems not to have stayed in the same local time rather to have co-rotated with the slowly rotating ground where the western part of Aphrodite Terra was below the center of the bow-shaped structure. Meridionally aligned filament-like structures similar to the bow-shaped structure in shape but in much smaller scale were also identified in the brightness temperature map on Dec. 7, and they propagated upstream of the zonal wind as well. The bow-shaped structure disappeared when LIR observed the same local time and longitude in the earliest opportunity on Jan. 16, 2016. Similar events, though their amplitudes were less than 1K, were found on Apr. 15 and 26, May 6 and 24-25, 2016, but they appeared in different local times and longitudes. A UV image obtained by UVI onboard Akatsuki almost at the same time clearly shows advection of UV markings on the background flow, of which the zonal velocity on Dec. 7, 8 and 9 are -96, -96 and -107 m/s, respectively. This finding suggests that a stationary gravity wave generated in the lower atmosphere propagates upward to emerge as the bow-shaped structure in the brightness temperature distributions at the cloud-top altitudes, and that the wind distribution in the lower atmosphere might be spatially and temporally more variable than believed.

2010年12月7日に金星周回軌道投入に失敗した金星探査機「あかつき」は太陽を周回する軌道を巡りながら次のチャンスを待った。奇しくもちょうど5年後の2015年12月7日、「あかつき」は姿勢制御用エンジンを利用するという史上初めての手段を用いて金星周回軌道投入に成功した。周回軌道投入の成否に関わらず、タイムラインによる金星観測プログラムが設定されていた。金星周回軌道投入成功後、直ちに観測プログラムは実行され、金星観測が開始された。

中間赤外カメラ (LIR) はボロメターアレイを検出器として用いて波長8〜12ミクロンの赤外線画像を取得するカメラである。高度65 km付近の雲層上端から発せられる熱赤外をとらえる。そのため、日照面と日陰面の区別なくどの位置から観測しても金星ディスク全体をとらえられる点が特徴である。2016年7月末の時点でLIRは800枚以上の金星画像を地上に送ってきている。

図は2015年12月7日05h26m UTにLIRが取得した画像から導出された金星雲頂高度輝度温度分布である。図を見てまず気づくのは、夕方ターミネータ付近の日照側（ディスク中心よりも左側）に、南北高緯度をつなぐ弓状の高温領域（東側）とそれに続く低温領域（西側）が10000 km以上にわたって南北方向に伸びていることである。中高緯度領域にある帯状構造や南極上空の高温領域がはっきりと識別できる。弓状構造の高温領域及び低温領域の温度はそれぞれ230〜231K、225〜226Kであった。この構造はその後少なくとも4日間は連続してほぼ同じ地形上の位置に存在していた。残念ながら12月12日以降は「あかつき」の軌道、姿勢、通信に関係する重要な作業を優先するために、観測データはない。次に同じ経度と地方時をLIRが撮像した2016年1月15日には弓状構造はなくなっていた。

12月7日から11日に観測された弓状構造の対地角速度は-1〜0°/dayであり、金星の対太陽自転角速度の-3°/dayとは明らかに異なっている。弓状構造の高温領域と低温領域の境界の赤道上での位置はアフロディーテ大陸の西側高地の上空に対応している。

輝度温度分布を詳しく調べると、低緯度領域にはより小さい1000 kmスケールの弓状温度構造がいくつか見られる。例えばそれらのうちの1つは (110°E, -20°S) に中心を持つ。スケールは異なるものの、これらの弓状構造の特徴は赤道上空でおよそ100 m/sの西向きの背景風に流されることなく金星固体と同じ角速度で回転しているように見える点と、

弓状構造が東向きに凸である点である。

紫外イメージャ(UVI) はそれぞれ SO_2 と未知の吸収物質による吸収帯に対応する波長 283 nm 及び 365 nm に中心を持つ 2 つのバンドで金星日照面を撮像する。弓状構造はほぼ同時刻に UVI によって撮像された波長 283 nm の紫外画像にもかすかに認められているが、波長 365 nm の画像でははっきりしない。波長 283 nm の紫外画像で明るい領域は輝度温度で高温領域に対応している。波長 283 nm 及び 365 nm 画像には過去の探査によってよく知られている Y 字型の構造がとらえられている。UVI 画像から雲追跡手法で求めた 12 月 7、8、9 日の緯度± 15 ° の内側の赤道領域での平均東西風速はそれぞれ-96、-96、-107 m/s であった。

その後、2016 年 4 月 15 日、26 日、5 月 6 日、24〜25 日の雲頂輝度温度分布にも、振幅は 1K 以下ながらも同様の弓状構造が検出されている。

弓状構造の起源としては、山岳波のように地表付近に起源がある重力波が上空に伝播して雲層上端での輝度温度変動及び紫外吸収物質のカラム量変動として出現していると解釈している。Bertaux et al. [2016] は VEX/VMC で観測された金星紫外画像を使って、山越え気流によって生成された定在重力波が平均風速の非一様分布をもたらしていると示唆した。今回、LIR 及び UVI が観測した弓状構造はより大規模な定在重力波が存在する直接的な証拠である。しかし、これまでの探査で知られている金星大気の中立層構造はそのような重力波の鉛直伝播を妨げる。今回、弓状構造を生成する重力波が見つかったことは、下層大気の風速に時間空間変動があることを示し、それが弓状構造が常に存在するわけではなく、ときどき出現することの理由かも知れない。

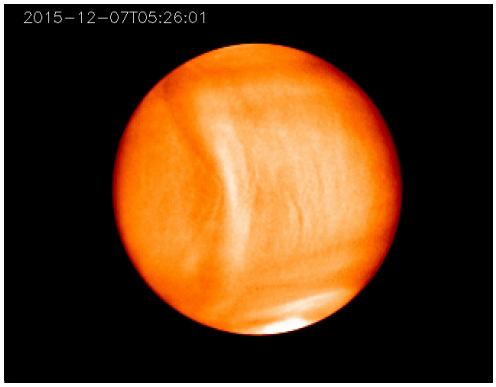

あかつき中間赤外カメラによる金星極域大気温度構造の解析

高村 真央 [1]; 神山 徹 [2]; 田口 真 [3]; 福原 哲哉 [4]; 今村 剛 [5]; 佐藤 隆雄 [6]; 二口 将彦 [7]; はしもと じょーじ [8]; 鈴木 睦 [9]; 岩上 直幹 [10]; 佐藤 光輝 [11]; 高木 聖子 [12]; 上野 宗孝 [13]; 中村 正人 [14]
[1] 立教・理; [2] 産総研; [3] 立教大・理・物理; [4] 立教大・理; [5] 東京大学; [6] 宇宙研; [7] 東邦大; [8] 岡大・自然; [9] JAXA・宇宙研; [10] なし; [11] 北大・理; [12] 東海大、TRIC; [13] 宇宙科学研究所; [14] 宇宙研

Investigation of thermal structures in Venus polar regions observed by Akatsuki/LIR

Mao Takamura[1]; Toru Kouyama[2]; Makoto Taguchi[3]; Tetsuya Fukuhara[4]; Takeshi Imamura[5]; Takao M. Sato[6]; Masahiko Futaguchi[7]; George Hashimoto[8]; Makoto Suzuki[9]; Naomoto Iwagami[10]; Mitsuteru SATO[11]; Seiko Takagi[12]; Munetaka Ueno[13]; Masato Nakamura[14]
[1] Rikkyo Univ.; [2] AIST; [3] Rikkyo Univ.; [4] Rikkyo Univ.; [5] The University of Tokyo; [6] ISAS/JAXA; [7] Toho Univ.; [8] Okayama Univ.; [9] ISAS, JAXA; [10] none; [11] Hokkaido Univ.; [12] Tokai Univ. TRIC; [13] ISAS, JAXA; [14] ISAS,JAXA

The polar dipole which locates at the center of the polar region shows higher temperature and the polar collars surrounding the polar region shows colder temperature relative to other regions. Infrared observations of Venus by the previous missions revealed these features.

Previous observations show that shapes of the polar dipoles can be characterized by three pattern which have a dipole shape, an elongated oval or a nearly circular structure and that these shapes change with time. [Garate-Lopez et al., 2013] The rotation period of polar dipole is 2.5 Earth days [Piccioni et al., 2007] and 2.8-3.2 Earth days [Schofield et al., 1983] in the south and north polar regions, respectively. It has not been clear that the difference and variability in the rotation period is due to just a temporal variation or influence of solar activity. Temperature of the Venusian atmosphere increases linearly with altitude. It is known that the mean cloud-top altitude decreases from 74 km at the mid-latitudes to 67 km at the high latitudes [Luz et al., 2011]. However, the observation by radio occultation showed that the temperature and altitude are not correlated in the polar region. The polar dipoles and polar collars are attributed to the residual mean meridional circulation (RMMC) enhanced by the thermal tide. In the high latitudes downward advection adiabatically heated by RMMC induces the warm polar dipole, and conversely, in the latitudes equatorward of the polar dipole, upward advection adiabatically cooled by RMMC induces the cold polar collar. [Ando et al., 2015]

The first Japanese Venus orbiter Akatsuki was launched in 2010. The Venus orbit insertion maneuver for Akatsuki in 2010 was failed, however, the second attempt to the Venus orbit insertion in 2015 was successful [Nakamura et al., 2011; 2016]. Akatsuki is a planetary meteorological satellite aiming at understanding the atmosphere dynamics of Venus.

Longwave infrared camera (LIR) observes thermal emission from the Venus cloud top and derives brightness temperature [Fukuhara et al., 2011]. LIR observe both dayside and nightside with an equal quality. Therefore, LIR can get temperature of a hemisphere facing to the spacecraft. Since Venus Express(VEX) was in a polar orbit of which the apoapsis was located at the south pole, VEX was suitable for observing the southern polar region. On the other hand, Akatsuki is in an equatorial orbit, which is suitable for simultaneous observations of both north and south polar regions.

We investigate thermal structure in the polar regions using brightness temperature distributions obtained by LIR. Figure shows an example of brightness temperature distribution derived by LIR. A polar dipole and a polar collar are clearly recognized. LIR has observed Venus sequentially every two hours except for the period while Akatsuki is close to periapsis. Temperature distributions of the polar regions, temporal variation of the shape of polar dipoles, the rotation period of the polar vortex by a cloud tracking method and north-south symmetry of polar phenomenon using brightness temperature distributions will be investigated to clarify the dynamics of Venusian atmosphere. In addition, comparing LIR results with results from other instruments, such as clout top altitudes derived from 2.02 micometer images obtained with a 2-micometer infrared camera (IR2), will provide additional hints for understanding the atmosphere dynamics of Venus polar regions.

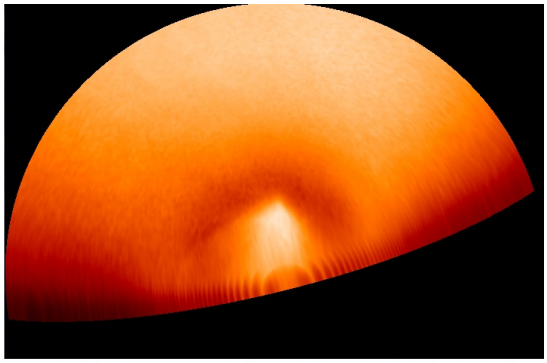

An example of a brightness temperature distribution which shows the polar dipole and polar collar

LIRによって観測された金星雲頂高度における温度構造とその時間変化

神山 徹 [1]; 田口 真 [2]; 福原 哲哉 [3]; 佐藤 隆雄 [4]; 二口 将彦 [5]; はしもと じょーじ [6]; 今村 剛 [7]
[1] 産総研; [2] 立教大・理・物理; [3] 立教大・理; [4] 宇宙研; [5] 東邦大; [6] 岡大・自然; [7] 東京大学

Spatial and temporal variation of thermal structures at the Venus cloud top level observed by LIR

Toru Kouyama[1]; Makoto Taguchi[2]; Tetsuya Fukuhara[3]; Takao M. Sato[4]; Masahiko Futaguchi[5]; George Hashimoto[6]; Takeshi Imamura[7]
[1] AIST; [2] Rikkyo Univ.; [3] Rikkyo Univ.; [4] ISAS/JAXA; [5] Toho Univ.; [6] Okayama Univ.; [7] The University of Tokyo

http://www.airc.aist.go.jp/teams/gsrt.html

Since the successful Venus orbit insertion-revenge of the Japanese Venus orbiter Akatsuki on December 7, 2015, the Longwave Infrared Camera (LIR) onboard Akatsuki has continuously observed Venus with the mid-infrared region (8-12 um). Mid-infrared observation provides Venus temperature distribution around the cloud top level (around 65km), and combining sequential observations, spatial and temporal variation of the temperature distribution can be investigated, which is one of fundamental information for studying Venus climate. Akatsuki is the first satellite orbiting an equatorial orbit, which enable LIR to provide Venus temperature field covering low to mid-latitude regions widely in both hemispheres. Since several planetary scale waves, such as Kelvin wave and Rossby wave, and thermal tides affect temperature field perturbations globally, investigation of spatial structures and temporal variations of temperature fields seen in LIR images may help to understand the activities of these waves. From such observation images, we found several global, both hemisphere symmetric and periodical variations whose directions were same as Venus' super-rotation (westward), in addition to some stationary structures (both global and local) as reported in the initial report of Akatsuki observations. In this study we will report the spatial and temporal temperature variations seen in LIR images and also report calibration and image processing procedures to clarify the structures.

2015年12月7日に成功裏に実施された金星探査機あかつきの金星軌道再投入から現在に至るまで, 他の観測機器同様に熱赤外線カメラ (LIR) は継続的に金星観測を行っている. LIRのカバーする熱赤外線波長 (8-12um) では雲頂高度 (~65km) からの熱放射 (輝度温度分布) を観測できる. また連続的に取得された観測データを組み合わせて解析をすることで, 温度場の構造を知るだけでなくその時間変化も捉えることができる. あかつきは赤道軌道に近い軌道上を回る最初の金星探査衛星であり, このような軌道は低緯度を中心として南北両半球の広い緯度帯を観測するのに適している. これまでに観測されているいくつかの惑星規模波動 (i.e. ケルビン波, ロスビー波, 熱潮汐波) は低緯度から高緯度帯にわたって全球的な温度擾乱場を作ることが知られており, 広い緯度帯をカバーできる観測はこのような惑星規模波動の活動性を理解するのに有効である. 実際に連続的に実施されたLIRの観測画像からは, 初期成果報告等で報告されている温度擾乱の定在構造だけでなく, 周期的に回転する惑星規模の温度擾乱構造がいくつも見られている. 本発表ではこのような赤道軌道上から得られたユニークな観測結果について報告するとともに, 輝度温度較正にかかる取り組みについて報告する.

あかつき電波掩蔽観測の初期結果

今村 剛 [1]; 安藤 紘基 [2]; あかつき電波科学チーム 今村　剛 [3]
[1] 東京大学; [2] 京産大; [3] -

Initial results of Akatsuki radio occultation

Takeshi Imamura[1]; Hiroki Ando[2]; Imamura Takeshi Akatsuki Radio Science Team[3]
[1] The University of Tokyo; [2] Kyoto Sangyo University; [3] -

Akatsuki's radio occultation experiments are performed when the spacecraft is hidden by Venus as viewed from the tracking station (Usuda Deep Space Center). Radio signals, stabilized by an onboard ultra-stable oscillator, are transmitted from the spacecraft and received at the tracking station after passing through the planetary atmosphere. Analysis of the recorded signals yields temperature profiles, sulfuric acid vapor profiles, and the ionospheric electron density profiles. A merit of Akatsuki's observation is that the location probed by radio occultation can be observed by the cameras a short time before the ingress or short time after the egress thanks to the equatorial orbit, enabling quasi-simultaneous observations. Since the dense Venusian atmosphere causes considerable ray bending, a spacecraft steering is required to compensate for this effect while the occultation geometry changes from ingress occultation to egress occultation. Eight Venus occultations have been observed till July 2016 and interesting features in the temperature profile are seen. Radio occultation observations of the solar corona have also been conducted in early June.

金星探査機「あかつき」の電波掩蔽（えんぺい）観測は気温の高度分布を精度 0.1 K、高度分解能 1 km 程度で取得し、光学観測を補完する。この観測では普段は探査機と地上局の間の通信に用いている電波を利用する。地上局から見て探査機が金星の背後に隠れる時と背後から出てくる時、探査機から送信される電波は金星大気をかすめるように通過して地上局に届く。このとき電波が金星大気の影響で屈折する結果として Doppler 周波数が変化する。これを分析すると大気の屈折率の高度分布がわかり、そこから気温の高度分布がわかる。高度 100 km 以上の屈折率からは電離層の電子密度も得られる。受信電波強度の変化からは硫酸雲の下に多く存在する電波吸収体である硫酸蒸気の分布がわかる。

電波掩蔽という手法自体は金星でも実績があるが、「あかつき」においては 5 台の大気観測カメラで得られる大気の水平構造の情報と組み合わせることにより 3 次元構造を推定するという狙いがある。「あかつき」は赤道周回軌道をとるため従来の極軌道の探査機と異なり中・低緯度を重点的に観測することも特色である。

金星大気の変動がもたらす微小な周波数変化を検出するために、基準周波数に対する周波数変動の割合が 10 のマイナス 12 乗以下という超高安定発振器 (Ultra-stable oscillator、USO) を搭載した。これまでの金星探査においてこのような安定度の USO を搭載したのは欧州の金星周回機 Venus Express だけである。「あかつき」から送信された GHz 帯の電波は臼田宇宙空間観測所のアンテナで受信され、ローカル信号のミキシングにより数百 KHz の信号に変換されたのち波形ごと記録される。このデータから周波数や電波強度の時系列を抽出する。観測時には、金星大気による電波の屈折を考慮して、探査機姿勢を変化させ高利得アンテナの向きを制御する。

これまでに 8 セットの電波掩蔽観測を実施した。1 セットごとに探査機が金星に隠れるときと現れるときの 2 箇所が観測される。これらのデータには、雲層の下で温度がよく安定していること、雲の上では温度場に細かな変動が多く見られること、高緯度の雲頂高度には顕著な温度極小があることなど、興味深い特徴が見られている。今後はこれらをカメラ群による撮像データを参照しつつ解析する。

2016 年 6 月上旬に探査機が地球から見て太陽の反対側を通過する外合時には、電波掩蔽の方法で太陽コロナの観測も実施した。

紫外線望遠鏡による系外惑星酸素大気検出の検討

堀越 寛己 [1]; 亀田 真吾 [1]; 村上 豪 [2]
[1] 立教大; [2] ISAS/JAXA

Feasibility studies for the detection of exoplanetary atomic oxygen exospheres with a UV space telescope

Hiroki Horikoshi[1]; Shingo Kameda[1]; Go Murakami[2]
[1] Rikkyo Univ.; [2] ISAS/JAXA

Many observations have been carried out for exoplanets since they were first discovered in 1995. To date, the number of detected exoplanets is more than 3000. Since exoplanetary atmospheric atoms and molecules absorb stellar photons during a transit, we can know atmospheric composition from the observation of stellar absorption line or band.

We simulate the detectability of atomic oxygen exospheres with a UV space telescope, assuming an Earth twin, Venus twin or Mars twin exists in the habitable zone of a low-temperature star. Stellar UV radiation dissociates or ionizes molecules in the planetary atmosphere; in particular, EUV radiation drives atmospheric heating. However, stellar radiations between 40 and 91.2 nm cannot be measured because of the absorption of neutral hydrogen in an interstellar medium. We estimate the EUV intensity at the habitable zone of a low-temperature star using empirically derived relations between the total hydrogen Lyman alpha (122 nm) intensity and the EUV intensity presented by Linsky et al. (2014). Moreover, we simulated the oxygen column density on an Earth twin, Venus twin and Mars twin in the habitable zone of a low-temperature star using the results of Kulikov et al. (2007) and Tian et al. (2008). We found that when an Earth twin in the habitable zone of a low-temperature star transits its host star, the transit depth of the OI emission line at 130 nm becomes much deeper than that of a Venus twin or Mars twin. We conclude that even a small UV telescope (˜20 cm) enables us to distinguish an Earth twin from a Venus twin and Mars twin and detect atomic oxygen exospheres of an Earth twin in a habitable zone of a low temperature star within a few transits.

NASA and ESA are planning to launch space telescope dedicated to exoplanets; however, their spectral ranges are limited to the visible and infrared regions. Therefore, we are planning to develop a UV space telescope dedicated to exoplanetary systems.

1995 年に系外惑星が発見されてから数多くの観測が行われ、検出された惑星の数は現時点で 3000 を超えている。今後は地球近傍の低温度星（3000～4000K）周りに数多くの惑星が検出される見込みである。また、一部の惑星では地球から見て惑星が主星の手前を横切る際に、主星の光を遮蔽するトランジット現象を利用して、大気組成に関する情報が得られている。大気を持たない惑星のトランジット時の主星光の減光率は波長に依存しないが、大気を持つ惑星の場合、大気中に含まれる原子・分子が特定の波長の光を吸収・散乱するため、分光観測によって大気組成に関する情報が得られる。

我々は低温度星のハビタブルゾーンに地球、金星、火星が存在すると仮定し、各惑星大気中の酸素原子の検出可能性について検討した。恒星の紫外線は惑星大気中の分子を解離・電離させ、特に極端紫外線（EUV）は大気の加熱源となる。しかし、波長 40～91.2nm の EUV 放射は星間空間中に存在する水素によって吸収・散乱されてしまうので観測することはできない。我々は Linsky et al. (2014) で示されている水素ライマン α 線（波長 122nm）強度と EUV 強度の関係式を用いて、低温度星のハビタブルゾーンにおける EUV 強度を推定した。さらに、Kulikov et al. (2007) と Tian et al. (2008) で示されている太陽からの EUV 放射の強度を変化させた場合の地球、金星、火星の酸素密度分布を用いて各惑星の酸素原子柱密度を計算した。結果として、低温度星のハビタブルゾーンに地球が存在した場合、高高度まで高密度な酸素原子が広がるため、OI 輝線（波長 130nm）でトランジット観測すると金星や火星がトランジットした場合に比べてトランジット深さが非常に深くなることが示された。従って、小型の紫外線宇宙望遠鏡（～20cm）による観測によって、地球、金星、火星は区別することが可能であり、数回トランジット観測すれば低温度星のハビタブルゾーンに存在する地球の酸素原子大気を検出することが可能であることが示された。

NASA や ESA で提案されている将来計画における観測波長域は可視～赤外のみである。そこで我々は系外惑星観測に特化した紫外線宇宙望遠鏡の開発を進めている。

Evaluation of hydrogen absorption cells for observation of the planetary coronas

Masaki Kuwabara[1]; Makoto Taguchi[2]; Kazuo Yoshioka[3]; Tokio Ishida[2]; Shingo Kameda[4]; Ichiro Yoshikawa[5]
[1] The Univ. of Tokyo; [2] Rikkyo Univ.; [3] The Univ. of Tokyo; [4] Rikkyo Univ.; [5] EPS, Univ. of Tokyo

Atomic hydrogen in the planetary exospheres resonantly scatters the solar Lyman-alpha emission at the wavelength of 121.567 nm forming planetary coronas. Imaging of the hydrogen corona allows us to probe a density distribution of the atomic hydrogen. The hydrogen absorption cell technique is a strong tool for the imaging of planetary coronas, because it enables us to obtain not only intensity distributions of the hydrogen coronas but also temperature distributions and D/H ratios, which are key parameters for estimating amount of planetary water lost in the past. Hydrogen absorption cells of which the clear aperture is enlarged to be twice as large as that of the cells for UVS-P onboard the Japanese Mars orbiter NOZOMI have been developed. We measured absorption profiles of them using the DESIRS beamline at Synchrotron SOLEIL in France, and evaluated dependences of optical thicknesses and FWHMs of the absorption profiles on 1) length and diameter of filaments, 2) filament temperature, 3) hydrogen gas pressure, 4) position of a beam in the cell, and 5) path length in the cell. A spare deuterium cell for NOZOMI/UVS-P was also reevaluated. Application of the absorption cell technique for future planetary missions will be also presented.

The spatial evolution of the mixing layer in the Kelvin-Helmholtz instability at the Martian ionopause

Sae Aizawa[1]; Naoki Terada[2]; Yasumasa Kasaba[3]; Manabu Yagi[4]; Yosuke Matsumoto[5]
[1] Geophysics, Tohoku Univ; [2] Dept. Geophys., Grad. Sch. Sci., Tohoku Univ.; [3] Tohoku Univ.; [4] AICS, RIKEN; [5] Chiba University

We investigate the growth of the mixing layer thickness in the Kelvin-Helmholtz (KH) instability using an extended-local MHD model to estimate the ion loss rate from the Martian ionopause. This instability is expected to play a major role in transporting mass, momentum and energy across the ionopause between the sheath flow and ionospheric plasmas. Since the mixing layer has a finite thickness between them, this layer has a potential for the removal of a huge amount of ions from Mars through its history. The recent MAVEN observation reported that the density ratio across the ionopause reaches as high as 100˜5000. With such a large density ratio, compressible effects are expected to modify the structure of the KH vortices and the evolution of the mixing layer by generating high-amplitude nonlinear fast-mode plane waves from ridges of the KH waves.

In order to reproduce a realistic Martian ionopause, we developed an extended-local MHD model with aperiodic boundary condition for the evaluation of traveling waves along the dayside Martian ionopause (˜6,000km). Spatial resolution is set with 3km to resolve the thin mixing layer. We find two factors that accelerate the growth of the mixing layer. Firstly, the KH wave with the fastest growing mode behaves like a wall to the leading vortex in the aperiodic condition. The sheath flow is stagnated by this wall-like structure and induces an enhanced vortex return flow, resulting in a deeper excavation of the ionospheric plasma. Secondly, fast-mode rarefaction waves generated by compressible effects make wall-like structures more effective by lowering pressure around antinodes of the KH waves. Such a pressure profile further accelerates the stagnation and the excavation. Thus, the mixing layer becomes about 1.5 times wider than that obtained from a periodic local model when the density ratio is 100. It indicates that more ionospheric plasmas will escape than expected. The ion loss rate drastically increases after reaching the nonlinear growth phase.

ひさきによって観測された金星熱圏極端紫外酸素大気光の周期変動の朝夕非対称

益永 圭 [1]; 関 華奈子 [2]; 寺田 直樹 [3]; 土屋 史紀 [4]; 木村 智樹 [5]; 吉岡 和夫 [6]; 村上 豪 [7]; 山崎 敦 [8]; 垰 千尋 [9]; Leblanc Francois[10]; 吉川 一朗 [11]
[1] 東大・理
; [2] 東大理・地球惑星科学専攻; [3] 東北大・理・地物; [4] 東北大・理・惑星プラズマ大気; [5] 理研; [6] 東大・理; [7] ISAS/JAXA; [8] JAXA・宇宙研; [9] NICT; [10] LATMOS-IPSL, CNRS; [11] 東大・理・地惑

Dawn-dusk difference of periodic oxygen EUV dayglow variations at Venus observed by Hisaki

Kei Masunaga[1]; Kanako Seki[2]; Naoki Terada[3]; Fuminori Tsuchiya[4]; Tomoki Kimura[5]; Kazuo Yoshioka[6]; Go Murakami[7]; Atsushi Yamazaki[8]; Chihiro Tao[9]; Francois Leblanc[10]; Ichiro Yoshikawa[11]
[1] Univ. Tokyo; [2] Dept. Earth & Planetary Sci., Science, Univ. Tokyo; [3] Dept. Geophys., Grad. Sch. Sci., Tohoku Univ.; [4] Planet. Plasma Atmos. Res. Cent., Tohoku Univ.; [5] RIKEN; [6] The Univ. of Tokyo; [7] ISAS/JAXA; [8] ISAS/JAXA; [9] NICT; [10] LATMOS-IPSL, CNRS; [11] EPS, Univ. of Tokyo

We report a dawn-dusk difference of periodic variations of oxygen EUV dayglow (OII 83.4 nm, OI 130.4 nm and OI 135.6 nm) in the upper atmosphere of Venus observed by the Hisaki spacecraft in 2015. Observations show that the periodic dayglow variations are mainly controlled by the solar EUV flux. Additionally, we observed characteristic ~1 day and ~4 day periodicities in the OI 135.6 nm brightness. The ~1 day periodicity was dominant on the duskside while the ~4 day periodicity was dominant on the dawnside. Although the driver of the ~1 day periodicity is still uncertain, we suggest that the ~4 day periodicity is caused by gravity waves that propagate from the middle atmosphere. The thermospheric subsolar-antisolar flow and the gravity waves dominantly enhance eddy diffusions on the dawnside, and the eddy diffusion coefficient or the wave filtering effect changes every ~4 days due to large periodic modulations of wind velocity of the super-rotating atmosphere. This implies that the ~4 day periodicity of the EUV dayglow may reflect the dynamics of the middle atmosphere of Venus. We also examined the effects of the solar wind on the dayglow variations by shifting measurements at earth to Venus. We did not find clear correlations between them. Howerver, since there are no local measurements of the solar wind at Venus, we remain the effect of the solar wind uncertain.

金星極域における東西風の準周期的変動について

安藤 紘基 [1]; 杉本 憲彦 [2]; 高木 征弘 [3]
[1] 京産大; [2] 慶大・日吉物理; [3] 京産大・理

Quasi periodic variation of the zonal wind in the Venus polar region

Hiroki Ando[1]; Norihiko Sugimoto[2]; Masahiro Takagi[3]
[1] Kyoto Sangyo University; [2] Physics, Keio Univ.; [3] Faculty of Science, Kyoto Sangyo University

Recently, infrared measurements performed in Venus Express mission showed that the center of the Venus polar vortex moves quasi-periodically with the period of 3-4 days for local time. This suggests that the zonal mean wind speed varies quasi-periodically. We reproduced the Venus polar vortex by using our Venusian general circulation model named AFES for Venus. As a result, the short-period fluctuation of the zonally averaged zonal wind is seen in the Venus polar vortex in our model. This fluctuation seems to be related to barotropic instability in the polar region. The wind speed increases in the case where the momentum flux is positive, otherwise it decreases. When the momentum flux is positive when the phase of the relative vorticity related to barotropic instability clines from west-south toward east-north direction. This short-period variation is similar to the vacillation observed in the Earth's polar vortex. Furthermore, our results also suggest that the behavior of the atmospheric circulation in the Venus polar region might be unstable, which is similar to that in the Earth's polar vortex.

欧州宇宙機関 ESA が打ち上げた金星周回機 Venus Express の赤外線観測によって、金星極渦の中心がローカルタイムに対して 3、4 日程度で準周期的に変動していることが明らかにされた。これは、平均東西風がその日数で準周期的に変動していることを示唆している。我々は、金星大気大循環モデル AFES for Venus を用いて金星極域の大気構造を再現したところ、観測と同様に平均東西風の速度が準周期的に変動していることを見出した。そして数値計算データを詳しく解析したところ、この風速振動が順圧不安定と関連があることが分かった。このような風速振動は、地球の極渦で見られるバシレーションと定性的に良く似ている。本発表では、渦度分布や運動量輸送量を示しながらその成因について言及する。

Venus Express/VIRTISの可視・赤外画像を用いたpolar ovalおよび極域大気の熱収支の研究

武藤 圭史朗 [1]; 今村 剛 [2]
[1] 東大・理・地惑; [2] 東京大学

Study of the heat balance of the polar oval and polar atmosphere of Venus using Venus Express/VIRTIS visible and infrared images

Keishiro Muto[1]; Takeshi Imamura[2]
[1] Earth and Planetary Science,The Univ. of Tokyo; [2] The University of Tokyo

For understanding heat balance in Venus atmosphere, it is necessary to understand the behavior of the sunlight absorber. In visible range, scant attention has been paid to the sunlight absorber, but there is remarkable absorption by polar oval in polar region. Polar oval is a circular feature observed near the South Pole in visible and ultraviolet wavelengths (Observation is absent for the North Pole). The mechanism producing the oval is not understood. Commencing with polar oval, it is important to understand thermal influence and distribution of the sunlight absorber. In our previous study, we studied the change of the shape of the polar oval in visible and ultraviolet images, and the whole shape of the polar oval was revealed using Venus Express/VMC visible images. In this study, we compare IR and visible images taken by VIRTIS onboard Venus Express to better characterize this feature. In images taken at 5 micrometers, which is the maximum wavelength that can be observed by VIRTIS, we can observe thermal radiation from the cloud top. Contamination of sunlight scattered by dayside clouds is removed by subtracting a cubic function fitted to the brightness temperature variation along the solar zenith angle; this procedure enables observation of thermal radiation even on the dayside. By analysis of this data, the temperature rises some degrees at the dark edge of the polar oval, but the mechanism of temperature increase is not understood. Calculation of the heat balance at the dark edge of the polar oval shows that the temperature variation across the polar oval is explained by the albedo variation. In visible range, local time dependence of the radiance was observed in polar region except polar oval. This suggests that the distribution of the visible absorber changes over time, and so albedo changes. What kind of influence this has on the heat balance of the cloud top is in discussion.

金星大気の熱収支にとって雲層高度における太陽光吸収物質の振る舞いが重要である。これまで太陽光吸収物質が注目されてこなかった可視波長においても極域においてpolar ovalが存在し顕著な吸収が有る。Polar ovalは金星南極域で可視、紫外領域において観測される環状構造であり、その生成メカニズムは未だわかっていない。このpolar ovalをはじめとして吸収物質がどう分布し、どのような熱的影響を与えているか理解することが重要である。我々はこれまでVenus Express/VMCの可視画像を用いてpolar ovalの形状の変動について研究し、全体形状の復元を行った。今回はVenus Expressに搭載されていたVIRTISの可視および赤外の画像を比較しpolar ovalの熱収支に着目して研究した。VIRTISで観測できる最大波長の5 μ mでの観測画像を用いることで金星の雲頂からの熱放射を見ることができる。しかし、昼面においては熱放射の他に太陽散乱光が観測されてしまう。そこで、輝度と太陽光天頂角の関係として3次関数を仮定し昼面における太陽散乱光を除去した。これにより、昼面においても雲頂からの熱放射を観測することができるようになった。このデータの解析によりpolar ovalの縁の暗部で温度が数Kほど上昇していることが判明したが、その温度上昇のメカニズムはわかっていない。このpolar ovalでの温度上昇はpolar ovalの熱収支について簡単な計算を行うことにより可視のアルベドの差によるもので十分説明できる。polar oval以外の極域においても可視波長での輝度にローカルタイム依存性が 見られた。これは可視波長での吸収物質の分布に時間変化が生じてアルベドが変化していることを意味する。このことが雲頂の熱収支にどのような影響を与えるかは考察中である。

中間赤外ヘテロダイン分光観測による金星中間圏の風速・温度鉛直分布導出

高見 康介 [1]; 中川 広務 [1]; 佐川 英夫 [2]; Krause Pia[3]; 青木 翔平 [4]; 笠羽 康正 [5]; 村田 功 [6]; 渡部 重十 [7]; 田口 真 [8]; 今村 剛 [9]; 佐藤 毅彦 [10]; 黒田 剛史 [11]; 寺田 直樹 [12]

[1] 東北大・理・地球物理; [2] 京都産業大学; [3] University of Cologne; [4] IAPS-INAF, Italy; [5] 東北大・理; [6] 東北大院・環境; [7] 北大・理・宇宙; [8] 立教大・理・物理; [9] 東京大学; [10] 宇宙研; [11] NICT; [12] 東北大・理・地物

The wind and temperature profiles in Venusian mesosphere using mid-IR heterodyne spectrometer

Kosuke Takami[1]; Hiromu Nakagawa[1]; Hideo Sagawa[2]; Pia Krause[3]; Shohei Aoki[4]; Yasumasa Kasaba[5]; Isao Murata[6]; Shigeto Watanabe[7]; Makoto Taguchi[8]; Takeshi Imamura[9]; Takehiko Satoh[10]; Takeshi Kuroda[11]; Naoki Terada[12]

[1] Geophysics, Tohoku Univ.; [2] Kyoto Sangyo University; [3] University of Cologne; [4] IAPS-INAF, Italy; [5] Tohoku Univ.; [6] Environmental Studies, Tohoku Univ.; [7] Cosmosciences, Hokkaido Univ.; [8] Rikkyo Univ.; [9] The University of Tokyo; [10] ISAS, JAXA; [11] NICT; [12] Dept. Geophys., Grad. Sch. Sci., Tohoku Univ.

The atmosphere on Venus has thick sulfuric acid clouds which cover the planet at altitudes between ~50 and ~70 km. The retrograde superrotating zonal (RSZ) wind reaches the velocity over 100 m/s around the cloud top altitude. In the lower thermosphere above 110 km, there exists subsolar-to-antisolar (SS-AS) flow generated by large temperature difference between dayside and nightside. Mesosphere in the altitude of 70-90 km is considered as the transition region of atmospheric dynamics from RSZ wind to SS-AS flow. And temperature in mesosphere is disturbed by given momentum with breaking atmospheric waves raised from the lower atmosphere. Venusian mesosphere has complicated dynamics and thermal structure.

Previous ground-based heterodyne observations in submillimeter (sub-mm) and middle infrared (mid-IR) wavelength ranges provide information of wind and temperature in mesosphere. Observations in sub-mm sense atmospheric properties in the altitude of 80-105 km [e.g., Clancy et al., 2008]. However, the sub-mm observations, particularly those using single-dish radio telescopes, often suffer from relatively low spatial resolution While, mid-IR heterodyne instruments can achieve diffraction-limit so that we can observe high spatial resolution of 3 arcsec with 60 cm diameter small telescope [Nakagawa et al., 2016]. Their resolution obtained latitudinal and local time (LT) dependency of wind and temperature. They decreased with latitude from 240 K to 150 K in temperature [Sonnabend et al., 2010] and from 160 m/s to 40 m/s in wind [Sornig et al., 2008]. In this study, we obtain the vertical profiles of wind and temperature in mesosphere and discuss latitudinal and LT dependency and the mechanism.

In order to obtain wind and temperature profiles, we need to achieve high spectral resolution 10^{6-7} so that we can spectrally resolve CO_2 absorption spectra at 10um band [Stangier et al., 2015; Nakagawa et al., 2016]. The vertical profiles are retrieved by forward and inverse calculations using Advanced Model for Atmospheric TeraHertz Radiation Analaysis and SimUlation (AMATERASU) [Baron et al., 2008]. Nakagawa et al. (2016) showed the sensitivity of mid-IR heterodyne technique to the mesospheric wind and temperature in the altitude range of 75-90 km and 65-90 km, respectively.

In this study, we develop the retrieval method for mesospheric vertical profiles of wind and temperature from observations and estimate the accuracy and validity. The observations on 5th September 2015 using Mid-Infrared LAser Heterodyne Instruent (MILAHI) were derived wind and temperature profiles with 5 km of altitudinal step and sensitivities in the altitude of 80-95 km and 70-100 km, respectively. The temperature profile showed inversion region above 90 km and agree with one of sub-mm [Clancy et al., 2012] and SOIR loaded on Venus Express [Mahieux et al., 2012]. The wind profile show two maximum points equal to 70 m/s at line of sight at 77 and 87 km and divided wind directions into westward and eastward. The wind profiles in this altitude range were derived for the first time with remote sensing. The results are compared with in situ observations of Pioneer Venus probes and simulations for Venus atmosphere VGCM to validate this method. In addition, we apply this method to observation data set in 2011 and 2012 using heterodyne instruments developed by NASA and Cologne University to estimation for latitudinal and LT dependency. Furthermore, we can also compare with dynamic variations at the cloud obtained imaging observations in infrared and ultra violet (IR2 [Satoh et al., 2016], LIR [Fukuhara et al., 2011], UVI) and radio occultation [Imamura et al., 2011] load on Venus orbiter Akatsuki to discuss relation between lower atmospheric activities and mesospheric wind and temperature.

金星大気の大規模な特徴として、高度約 50-70km の厚い硫酸雲、そしてその雲頂付近におけるスーパーローテーションと呼ばれる速さ 100m/s 以上の東西風が挙げられる。一方、高度 110km 以上に位置する熱圏下層では、昼と夜の温度差によって生じる昼夜間対流が支配的である。両者に挟まれた高度 70-110km に位置する中間圏は、異なる惑星スケールの大規模風速場が遷移する高度域に当たる。下層大気から上昇してくる大気波動が砕破することによって大気に運動量が受け渡され、風速場や温度構造が大きく変化する複雑な領域である。中間圏・下部熱圏における温度場、そして特に風速場の直接観測は過去の観測例が限られており、これまで大気波動や背景場に与えるその効果を観測的に明らかにすることができなかった。

過去の観測例では、サブミリ波・中間赤外領域のヘテロダイン分光観測により、中間圏の風速と温度が報告している。例えばサブミリ波の観測から、高度 80-105km の温度・風速が導出されている [e.g., Clancy et al., 2008] が、この波長域の観測では、単一鏡を利用した場合に空間分解能が 10 秒角前後となり惑星ディスクを十分に空間分解できない。一方で、

中間赤外では、口径 60 cm の望遠鏡を利用して金星のディスクに対して 3 秒角 [Nakagawa et al., 2016] で観測が行える。この空間分解により、風速と温度の緯度変化をとらえることが可能であり、低緯度から高緯度間で温度は 240K から 150K [Sonnabend et al., 2010]、風速は 160m/s から 40m/s [Sornig et al., 2008] におよぶ大きな空間非一様性が存在することが確認されている。本研究では、中間赤外ヘテロダイン分光による中間圏の風速、温度鉛直分布の取得によって、その時空間変動とその要因について明らかにすることを目指す。

中間圏の風速、温度の鉛直分布は、波長 10um 帯の CO_2 吸収スペクトルを解析することで得られる。波長分解能 10^{6-7} を有する中間赤外ヘテロダイン分光器で吸収線を分解することにより、吸収線の圧力拡がり情報をもとに、気温・風速の鉛直分布を導出することが可能である [Stangier et al., 2015; Nakagawa et al., 2016]。放射伝達および反転解析モデルには、Advanced Model for Atmospheric TeraHertz Radiation Analaysis and SimUlation (AMATERASU) [Baron et al., 2008] を利用する。Nakagawa et al. (2016) では、同手法より風速が 75-90km、温度が 65-90km の高度範囲で求められることをモデルスペクトルを用いて検証した。

本研究では、実際に得られた金星観測データを用いて、中間圏の風速・温度鉛直分布の導出手法とその精度・妥当性の検証結果を報告する。マウイ島・ハレアカラ山頂の 60cm 望遠鏡に実装された東北大開発の赤外ヘテロダイン分光器 Mid-Infrared LAser Heterodyne Instrument (MILAHI) を用いて、2015 年 9 月 5 日に観測を行った。その結果、鉛直分解能 5km で風速・温度がそれぞれ高度 80-95km、70-100km に感度があることが確認された。温度分布では、高度 90km の上方で温度逆転層がみられ、サブミリ波観測 [Clancy et al., 2012] や Venus Express に搭載の SOIR の結果 [Mahieux et al., 2012] と一致する。風速鉛直分布では、高度 77km と 87km 付近でそれぞれ西向き、東向きに視線方向 70m/s の風が流れていると推定した。この高度領域の風速についてリモートセンシングによる鉛直分布の導出はこれが初となり、パイオニアビーナスプローブのその場観測結果や金星大気 VGCM 結果との比較によって、その妥当性を議論する。本研究では、2011、2012 年に NASA・ドイツで開発された同ヘテロダイン装置で取得された金星観測データにも我々のリトリーバル手法を適用し鉛直分布を求め、時空間変動について検証を行う。また、金星探査機あかつき搭載の赤外・紫外撮像観測（IR2[Satoh et al., 2016]、LIR[Fukuhara et al., 2011]、UVI）や電波掩蔽 [Imamura et al., 2011] によって得られる金星雲層の大気変動と比較することによって、中間圏風速・温度の時空間変動と下層大気活動との関係性を明らかにしていく。

Optical ground-based observation of Venusian lightning in 2015

Masataka Imai[1]; Yukihiro Takahashi[1]; Mitsuteru SATO[2]
[1] Cosmosciences, Hokkaido Univ.; [2] Hokkaido Univ.

Lightning is one of the fundamental atmospheric phenomena and it was produced by strong convective clouds on the Earth. We have known that lightning also exists on the giant planets such as Jupiter and Saturn, and these planets are well known having intense atmospheric convection. Besides with their impacts on chemical reaction, lightning can be an important implications for the atmospheric dynamics.

On Venus, lightning explorations were started in 1970s from several spacecraft such as Venera series and Pioneer Venus Orbiter [e.g. Ksanfomaliti et al., 1979; Taylor et al., 1979], and also previous ground-based observations challenged to detect the lightning flash [e.g. Hansell et al., 1995]. It has been known that this planet has severe environment with high pressure and temperature and fast zonal atmospheric winds named Superrotation. Recently, Japanese Venus exploration AKATUSKI and one of its camera IR2 firstly success to reveal the strong convective cloud formation in the middle layer of Venus. However, Venusian lightning activity has been a mystery over a half century, and we still do not get over the ambiguity of evidential measurements of previous studies.

In these surroundings, a new type of lightning detector, LAC (Lightning and Airglow Camera) onboard AKATSUKI [Takahashi et al., 2008] are ready to start its lightning exploration. We expect that LAC success to detect the lightning flash, and we began to support the LAC observation from ground. 1.6-m optical telescope named Pirka was operated to observe night side of Venus on July, 2015 around the season of inferior conjunction. Using the liquid crystal tunable filter (LCTF: FWHM ˜10 nm) and 777.4 nm strong emission line wavelength, which laboratory experiments suggest, total ˜2 hours sequent images were obtained. Exposure time of each image is 0.035 s and after biasing (subtracting) with the two previous and the two following images are investigated. Considering the point spread function and point fluctuation caused by seeing effect, 3x3 and 5x5 pixels window was adopted to search the strong emission region on Venus night side disk.

As a results, we did not success to find the significant emission region larger than 3 times of background noise standard deviation. Our detection limit is an order of 10^7 J at observation wavelength and it is two or three times better than [Hansel et al., 1995]. Previous observations detected six or seven 10^8–10^9 J magnitude lightning flushes in ˜3 hours, therefore our result shows negative possibility of the existence of lightning. However, it can be considered that the convective activity on Venus has strong temporal variation, and final conclusion will be provided from the LAC observations.

あかつき・Venus Express継続観測から明らかにする高高度金星雲

高木 聖子 [1]; MAHIEUX Arnaud[2]; WILQUET Valerie[2]; ROBERT Severine[2]; DRUMMOND Racheal[2]; VANDAELE Ann Carine[2]; 岩上 直幹 [3]
[1] 東海大、TRIC; [2] BISA; [3] なし

High altitude Venus cloud structure observed by SOIR/Venus Express and AKATSUKI

Seiko Takagi[1]; Arnaud MAHIEUX[2]; Valerie WILQUET[2]; Severine ROBERT[2]; Racheal DRUMMOND[2]; Ann Carine VANDAELE[2]; Naomoto Iwagami[3]
[1] Tokai Univ. TRIC; [2] BISA; [3] none

The Venus cloud consists of a main cloud deck at 47-70 km, with thinner hazes above and below. The upper haze on Venus lies above the main cloud surrounding the planet, ranging from the top of the cloud (70 km) up to as high as 90 km.

The Solar Occultation in the InfraRed (SOIR) instrument onboard Venus Express (ESA) was designed to measure the Venusian atmospheric transmission at high altitudes (65-165 km) in the infrared (2.2-4.3 um) with high spectral resolution. We investigated the optical properties of the Venus haze above 90 km using the SOIR solar occultation observations. Vertical and latitudinal profiles of extinction, optical thickness, and mixing ratios of haze were retrieved. We find that haze extinction and optical thickness at low latitudes are two times higher than those at high latitudes. One of the noticeable results is that haze mixing ratio increases with altitude above 90 km at high and low latitudes. Therefore we speculate that haze could be produced at such high altitudes.

On December 7, 2015, AKATSUKI (JAXA) arrived at Venus after orbit insertion. Some instruments onboard AKATSUKI will observe characteristics of cloud and haze particles. In this presentation, we will report high altitude Venus cloud structure obtained from SOIR/Venus Express and AKATUSKI limb observation and also report a study plan to elucidate Venus cloud including haze layer creation and maintain process.

金星を一様に覆う雲の大局的な振る舞いを高時間・高分解能で捉えることができるのは、周回軌道からの継続観測のみである。過去の金星観測により、主成分濃硫酸の雲層 (45-70 km) の上にもや層 (70-90 km) が重なる金星雲が確認されている。しかしその知見は観測不足故に断片的であり、金星雲の描像の理解は停滞している。

Venus Express(ESA) に搭載された赤外分光計 Solar Occultation at InfraRed (SOIR, 2.3-4.2 um) は、太陽掩蔽法により高高度 (65-165 km) の金星大気・雲を 2006 年より継続観測した。本研究では SOIR のデータ解析により、もや層の新たな知見のほか、90 km 以上の「上部もや層」の存在やその知見を初めて観測から統計的に明らかにした。しかし、Venus Express は低緯度・夕方における観測が少ない。そのため、これまでの本研究で、高高度に存在するもやの緯度・ローカルタイム依存性が見受けられるものの決定的とは言い切れない。また、もやが 2006 年から数年かけて徐々に増加する Braak et al.(2002) とは逆の傾向を確認しているが、低緯度観測・解析期間不足により、全球的・長期的な連続する高高度におけるもやの時間変動は得られていない。長年謎の金星雲生成・維持メカニズムの解明を将来目標に、全球的かつ長期的な高高度に存在するもやの振る舞いを明らかにするためには、不足部分を補う観測が必要である。

2015 年 12 月 7 日、あかつきは赤道周回軌道に投入され、以降数年にわたり継続観測を実施する。あかつきは複数波長を用いて低緯度及び様々なローカルタイムにおける観測を豊富に行い、Venus Express に対する相補的役割を果たす。今後、あかつき・Venus Express の両観測を扱うことで、全球的かつ長期的な高高度に存在するもやの振る舞いを明らかにすることができる。本発表では、あかつきリム観測の初期解析を含むこれまでの研究成果及び研究計画を報告する。

Venus Express/VMCの可視・紫外画像解析による金星雲頂の模様と風速場の関係

奈良 佑亮 [1]; 今村 剛 [2]; 村上 真也 [3]
[1] 東大・理・地惑; [2] 東京大学; [3] 宇宙研

Relationship between wind field and cloud top features of Venus revealed by visible and ultraviolet images obtained by VMC

Yusuke Nara[1]; Takeshi Imamura[2]; Shin-ya Murakami[3]
[1] EPS, Univ. of Tokyo; [2] The University of Tokyo; [3] ISAS/JAXA

In the study of material cycle related to cloud generation and spatial distribution of albedo on Venus, it is important to consider contribution of three-dimensional motion in the cloud layer and transportation of sunlight absorber accompanied by the motion, because most of the sunlight is absorbed in the cloud layer. By using ultraviolet images which reflect unidentified absorber, Venusian cloud motion is well studied but, to understand vertical motion caused by solar heating as well as horizontal motion, the study of multiple altitudes taken by multiple wavelengths is necessary. Hueso et al. (2015) derived the three-dimensional motion of Venusian cloud from images of several wavelengths taken by VIRTIS on Venus Express although they did not associate the cloud motion with morphology and did not investigate daily variation of it. Moreover, equatorial region is not included in that study due to constraint of the equipment.

In this study, by using ultraviolet and visible images obtained by VMC on Venus Express, we tried to extract the three-dimensional motion of Venusian cloud and compare them with the cloud morphology. The ultraviolet images reflect distribution of unidentified absorber at an altitude of about 70 km and the visible images reflect thickness of cloud at an altitude of 60 km. So far, because there are few studies used visible images, we lack the knowledge about them obtained by VMC. To improve the reliability of estimation of wind fields, we corrected distortion of the images and removed streaky noise fixed to the detector.

We discuss the relationship between the cloud motion observed by the two wavelengths and morphology, the variation of albedo and the vertical motion caused by solar heating.

金星の雲形成やアルベドの分布に関わる物質循環を理解するためには、雲層内の3次元的な運動やそれに伴う太陽光吸収物質の輸送を把握することが重要である。金星昼面においては、これまで未同定太陽光吸収物質の空間分布を捉える紫外波長での画像が雲の運動の研究に用いられてきたが、太陽光により加熱された大気によって引き起こされる物質循環を理解するためには、複数波長での撮像による複数高度の情報と、雲そのものの空間分布の情報が必要である。Hueso et al. (2015) は欧州の金星探査機 Venus Express に搭載されてた分光撮像装置 VIRTIS の観測結果を用いて複数高度の大気の運動を求めているが、雲の形態との関連付けはされておらず、風速場の日々の変化は調べられていない。また、観測機器の制約から赤道域の風速場については調べられていない。

そこで本研究では、Venus Express に搭載されていた撮像装置 VMC により得られた、高度約 70km の雲頂の吸収物質の分布を反映している紫外画像に加え、低コントラストながら模様が存在する、雲頂より低い高度約 60km の雲そのものの厚さを反映している可視画像を用いて金星の雲の3次元的な運動を、風速場を導出することで捉えることを試みた。これまで紫外画像を用いた研究は数多くあるが、可視画像を用いた研究は少なく、VMC の可視画像に関する知見がほぼ無いため、検出器の歪曲収差の補正や検出器に固定されたノイズの除去をおこない、風速場推定の確度を向上させた。

2波長で求めた雲の移動ベクトルと雲の形態を比較することで、アルベドの分布や、過熱された大気により引き起こされる上下の物質循環について議論する。

Venus Express搭載VIRTISの画像データを用いた金星夜面の雲移動ベクトルと雲分布の関係

小美野 将之 [1]; 中村 正人 [2]; 今村 剛 [3]
[1] 東大・理・地惑; [2] 宇宙研; [3] 東京大学

Relationship between the cloud distribution and cloud-tracked winds on Venus night-side obtained from images taken by VIRTIS

Masayuki Omino[1]; Masato Nakamura[2]; Takeshi Imamura[3]
[1] EPS, Univ. of Tokyo; [2] ISAS; [3] The University of Tokyo

Venus is covered by a thick layer of clouds, and the contribution of various atmospheric motions such as small-scale turbulent flows, convection in the cloud layer, planetary scale waves, the meridional circulation, etc. is imagined on the generation and maintenance of those clouds but the mechanism of them are unexplained yet. Investigating the relationship between the cloud distribution and the wind velocity field is important to deepen our understanding for the mechanism of the cloud generation and of the atmospheric circulation, but enough studies are not done yet.

In this study, we are investigating the relationship between the cloud distribution and the distribution of the wind velocity by tracking the clouds using the images of VIRTIS on board Venus Express. Specifically, we are investigating the atmospheric motion of Venus night-side by using 1.74 micrometer images which is a wavelength known as the 'atmospheric window'. The cloud distribution is visualized by the thermal radiation from the substratum atmosphere in near infrared night-side images. Using a pair of such images which is temporally continuous, the wind velocity is derived by extracting the part where the cloud feature is identical by calculating phase correlation between the first image and the second image and by dividing its moving distance by time interval of two images.

金星はその全球が分厚い硫酸の雲で覆われており、それらの雲の生成や維持の上では、小規模な乱流、雲層内の対流、惑星スケールの波動、子午面循環など様々な大気運動の寄与が想像されるがそのメカニズムは未だ解明されていない。このような雲の生成や大気循環のメカニズムに対する理解を深める上で、金星大気における雲構造とその周辺における風速場を解明することが重要であるが未だ不十分である。

本研究では、欧州の金星探査機 Venus Express に搭載されていた可視近赤外分光撮像装置 VIRTIS の分光画像データを用いて雲追跡を行うことにより金星大気における雲の分布と風速の分布の関連性について調べている。具体的には、金星の分厚い雲を通って出てくる「大気の窓」と呼ばれる波長である 1.74 μ m の画像データを用いることで、金星夜面における大気運動について調べている。近赤外夜面画像では下層大気からの熱放射を光源として雲量の分布が可視化される。時間的に連続したこのような画像を用いて、1 枚目と 2 枚目の画像間で位相相関を計算することにより画像間で濃淡の特徴が一致している部分を抽出し、その移動量を二枚の画像の時間間隔で割ることにより風速を導出する。

AKATSUKI IR1 camera status

Naomoto Iwagami[1]
[1] none

Availabilities of main products are summarized. They are (1) dayside images for dynamics by cloud tracking, (2) nightside images for deducing H2O abundance and surface characteristics by differencial spectroscopy and (3) nightside images for questing active volcanos.

金星周回軌道における「あかつき」初期科学成果の概要

佐藤 毅彦 [1]; 中村 正人 [2]; 今村 剛 [3]; 山崎 敦 [4]; 鈴木 睦 [5]; 上野 宗孝 [6]; 山田 学 [7]; 福原 哲哉 [8]; 小郷原 一智 [7]; 大月 祥子 [9]; 村上 真也 [10]; 佐藤 隆雄 [10]; 渡部 重十 [11]; 岩上 直幹 [12]; 田口 真 [13]; 高橋 幸弘 [11]; はしもとじょーじ [14]; 堀之内 武 [15]; 高木 征弘 [16]; 神山 徹 [17]
[1] 宇宙研; [2] 宇宙研; [3] 東京大学; [4] JAXA・宇宙研; [5] JAXA・宇宙研; [6] 宇宙科学研究所; [7] 宇宙研; [8] 立教大・理; [9] 専修大; [10] 宇宙研; [11] 北大・理・宇宙; [12] なし; [13] 立教大・理・物理; [14] 岡大・自然; [15] 北大・地球環境; [16] 京産大・理; [17] 産総研

Overview of initial scientific results of Akatsuki in Venus orbit

Takehiko Satoh[1]; Masato Nakamura[2]; Takeshi Imamura[3]; Atsushi Yamazaki[4]; Makoto Suzuki[5]; Munetaka Ueno[6]; Manabu Yamada[7]; Tetsuya Fukuhara[8]; Kazunori Ogohara[7]; Shoko Ohtsuki[9]; Shin-ya Murakami[10]; Takao M. Sato[10]; Shigeto Watanabe[11]; Naomoto Iwagami[12]; Makoto Taguchi[13]; Yukihiro Takahashi[11]; George Hashimoto[14]; Takeshi Horinouchi[15]; Masahiro Takagi[16]; Toru Kouyama[17]
[1] ISAS, JAXA; [2] ISAS; [3] The University of Tokyo; [4] ISAS/JAXA; [5] ISAS, JAXA; [6] ISAS, JAXA; [7] JAXA/ISAS; [8] Rikkyo Univ.; [9] Senshu Univ.; [10] ISAS/JAXA; [11] Cosmosciences, Hokkaido Univ.; [12] none; [13] Rikkyo Univ.; [14] Okayama Univ.; [15] Hokkaido University; [16] Faculty of Science, Kyoto Sangyo University
; [17] AIST

The 4 cameras (UVI, IR1, IR2, and LIR) onboard Akatsuki successfully obtained the first-light Venus images after the spacecraft was inserted to an elliptical orbit around Venus on 7 December 2015. After the first light, observations were paused due to the orbit correction maneuver, initial tests of spacecraft bus, and evaluation of thermal environment. The observations resumed in mid-January 2016. By examining acquired images for sensitivity and resolution, it is confirmed that the 4 cameras function as expected and the project has decided to start regular observations in April 2016. Operation of LAC is in progress because it can only be switched on while the spacecraft is in eclipse AND the sensor requires high voltage. As of this writing, the voltage nears its nominal and we expect to start observations with LAC during the eclipses in 4Q of 2016. Radio occultation measurements using USO are being done whenever the geometry of spacecraft-Venus-Earth is favorable.

The Akatsuki mission is to investigate the structure and dynamics of Venus atmosphere in 3D by combining the data from multiple instruments. The data will be reviewed and obtained 3D pictures of Venus atmosphere will be discussed.

「あかつき」搭載の4カメラ（UVI, IR1, IR2, LIR）は、2015年12月7日の周回軌道投入直後の数日間にファーストライト画像の取得に成功した。その後しばらく、周回軌道の修正、姿勢制御を含むバス系の点検、そして熱環境の確認が続き、2016年1月中旬から試験観測を再開した。画像データを通じて感度・解像度が期待通りであることが確認できた4カメラは、2016年4月から定常観測に移行した。それ以来、順調にデータを蓄積している。日陰通過時にしか装置をオンできずしかも高電圧を要するLACについてはまだ立ち上げが続いているが、所定の高電圧まであと一歩のところに来ており、2016年第4四半期の日陰通過時には本観測を行える見込みである。USOを用いた電波掩蔽観測もその観測機会毎に良好なデータ取得を行っている。

「あかつき」の特徴は、複数の機器からのデータを組合わせて、金星大気の構造と運動を三次元的に明らかにすることにある。これまでのデータを概観し、そしてどのような三次元的描像が得られてきたかを紹介する。

あかつきIR2による金星夜面強化観測

佐藤 隆雄 [1]; 佐藤 毅彦 [2]; 中村 正人 [3]; 上野 宗孝 [4]; 鈴木 睦 [5]; はしもと じょーじ [6]; 榎本 孝之 [7]; 高見 康介 [8]; 中川 広務 [8]; 笠羽 康正 [9]
[1] 宇宙研; [2] 宇宙研; [3] 宇宙研; [4] 宇宙科学研究所; [5] JAXA・宇宙研; [6] 岡大・自然; [7] 総研大・物理・宇宙; [8] 東北大・理・地球物理; [9] 東北大・理

Initial report of an improved nightside observation by Akatsuki IR2

Takao M. Sato[1]; Takehiko Satoh[2]; Masato Nakamura[3]; Munetaka Ueno[4]; Makoto Suzuki[5]; George Hashimoto[6]; Takayuki Enomoto[7]; Kosuke Takami[8]; Hiromu Nakagawa[8]; Yasumasa Kasaba[9]
[1] ISAS/JAXA; [2] ISAS, JAXA; [3] ISAS; [4] ISAS, JAXA; [5] ISAS, JAXA; [6] Okayama Univ.; [7] Space and Astr., SOKENDAI; [8] Geophysics, Tohoku Univ.; [9] Tohoku Univ.

The 2-micron camera named IR2 onboard Akatsuki has continuously observed the nightside of Venus with three narrow-band filters (1.735, 2.260, and 2.320 micron) since the late of March, 2016. The main roles of nightside observation by IR2 are (i) to study the dynamics in the lower atmosphere with the cloud-tracked winds, (ii) to deduce CO distribution which is thought to be a good tracer of the atmospheric circulation, and (iii) to investigate aerosol properties of the lower clouds.

Although the nightside images collected until the middle of May, 2016 show the quality enough to be used for deriving the cloud-tracked winds, they are not good enough to be used for conducting studies requiring photometric accuracy. This is due to the contamination by the stray light from the dayside of Venus and the unwanted artifacts which arise electrically when the significantly bright target is read out. To evaluate how the stay light from the dayside contaminates nightside data, 2.020-micron observation was added to the nightside observation. Non negligible count of nightside at 2.020 micron can be regarded as the stray light from the dayside because thermal radiation at this wavelength cannot escape to space due to CO_2 absorption. To reduce the unwanted artifacts, the observation scheme was changed so that the dayside of Venus is out of the detector. This improved observation scheme has been executed since the end of June, 2016.

In this presentation, we will present the initial report of this improved nightside observation.

鉛直1次元モデルを用いた金星の雲形成の研究

下川 真弘 [1]; 今村 剛 [2]; 杉山 耕一朗 [3]; 中村 正人 [4]
[1] 東大・地惑・宇宙研; [2] 東京大学; [3] 松江高専; [4] 宇宙研

One-dimensional modeling of Venusian clouds

Masahiro Shimokawa[1]; Takeshi Imamura[2]; Ko-ichiro Sugiyama[3]; Masato Nakamura[4]
[1] Earth and Planetary Science, UTokyo / ISAS; [2] The University of Tokyo; [3] Matsue College of Technology; [4] ISAS

Venusian clouds, mainly consisting of sulfuric acid, lies on 45-70 km altitude and highly influence on climate of Venus because of high albedo. Besides, zonal wind velocity from super-rotation peaks near 70 km altitude, and thermal tidal waves, caused at cloud layer where sunlight is absorbed, propagate momentum of atmosphere. Thus it is important to know how Venus cloud formation occurs and what physical processes the thickness of clouds are adjusted, for understanding the dynamics of Venusian atmosphere. We have calculated one-dimensional modeling of Venus clouds considering photolysis of sulfuric acid and studied the process of Venus cloud formation.

In this study we watched vertical distribution of liquid cloud components of sulfuric acid and water at 40-75 km altitude, for calculating time development of number density of each sulfuric acid and water in liquid and gas phase. Partitioning of these phases is judged at every time step of calculation, although supersaturation and energy balance with vaporizing and condensation are not considered, and supersaturated gas materials are just regarded as liquid. Physical factors affecting each total number density we considered are liquid sedimentation due to gravity, eddy diffusion and atmospheric chemistry at upper clouds. Sedimentation occurs in liquid components regarded as droplets which have constant radius, and we calculate the downward transportation of those droplets by gravity. The radius of droplets are determined from observation. Eddy diffusion expresses totally on transportations of thermal convection, turbulence and large-scale atmospheric movement, calculated by given constant coefficient. In atmospheric chemistry we consider a photochemical reaction near 62 km altitude with production of sulfuric acid and consumption of water (Yung and DeMote, 1982 / Krasnopolsky and Parshey, 1981). We can also calculate the effect of meridional circulation, which vertically becomes upward wind at tropical region and downward wind at high latitude.

For initial conditions, volume mixing ratio of each material is homogeneous at every altitude except at lower boundary. Thus we watched the behavior of cloud formation with or without effects of respective physical factors. At upper boundary the gradients of volume mixing ratio are zero, and at lower boundary that ratio is given by radio occultations for sulfuric acid, and ground observations for water (Knollenberg and Hunten, 1980). Results of liquid distributions are compared to calculations by Imamura and Hashimoto, 1998 and observation results, and checked if and how each physical factor influences on cloud formation. Moreover, time scales of diffusion and vertical wind are expressed as $L*L/K$, L/w, respectively, where L is a scale of length, K is the diffusion coefficient and w is the velocity of vertical wind, respectively. Therefore we compared these time scales with varying K and w, and estimated how atmospheric dynamics such as convection and meridional circulation affect cloud formation.

We are going to do further studies of each physical factor to contribute to cloud structure by considering latitudinal effects such as meridional circulation and chemical production with two-dimentional modeling. Results of this study will make use of interpretations of observed data by Akatsuki and contribute to atmospheric chemistry and dynamics of Venus.

硫酸を主成分とする金星雲は高度 45~70 km に存在し、高アルベドであることから金星気候に大きく影響を与える。また高度 70 km 付近においてスーパーローテーションによる東西方向の風速がピークを持つ上、太陽光を吸収した雲層で励起される熱潮汐波が大気の運動量伝播を担っていることから、金星の雲形成や、雲の厚さがどのような物理過程により調節されているかを知ることは金星の大気力学を理解する上でも重要である。我々は硫酸の光生成化学を考慮した鉛直 1 次元における雲形成モデルを計算し、金星雲の形成過程に関する研究を行った。

本研究では高度 40~75 km における硫酸および水の数密度の時間発展を液相と気相それぞれについて高度ごとに計算し、液相である雲成分の高度分布を観察した。計算の時間ステップごとに各物質の総量から液相と気相への分配を行っているが、蒸発および凝縮に伴う過飽和やエネルギー収支は考慮せず、硫酸と水の混合により定まる各物質の飽和蒸気圧を超えた分の気相をそのまま液相として扱っている。数密度を変化させる物理的要素については、液相の重力沈降、渦拡散、雲層上部での大気化学を想定した。重力沈降では液相を一定粒径の雨粒と仮定し、その雨粒に作用する重力による鉛直下向きの輸送を計算している。雨粒の粒径は観測結果をもとに与えた。渦拡散では熱対流や乱流、大規模な大気運動に伴う輸送を総じて表現し、全高度で一定の拡散係数を与えて計算を行っている。大気化学の項では高度 62 km 付近で硫酸の生成と水の消滅を伴う光化学反応を仮定し、計算している (Yung and DeMote, 1982 / Krasnopolsky and Parshey, 1981, 1983) 。また、特定の緯度を設定して計算を行う際に子午面循環を考え、鉛直風として赤道域での上昇流や高緯度での下降流の効果を取り入れることも可能である。

初期状態としては、各物質の大気に対する体積混合比が下端を除く全高度で一様になるように与え、上記の各物理的要素を考慮した場合と除いた場合についてそれぞれ雲形成の様子を観察した。上端では混合比の勾配をゼロとし、下端では 電波掩蔽観測による硫酸蒸気や地上観測による水蒸気の観測結果を境界条件として用いている (Knollenberg and Hunten, 1980) 。得られた液相分布は Imamura and Hashimoto, 1998 による計算結果や観測結果と比較することで、要素ごとに雲形成への影響の可否や程度を調べた。

また渦拡散係数を K, 鉛直風速を w とすると、鉛直スケール L に対する拡散及び鉛直風の時間スケールはそれぞれ

L∗L/K, L/w と表されることから、 K や w を変化させた際の時間スケールについて比較し、対流や子午面循環などの大気力学作用が雲形成をどう変化させるのかを推量するに至った。

今後は現在の鉛直 1 次元構造に加え、緯度方向による子午面循環や大気化学の影響を考慮した 2 次元構造へと拡張し、各物理的要素の雲構造への寄与を詳細に研究する予定である。研究の成果は JAXA により運用されている金星探査機「あかつき」による観測結果を解釈する上で有用であり、大気化学や大気力学への貢献が期待される。

Simulation of the ancient Martian climate with denser pure CO2 atmosphere using a general circulation model, DRAMATIC MGCM

Arihiro Kamada[1]; Yasumasa Kasaba[2]; Naoki Terada[3]; Takeshi Kuroda[4]
[1] Geophysics, Tohoku Univ.; [2] Tohoku Univ.; [3] Dept. Geophys., Grad. Sch. Sci., Tohoku Univ.; [4] NICT

The fluid traces on the Martian surface are thought to be made before ˜3 billion years ago. If they were made by the liquid H_2O, the environment of the ancient Mars should be suitable for huge amount of liquid water, under higher temperature of larger atmospheric pressure than today. Several modeling studies have been performed to investigate this possibility. The solar insolation at that time is thought to be ˜75% of today from a standard stellar evolution model. In this condition, the study by a Martian General Circulation Model (MGCM) assuming the pure CO_2 atmosphere could not reproduce the surface temperature higher than 273K with surface pressure in 0.1-7bars [Forget et al., 2013, hereafter F13), which is so-called the 'Early faint Sun paradox'. On the other hand, according to the study of Graedel et al. [1991], early solar mass was possibly heavier, and, then, the luminosity was possibly higher than expected (100˜150% of the present value). It may work to make the temperature of the early Martian environment above the H_2O melting point. From this viewpoint, we are starting to reproduce dependence of the ancient Martian environment on the solar luminosity between 75% and 150% of the present value using our MGCM, DRAMATIC [e.g., Kuroda et al., 2005]. It can also provide the threshold conditions between 'frozen' and 'liquid' conditions of Martian-like planets with pure CO_2 atmospheres.

At first, in order to check the validity of our model, we simulated the possible climate on early Mars with 75% of today's solar luminosity under the pure CO_2 atmosphere with globally-averaged surface pressure of 0.1-2bars(realistic pressure range of early Mars). The obliquity, eccentricity, surface albedo and thermal inertia are set to be the same as F13 for the comparison with this result. Our model has the vertical 49 layers with the model top of ˜90 km height (2-3 km of layer thickness in most altitude range), while F13 has 15 vertical layers and the model top of ˜50 km height (detailed layer thicknesses are not shown in F13). This difference enables our model to emulate CO_2 ice clouds up to the upper level where thick CO_2 ice clouds (30˜40km thickness) are formed globally. The radiative effects of CO_2 ice on the surface are also considered in solar and infrared wavelengths, although the radiative effects of dust are not considered.

In the results of our simulations, the global mean surface temperature increased with pressure. The thickness and distribution of CO_2 ice clouds was sensitive to the definition of super-saturation, and optical thickness of CO_2 ice clouds becomes globally ˜30% thicker in the no super-saturation case than in the 35% super-saturation case, but much thinner than that of F13, and the distribution of CO_2 ice clouds does not change very much in both cases. The radiative effects of CO_2 ice clouds affect to increase the global-mean temperature for several K in maximum, while ˜10 K in F13, due to the difference of the layer thickness in the models. In low and mid-latitudes where many fluid tracers are left, the temperature changes seasonally between 220 and 250 K at surface pressure above 0.5bar. Our result is consistent with F13 that the ancient climate could not keep the temperature above 273K with the solar luminosity of 75% of today.

Next, we started to simulate the solar luminosity above 100% of the present value with the surface pressure between 0.5 to 2 bars. In the case of surface pressure with 0.5 bars, annual mean surface temperatures greatly increase with solar luminosity and overcome 273K with the solar luminosity of between 125% and 150% (54% - 64% of the Earth's solar intensity). Moreover, high temperature area is distributed in mid-low latitudes, where valley networks are mostly discovered. Hereafter, we are starting to investigate in the cases of surface pressure of 1.0 bar and 2.0bar and detailed threshold of solar intensity of overcoming the H_2O melting point.

表面構造の測色観測による木星大気ダイナミクスの研究

岩崎 和人 [1]; 鈴木 秀彦 [2]; 田部 一志 [3]; 弘田 澄人 [4]
[1] 明治大; [2] 明治大; [3] 月惑星研究会; [4] かわさき宙と緑の科学館

Study on dynamics of Jovian atmosphere by a colorimetric observation of surface structures

Kazuto Iwasaki[1]; Hidehiko Suzuki[2]; Isshi Tabe[3]; Sumito Hirota[4]
[1] Meiji Univ.; [2] Meiji univ.; [3] ALPO-Japan; [4] Kawasaki municipal science museum

Stripe patterns called belts or zones with various colors persist on Jovian surface. Anticyclonic vortices called an oval with various scales and colors are maintained and drifted in the boundary between zones and belts. Some ovals have different colors despite they are formed simultaneously in same latitude region. Color changes of ovals after an interaction with other ovals were also reported. Such results suggest a strong relationship between dynamics of Jovian atmosphere and colors of local structures. However, detailed mechanisms for such color variations are still unknown. Recently, it is suggested that the color of Jovian surface structures are determined by the mixing ratio of two chromophores [Ordonez-Etxeberria et al., Icarus, 2015]. In this study, colors of remarkable Jovian structures like the great red spot (GRS), bands, and zones are focused on as a tracer of the Jovian atmospheric dynamics. It is essential to monitor the Jovian surface continuously to quantify color variations with various temporal scales. However, it is difficult to make a continuous monitoring of Jupiter with large telescopes due to limited machine time. Instead, large amounts of image data reported by amateur astronomers in the world have potential to achieve the continuous monitoring by combining them (e.g. Archive by Association of Lunar and Planetary Observers in Japan: http://alpo-j.asahikawa-med.ac.jp/). However, quantitative color comparison between color images acquired by different optics and sensors are principally difficult. It is necessary to have standard spectra to correct a white balance of these color images. Thus, a portable device which can observe visible spectra of Jovian surface with resolving spatial structures was developed [Iwasaki et al, JPGU, 2016]. On a night of Dec 15 2015 and two nights of May 2016, spectroscopic observations of Jovian surface using the device and a 40cm diameter telescope in Kawasaki municipal science museum have been conducted. By these observations, it was confirmed that apparent variations in the Jovian color due to the absorption caused by earth's atmosphere were not negligible. To make a correction to observed spectra, a simultaneous observation of spectrum of a standard star (whose absolute spectrum is known) is required. In this talk, a method to remove effects of terrestrial absorptions from observed data by using spectrum of a standard star and its verification are presented.

木星表面には緯度毎に縞 (Belt)、帯 (Zone) と呼ばれる特徴的な縞模様が複数存在し、その境界にはオーバルと呼ばれる大小様々なスケールの渦が維持生成されている。オーバルの中には同時期・同緯度で発生したにも関わらず白色や赤褐色といった異なる色を持つものや、オーバル同士の相互作用の結果、みかけの色が変化するものも観測されている。各種構造の色の違いや変動は雲頂高度の違いや、雲に含まれる元素成分の違いなどに起因するなどと言われているが、詳しいメカニズムは未解明である。さらに最近では、色度図を用いた解析手法により木星表面の色は白色と橙色の２つの物質の混合で決まるといった報告もある [Ordonez-Etxeberria et al., Icarus, 2015]。そこで本研究では、スケールの長期変動やより小さい渦とのの相互作用によってその色の変化が報告されている大赤斑（GRS）や、色に経年変化がみられる縞・帯といった木星大気の特徴的な表面構造に着目し、表面構造における「色」の変化から惑星大気ダイナミクスの解明を目指す。刻一刻と激しく変動する木星表面構造の運動と色の変動を定量化するためには、継続的な木星表面の監視が不可欠である。大型望遠鏡を占有し木星の監視を連続的に行うことは限られたマシンタイムの観点から現実的ではないが、木星表面の精緻な構造を捉えたカラー画像に関しては、世界各地のアマチュア天文家によって報告されている膨大なデータを有効に活用できる可能性がある（例えば月惑星研究会のアーカイブ：http://alpo-j.asahikawa-med.ac.jp/）。これらの画像は、異なる光学系とイメージセンサーによって撮像された上に、画像の処理系の違いも加わり色彩の定量的な相互比較は一般的には困難である。しかし、カラー画像のホワイトバランスを統一調整するための参照スペクトルが同時に存在すれば、世界各地で得られたカラー画像の色彩を直接比較可能な状態に補正することが可能になると考えられる。そこで、本研究では木星の表面構造の任意の部分をピンポイントで分光観測可能な可搬型の分光ユニットを開発した [Iwasaki 他, JPGU,2016]。これまでに、かわさき宙と緑の科学館の所有する口径 40cm の反射望遠鏡と本装置を組み合わせ、2015 年 12 月および 2016 年 5 月の 2 晩において木星表面構造の分光観測を実施した。これらの観測によって、地球大気の吸収による色度の変化が宇宙空間で測定された木星表面の各種模様間の色差（色度図上での距離）に比べて無視できない程の変動を与えることが確認された。地球大気による色度の変動は観測地域における大気の透明度に依存するため、これを精密に補正するためには、観測晩毎に絶対スペクトルもしくは反射スペクトルが既知の惑星の参照スペクトルを同時に撮像し、大気吸収による影響を評価する必要がある。本発表では、地球大気の吸収による色度の変化を正確に補正し宇宙空間におけるスペクトルに換算する手法について検討・検証した結果について報告する。

Increase of hot ion fraction on Io plasma torus after an outburst in 2015

Masato Kagitani[1]; Fuminori Tsuchiya[2]; Mizuki Yoneda[3]; Tomoki Kimura[4]; Kazuo Yoshioka[5]; Go Murakami[6]; Chihiro Tao[7]; Takeshi Sakanoi[8]; Yamazaki Atsushi Hisaki (SPRINT-A) project team[9]
[1] PPARC, Tohoku Univ; [2] Planet. Plasma Atmos. Res. Cent., Tohoku Univ.; [3] none; [4] RIKEN; [5] The Univ. of Tokyo; [6] ISAS/JAXA; [7] NICT; [8] Grad. School of Science, Tohoku Univ.; [9] -

Volcanic gases (mainly composed of SO_2, SO and S) originated from jovian satellite Io are ionized by interaction with magnetosphere plasma and then form a donut-shaped region called Io plasma torus. Ion pickup is the most significant energy source on the plasma torus thought, additional energy source by hot electron is needed to explain energy balance on the neutral cloud theory (Daleamere and Bagenal 2003). In fact, in-site measurements by Galileo indicates some injections of energetic particles in the middle magnetosphere. Recent EUV spectroscopy from the space shows fraction of hot electron increases as increase of radial distance in the plasma torus (Yoshioka et al. 2014 and Steffl et al. 2004). On this study, we focus on variability of hot electron fraction derived from EUV diagnostics measured by HISAKI/EXCEED after a volcanic outburst in 2015.

We have made spectral fitting as the following method. First, we made series of EUV spectra averaged over 3 days during January through May 2015. Next, assuming azimuthal homogeneity of Io plasma torus, onion-peeling is conducted to reduce line-of-sight integration effect. Then, we made fitting of observed EUV spectra (60 - 140 nm) with CHIANTI model spectra by changing electron density and temperature, mixing ratio of ions (S^+, S^{++}, S^{+++}, O^+ and O^{++}) and fraction of hot electron (Te = 100 eV).

Based on observation of neutral sodium and oxygen (Yoneda et al., 2015), neutral densities started to increase at around DOY = 10, were at maximum at around DOY = 50, and have backed into the initial levels at around DOY = 120. In contrast, plasma diagnostics indicates that hot electron fraction at 7.0 jovian radii was less than 2 % before DOY = 50, started to increase after DOY = 50, and have reached 8(+/-1) % at DOY = 110. EUV emission from aurora was also activated after DOY = 50 as increase of hot electron fraction on the plasma torus. The results suggest that the inward transportation of hot electron was activated after increased of neutral supply on the plasma torus caused by the outburst.

ひさき衛星極端紫外光観測と地上可視光観測による木星衛星イオの硫黄イオントーラスの時空間変動

宍戸 美日 [1]; 坂野井 健 [2]; 鍵谷 将人 [3]; 土屋 史紀 [4]; 吉川 一朗 [5]; 山崎 敦 [6]; 吉岡 和夫 [7]; 村上 豪 [8]; 木村 智樹 [9]
[1] 東北大・理・地物; [2] 東北大・理; [3] 東北大・理・惑星プラズマ大気研究センター; [4] 東北大・理・惑星プラズマ大気; [5] 東大・理・地惑; [6] JAXA・宇宙研; [7] 東大・理; [8] ISAS/JAXA; [9] RIKEN

Variation in SII, SIII and SIV brightness distribution of Io plasma torus based on Hisaki/EXCEED and ground based observation data

Mika Shishido[1]; Takeshi Sakanoi[2]; Masato Kagitani[3]; Fuminori Tsuchiya[4]; Ichiro Yoshikawa[5]; Atsushi Yamazaki[6]; Kazuo Yoshioka[7]; Go Murakami[8]; Tomoki Kimura[9]
[1] PPARC, Tohoku Univ.; [2] Grad. School of Science, Tohoku Univ.; [3] PPARC, Tohoku Univ; [4] Planet. Plasma Atmos. Res. Cent., Tohoku Univ.; [5] EPS, Univ. of Tokyo; [6] ISAS/JAXA; [7] The Univ. of Tokyo; [8] ISAS/JAXA; [9] RIKEN

We report the time and spatial variation of sulfur ion emission line from the Io plasma torus to understand the dynamical process in the torus associated with Io's volcanic event during the period from December 2014 to March 2015, using the data obtained by Hisaki/EXCEED. A large quantity of gas is ejected from Io's volcanoes, principally oxygen and sulfur atoms and their compounds. Once they are ionized through electron impact and charge exchange, the ions are accelerated to the nearly corotational flow of the ambient plasma to form a torus of ions (the Io plasma torus, about $6R_J$ from the center of Jupiter) surrounding Jupiter. The fresh ions lose their pickup energy to the ambient electrons through Coulomb collisions. Ultimately, the torus electrons lose energy by transiting electron energy state of ions into higher states, leading to the prodigious extreme ultraviolet (EUV), ultraviolet, and visible emissions from the torus. During the period from December 2014 to March 2015, Io's outburst was observed by EXCEED, and the increase in the pickup ions were anticipated along with the increase in the neutral gas. To investigate energy flow from ions to electrons in this period, we derived sulfur ion temperature parallel to magnetic field lines from the emission scale height of the ion along the field line. From images of sulfur ion emission at 76.5nm(SII), 68nm(SIII) and 65.7nm(SIV) observed by EXCEED, we identified the time variation of sulfur ion temperature associated with enhanced volcanic activities, and interpreted that this was due to increase in the ion-pickup process. We also carried out the measurement of SII 673.1 nm emission with visible spectrograph on T60 telescope at Haleakala, Hawaii, which has high spatial resolution and found the similar variation in ion temperature. We also evaluated the spatial resolution of EXCEED by comparing the scale height which was derived from EXCEED and T60, and corrected the value of the defocused scale height by EXCEED. We will use a homogeneous model for mass and energy flow in the torus by Delamere and Bagenal (2003) to investigate the time variability of the ion and electron temperature changes during the Io's outburst period.

今回我々は、2015年1月中旬から3月下旬の期間に発生したイオトーラス増光期間中における EXCEED の紫外観測ならびに地上ハレアカラ望遠鏡可視観測データを用いて、イオトーラス中の硫黄イオン温度及び電子温度の時間変化を明らかにした。さらにこの現象に関して、0次元時間発展モデルを用いて得られたイオン及び電子の加熱機構の検証結果を報告する。木星の衛星イオの軌道 ($6R_J$) には、イオの火山ガスに起因するプラズマトーラスが形成される。このトーラス中の硫黄・酸素イオンは、電子 (5eV-1keV) との衝突励起により極端紫外から可視に渡る広い波長範囲で発光する。常に明るく光るプラズマトーラスの発光を維持するには電子の温度を 5eV 程度に加熱し続ける必要があり、その主要な加熱源の一つとして火山ガスの電離により生じる数 100eV のピックアップイオンから電子へのクーロン衝突が考えられている。2015年1月から2015年3月にかけて、「ひさき」衛星に搭載された極端紫外線分光撮像装置 EXCEED により、イオ火山噴火に伴うイオトーラス増光現象 (アウトバースト) が観測された。本研究は、EXCEED の紫外分光データならびに地上ハレアカラ T60 望遠鏡による硫黄イオン 673.1nm 可視光イメージング観測データを用いて、トーラス増光現象期間におけるイオン温度の時間変化の特徴を調べることにより、電子の加熱機構を検証することを目的とする。イオトーラスの南北方向の発光強度分布は磁力線方向のイオン温度を反映しており、発光分布のスケールハイトからイオン温度を推定することができる。可視イメージング観測が1価の硫黄イオンの発光分布を約1秒角の高空間分解能で撮像できるのに対し、EXCEED は広い波長域のスペクトル観測から、多価の硫黄イオンと電子温度の情報を得ることができる。EXCEED が観測した1価、2価、3価の硫黄イオン ([SII]76.5nm、[SIII]68nm 及び [SIV]65.7nm) の2次元発光分布から動径幅 $2R_J$（dawn 側、dusk 側ともに $5R_J$ − $7R_J$）の南北方向発光強度分布を求め、スケールハイトを導出したところ、アウトバーストによるトーラスの増光が開始するタイミング (2015年1月中旬) よりも 10 − 20 日ほど遅れてスケールハイトが上昇し始めた。トーラスが約 30 日間かけて約 100R 増光し、その後さらに約 30 日かけて元の明るさまで減光する間、当初 $1.2R_J$(FWHM) あったスケールハイトは緩やかに上昇し続け、2015年3月下旬には $1.3R_J$(FWHM) まで増加した。ここで、EXCEED の観測から導出されるスケールハイトは空間分解能の影響を受けているため、ハレアカラ地上可視光イメージング観測から同様に1価の硫黄イオンのスケールハイトと発光強度を導出し、これと EXCEED の結果を比較することでそれから得られた硫黄イオンのスケールハイトの値を補正した。今後は EXCEED の観測からイオン温度を導出し、トーラスの0次元時間発展モデル [Delamere and Bagenal 2003] で再現することで、トーラス中のプラズマの増加に伴うイオン及び電子の加熱機構の検証を行う。

木星磁気圏サブストームと関係するnKOM放射の特徴についての研究

水口 岳宏 [1]; 三澤 浩昭 [2]; 土屋 史紀 [1]; 小原 隆博 [3]
[1] 東北大・理・惑星プラズマ大気; [2] 東北大・理・惑星プラズマ大気研究センター; [3] 東北大・惑星プラズマセンター

Study of the characteristics of nKOM emissions correlating with substorm-like events in the Jovian magnetosphere

Takahiro Mizuguchi[1]; Hiroaki Misawa[2]; Fuminori Tsuchiya[1]; Takahiro Obara[3]
[1] Planet. Plasma Atmos. Res. Cent., Tohoku Univ.; [2] PPARC, Tohoku Univ.; [3] PPARC, Tohoku University

Jupiter has the largest magnetosphere in the planets of our solar system, which has been produced by its rapid rotation period (about 10 hours), strong intrinsic magnetic field and internal source of heavy plasma originated from Io plasma torus (IPT).

The observations by the Galileo orbiter revealed that there were quasi-periodic phenomena in the Jovian magnetotail, such as radial flow bursts of energetic particles [Krupp et al., 1998, Woch et al., 1998] and the variation of radial and north-south component of the magnetic field [Krupp et al., 1998], which imply magnetic reconnections and the periodic thinning and thickening of the plasma sheet. The signatures of these events were similar to the terrestrial substorm, so they are called ”substorm-like events (SLE)” [Woch et al., 1998]. Furthermore, the Cassini spacecraft performed Jupiter flyby around the end of 2000 and observed the Jovian magnetosphere in collaboration with Galileo.

It is known that there are radio emissions from the Jovian magnetosphere which correlate with SLE. In the preceding studies, Louarn et al. (2001, 2014) reported the narrow-band KilOMetric radiation (nKOM) correlated with inward flow burst and variation of the north-south component of the magnetic field during SLE. X-lines where the SLEs are thought to start were located at around 60-80 Jovian radii (R_J) [Woch et al., 2002], while the source of nKOM is suggested to be located at the outer edge of the IPT (6 - 10 R_J) [Reiner et al., 1993]. The report implies that the generation process of nKOM relates to the reconnection at the magnetotail. However, it has not been revealed well yet how inner (6 - 10 R_J) and outer (60 - 80 R_J) magnetospheres couple each other during SLE.

The purpose of this study is to reveal the coupling process of the formation of the source of nKOM at the inner magnetosphere (6 - 10 R_J) and the reconnection at the magnetotail (60 - 80 R_J). To study this process is important in order to understand the radial transport of the energy and the magnetic flux tube in the Jovian magnetosphere and the proceeding processes of the global dynamics of the Jovian magnetosphere (as suggested by Kivelson et al. (2005)).

In this study, we have analyzed nKOMs obtained by Galileo and Cassini to discuss their characteristics, such as its time series variation and the location of the formation of their sources. We obtained that the positions of the formation of new nKOM sources were not fixed on specific localtime. Additionally, we have also estimated the lifetime of energetic electrons which are thought to correlate with nKOM emission by adapting method for the energetic plasmas in terrestrial magnetosphere suggested by Wentworth et al.(1959) As the result, It is suggested that the electron of about 10 keV is necessary to explain the duration of nKOM emission (several rotation periods).

In this presentation, we will show preliminary results on occurrence characteristics of nKOM observed by both Galileo and Cassini relates with inward flow burst caused by the Jovian SLE and lifetime of energetic electron to explain the duration of nkOM emission.

木星磁気圏プラズマ変動期における準周期的オーロラ電波の出現特性

三澤 浩昭 [1]; 土屋 史紀 [2]
[1] 東北大・理・惑星プラズマ大気研究センター; [2] 東北大・理・惑星プラズマ大気

Occurrence characteristics of Jupiter’s quasi-periodic auroral radio emission in the megnetospheric plasma enhancement period

Hiroaki Misawa[1]; Fuminori Tsuchiya[2]
[1] PPARC, Tohoku Univ.; [2] Planet. Plasma Atmos. Res. Cent., Tohoku Univ.

http://pparc.gp.tohoku.ac.jp/

Around Jupiter’s oppositions to the earth in 2014 and 2015, remote observations for Jupiter had been made continuously by the HISAKI satellite. In particular in the 2015 campaign period, sudden enhancement of Iogenic plasma emissions occurred in the middle of Jan. and the enhancement had lasted for more than two months. This phenomena would give a valuable opportunity to investigate what parameters and/or processes control magnetosphere’s variations.

In the last SGEPSS meeitng, we showed some occurrence features of Jupiter’s auroral radiations in hectometric wave range (HOM) for the Iogenic plasma enhancement period, particularly for their occurrence probability/intensity. In this presentation, we will introduce occurrence timing and/or spectral features of Jupiter’s auroral radio emission in the decametric wave range (DAM) in particular non Io-DAM’s "QP burst" (see Panchenko et al., 2010, 2013) for the particular period based on the analyses of the WIND spacecraft data. A preliminary analysis shows that the recurrence period of the QP bursts was shorter during the Iogenic plasma enhance period, which seems to be different from that of the known recurrence feature of the Iogenic plasma (i.e. System-IV). We will introduce the preliminary results and discuss effects of the plasma enhancement on the auroral radio activities.

Acknowledgements: We would greatly appreciate M. Kaiser, J.-L. Bougeret and the WIND/WAVES team for providing the radio wave data.

地上電波観測による木星デカメータ電波Sバースト放射源の鉛直分布の研究

佐々木 悠朝 [1]; 熊本 篤志 [2]; 加藤 雄人 [3]; 三澤 浩昭 [4]
[1] 日工大高校; [2] 東北大・理・地球物理; [3] 東北大・理・地球物理; [4] 東北大・理・惑星プラズマ大気研究センター

Study on the vertical distribution of Jovian decametric S-burst sources based on the ground-based radio observation

Yuasa Sasaki[1]; Atsushi Kumamoto[2]; Yuto Katoh[3]; Hiroaki Misawa[4]
[1] NIT high.; [2] Dept. Geophys, Tohoku Univ.; [3] Dept. Geophys., Grad. Sch. Sci., Tohoku Univ.; [4] PPARC, Tohoku Univ.

Jovian decametric (DAM) radiation has been studied based on analysis of a simultaneous S-burst event in the multiple frequency bands obtained by ground-based observation.

In Jovian ionospheric Alfven resonator (JIAR) model proposed by Ergun et al. [2006] and Su et al. [2006] based on the theory and observations of the Earth's ionospheric Alfven resonator (IAR), eigen-frequencies of JIAR are expected to determine the repetition rate of S-burst of Jovian DAM radiation. In the Earth's IAR, the fundamental and higher harmonics eigen-frequencies were analytically calculated and depend on the Alfven speed in the lower ionosphere and the ionospheric scale height [Lysak, 1991; 1993]. So, we can estimate Jovian ionospheric scale height using the repetition frequencies of the S-burst emissions determined from the observation.

In this study, we used dataset from observation of Jovian DAM radiation in Io-B source condition with a logperiodic antenna at Yoneyama observatory of Tohoku University and a wideband receiver, whose frequency range is from 20 MHz to 40 MHz, since 2012. Previous studies reported that intense S-burst events were often found in Io-B source condition.

We especially focus on a simultaneous S-burst event in two different frequency bands (˜23.5 MHz (DAM1) and ˜27.0 MHz (DAM2)) found at 15:56 UT on 24 November 2014. If the emissions are radiated at the local electron cyclotron frequency, the geometric distance of the sources are estimated to be ˜1.085 Rj (DAM1, ˜23.5 MHz) and ˜1.040 Rj (DAM2, ˜27.0 MHz) based on the VIPAL magnetic field model [Hess et al., 2011] at the location of Io UV footprint [Bonfond et al., 2009]. The repetition frequencies are determined to be 22.3 Hz (DAM1) and 28.5 Hz (DAM2).

Assuming that the two emission sources are considered to be on the same magnetic field line or on the different close magnetic field lines and that the repetition frequencies of DAM1 and DAM2 are respectively equal to the fundamental and harmonic eigenmode of JIAR, the Jovian ionospheric scale height is estimated to be ˜1400 km or ˜1800 km.

In the above discussion, we have considered the simplified JIAR model that made by the incident Alfven wave and the reflected Alfven wave at the position where the ionospheric plasma density becomes maximum. In the presentation, we will show further discussion that the JIAR model in consideration of the multi-layer for high distribution of the plasma density.

土星オーロラ電波放射の季節変動：太陽風活動度及び太陽紫外線強度との相関

佐々木 歩 [1]; 笠羽 康正 [1]; 木村 智樹 [2]; 垰 千尋 [3]
[1] 東北大・理; [2] 理研; [3] NICT

The seasonal variation of Saturn's auroral radio emissions: The correlation with solar wind activity and solar EUV flux

Ayumu Sasaki[1]; Yasumasa Kasaba[1]; Tomoki Kimura[2]; Chihiro Tao[3]
[1] Tohoku Univ.; [2] RIKEN; [3] NICT

Saturn emits intense radio emissions, Saturn Kilometric Radiation (SKR), from the northern and southern polar regions in 3-1200 kHz. SKR is generated by field-aligned energetic auroral electrons via the Cyclotron Maser Instability (CMI) at local cyclotron frequency. Evaluation of Saturn's rotation period is based on the occurrence period of SKR because the SKR source is fixed in the planetary magnetic field with highly anisotropic beaming and forms a corotating searchlight of radio emission. For the Saturn's magnetic field direction, the right-handed circularly polarized (RH) emissions are from the northern region and the left-handed (LH) ones from the southern region. Cassini observations in the southern summer (2004-2009) showed that the period of SKR daily variation is variable [Kurth et al., 2008]. It was slightly longer in the southern (summer) hemisphere [Gurnett et al., 2009], but close to each other near the equinox (September 2009) [Gurnett et al., 2010]. We also studied the flux variation between northern and southern SKR in 2004-2010, and showed that the LH (summer, south) is stronger than the RH (winter, north) in average [Kimura et al., 2013]. Those characteristics could be related to the north-south asymmetry in the polar ionospheric conductivities, which are related to the seasonal variations of the solar EUV flux illuminating to the polar region. However, its comprehensive explanation has not yet been established. In 2010-2013, the observations during the northern summer also show northern and southern SKR periods merge together without clear separation [Provan et al., 2014; Fischer et al., 2015]. In 2015, both SKR periods at last becomes to be separated [Ye et al., 2016].

In this study, we extend our last SKR flux variation study in 2004-2010 [Kimura et al., 2013] toward the northern summer (-2015 DOY264). We note that the simple extension of the analysis period is not adequate because of the bias in the Cassini orbit. Since the SKR is stronger in the dawn side, we only used the data when Cassini was at the dawn side (2h-10h LT). And, in order to avoid the visibility effect of SKR caused by its propagation, we also limited the data by the Cassini's latitude (-5 to +30deg (RH), +5 to -30deg (LH)) and the distance from Saturn (10 - 100 Rs). However, because of Cassini's apokrone after 2007 was gradually shifted from dawn to dusk, the same criteria prevents from collecting enough dataset for the analysis.

For this study, we kept the same latitude and distance criteria but didn't adopt LT condition. In the data when Cassini was close from the equator, both northern and southern SKR are observed simultaneously. Therefore we selected the data when Cassini was in the latitude within +-5deg and verified the result. The variation of SKR peak intensity was evaluated by a running median with a window of +-35 days. In this result, the intensity of LH component in 2004-2009 (south, summer) was ~+10 dB stronger than RH (north, winter), which is consistent with the result in Kimura et al. (2013). In 2010-2012, the both SKR intensities got close to each other. After 2013, RH (north, summer) was stronger by a few dB than LH (south, winter). Those variations of the flux ratio between Northern and Southern SKR after 2010 seems to be linked with those of the Northern and Southern SKR periods. We also note that the flux ratio was more than 10 in southern summer but only 2.5~5 in northern summer, in the analyzed term. On the other hand, in order to check the LT dependence effect, we divided the data with 4 LT sectors (3-9h, 9-15h, 15-21h, 21-3h). We could confirm that the south-to north ratio changed from 10 to 0.2 and reversed in the 3-9h and 9-15h sector and didn't clearly reverse in 15-21h and 21-3h sector.

In this paper, we will also show the correlations of the SKR flux variations to the solar activity, solar EUV flux in 2004-2015, as the extension of the results in 2004-2010 done by Kimura et al. [2013].

土星は、Saturn Kilometric Radiation（SKR）と呼ばれる強力な電波放射を 3-1200kHz で南北両極のオーロラ発光領域上空から放射している。この電波は、沿磁力線加速されたオーロラ降下電子からサイクロトロンメーザー不安定性によって励起され、放射源におけるその場のサイクロトロン周波数で放射される。背景磁場に対して強い放射異方性を持ちながら、磁場に固定されて土星と共回転している特性から、土星の自転周期の評価に用いられてきた。SKR は土星磁場の向き (地球と逆) に従い、北側からは右旋円偏波（RH）、南側からは左旋円偏波（LH）で放射されるため、円偏波度を用いて南北要素を分離可能である。この性質を利用した Cassini 探査機による土星南半球夏季の観測 (2004-2010) から、自転に伴うとされてきた SKR 日変動周期が時間変動すること [Kurth et al., 2008]、この周期は南北で差があり南（夏側）でより長いこと [Gurnett et al., 2009]、春分点（2009 年 9 月）付近に向かって南北間の周期差が縮小したこと [Gurnett et al., 2010] 等の特性が発見された。さらに Kimura et al. (2013) では 2004-2010（南半球夏~春分点直後）の南北 SKR 強度長期変動を追跡し、この期間には LH 成分（南半球・夏側）が RH 成分（北半球・冬側）よりも平均的に強いことを見出した。これらの統一的な原因として、土星の極域沿磁力線電流量・降下電子量・オーロラ活動量に対する極電離圏電気伝導度（太陽輻射に照らされる夏側がより高い）による制御、及びこの電気伝導度の季節変動・太陽紫外線輻射量への応答が示唆されるものの、結論は確立されていない。2010~2013 年まで（北半球春~初夏）には、南半球夏季にはっきり見られた南北日変動周期の相違が不明瞭 [Provan et al., 2014; Fischer et al., 2015] であることも問題である。

我々は「北半球夏季」条件も網羅すべく、南北 SKR 強度の季節変動について、南半球夏˜春分点 (2004-2010) の解析 [Kimura et al., 2013] を北半球夏 (現時点で入手可能なのは 2015DOY264 まで) に拡張した。ただしこの延長には、Cassini 土星周回軌道の偏りが問題となる。土星 SKR の放射は朝側領域でより強く、また極域上空に位置する放射源位置とそこからの電波指向性の影響で近距離 (10 Rs 以内 (Rs：土星半径)) や高緯度側・反対半球側（北側放射：磁気緯度+30˜-5 deg 以外、南側放射：同+5˜-30 deg 以外）では観測電波強度が低下する。このため、Kimura et al. (2013) では Cassini の位置を「朝側領域（ローカルタイム（LT）：2˜10h)、土星からの距離 10-100Rs、RH(北側)・LH（南側）に対しそれぞれ磁気緯度+30˜-5 deg・+5˜-30 deg」に絞って解析した。しかし 2007 年以降、Cassini 軌道は遠土点がそれまでの朝側から夕側へと移行し、また軌道傾斜角も 2015 年初頭に至るまで大きく、この制限、特に LT
の制約を維持すると採用可能データ量が著しく減少する。

このため本研究では、磁気緯度と土星距離に関しては Kimura et al. (2013) と同条件を用いるものの、LT に対する制約を外して南北 SKR のピークフラックス及びその比を調査した。赤道面を離れると北・南両極からの電波の同時観測は困難なため，両者は異なる LT で観測された量となる。このため南北比については磁気緯度± 5deg に絞り、南北同時観測データだけを選別して検証した。衛星位置による見かけの変化を避けるため、± 35 日幅（70 日間）で running median を取ったところ，2009 年までは平均的に LH 成分が˜10dB ほど強く、2010˜2012 年の間は明瞭な差はなく、2013 年以降は RH 成分が数 dB ほど強くなる様子が見えた。2010 年までの結果は Kimura et al. (2013) の結果と同様の傾向である。周期逆転については遷移がはっきりしなかったものの、南北比については 2013 年以降 RH 成分が数倍卓越し逆転する様相が見えた。ただし、冬半球側に対する夏半球側のフラックスは 2004 年（南半球夏）では 10 倍以上あるのに比べ、2015 年（北半球夏）では 2.5˜5 倍程しか差がない．なお、LT 依存性の影響を確認すべく、観測データを 4 つ（3-9h、9-15h、15-21h、21-3h）に区切り、南北比を解析した。データが存在する期間に偏りが生じるものの、同じ解析期間で、3-9h 側及び 9-15h 側では南北比が約 10 から 0.2 へ変化し逆転する様相が、15-21h 側と 21-3h 側では 1 付近の値を取り、判然としない様相が見てとれた。

本講演では、Kimura et al. (2013) で行われた 2004-2010 の SKR －太陽紫外線強度・太陽風活動度相関解析の 2015 年までの延長についての、その進捗も述べる。

Total flux measurement of Jupiter's synchrotron radiation at 325MHz during the HISAKI-JUNO campaign period

Fuminori Tsuchiya[1]; Hiroaki Misawa[2]; Hajime Kita[3]
[1] Planet. Plasma Atmos. Res. Cent., Tohoku Univ.; [2] PPARC, Tohoku Univ.; [3] Tohoku Univ.

Ground-based radio monitoring of Jupiter's synchrotron radiation is a useful probe to investigate time variability of Jupiter's electron radiation belt. Previous studies showed correlation between short-term variation in intensity of the synchrotron radiation and the solar EUV flux, suggesting enhancement of radial diffusion in the radiation belt driven by electric field fluctuations generated in Jupiter's upper atmosphere. In addition, some reports reported a possible relationship between the synchrotron radiation and the solar wind. But more observations are needed to obtain a definitive conclusion. Here, we will report a preliminary result of the total flux measurement of Jupiter's synchrotron radiation with Iitate planetary radio telescope (IPRT) from May to July in 2016. During this period, the JUNO spacecraft was approaching to Jupiter and monitored the solar wind parameters upstream of Jupiter. HISAKI observed the brightness of both Io plasma torus and Jupiter's aurora, and monitored magnetosphere activity in the Jovian magnetosphere. For the total flux measurement of the synchrotron radiation, a backend receiver of IPRT was replaced to improve sensitivity of the measurement. The new receiver consists of a base-band down-converter and a digital waveform receiver developed by NICT (VSSP32). We will report overview of the new receiving system and preliminary results of the total flux measurement of Jupiter's synchrotron radiation during the HISAKI-JUNO campaign period.

ひさき衛星による木星観測と磁気圏グローバルMHDシミュレーションの連携解析

木村 智樹 [1]; 深沢 圭一郎 [2]; 土屋 史紀 [3]; 垰 千尋 [4]; 村上 豪 [5]; 北 元 [6]; 八木 学 [7]
[1] RIKEN; [2] 京大・メディアセンター; [3] 東北大・理・惑星プラズマ大気; [4] NICT; [5] ISAS/JAXA; [6] 東北大・理・惑星プラズマ大気; [7] AICS, RIKEN

Synergetic analysis of the global MHD simulation with Hisaki EUV monitoring of Jupiter’s magnetosphere

Tomoki Kimura[1]; Keiichiro Fukazawa[2]; Fuminori Tsuchiya[3]; Chihiro Tao[4]; Go Murakami[5]; Hajime Kita[6]; Manabu Yagi[7]
[1] RIKEN; [2] ACCMS, Kyoto Univ.; [3] Planet. Plasma Atmos. Res. Cent., Tohoku Univ.; [4] NICT; [5] ISAS/JAXA; [6] Tohoku Univ.; [7] AICS, RIKEN

The Hisaki satellite has been monitoring our solar system planetary environments with the first-ever continuity since its launch in September 2013. New dynamics of the planetary particle acceleration, plasma heating, and atmosphere are discovered by the continuous monitoring. This study investigates the physical origin for the observed global dynamics of Jupiter’s aurora and plasma torus based on analysis of the global magnetohydrodynamic simulation established by Fukazawa et al. [2005]. Essential electromagnetic parameters, e.g., field-aligned currents, are extracted from the MHD simulation data. Associating with the solar wind, planetary rotation, and plasma loading from the satellites, we quantitatively explore the variability in these parameters which is responsible for the observed auroral and torus dynamics.

２０１３年９月の打ち上げ以降、惑星分光観測衛星ひさきは、太陽系の惑星環境を、史上最も連続的に長期監視している。蓄積された大量の監視データから、今までの時間的に疎な観測では得られなかった、新しい惑星プラズマ加速・加熱過程や、大気物理の動力学が発見された。本研究では、ひさきの木星磁気圏観測で発見された、オーロラやイオプラズマトーラスの巨視的変動を物理的に解釈するため、Fukazawa et al. (2005) で確立されたグローバルMHDシミュレーションを解析し、観測を再現しうる磁気圏変動の特定を試みる。太陽風、惑星自転、衛星プラズマ供給に起因した、沿磁力線電流等の物理量変動を抽出し、それらが観測されたオーロラ強度やプラズマトーラス加熱量を再現しうるか定量的検証を行っている。本発表では、研究目的、アプローチ、体制と、実施の現状を報告する。

電離圏ポテンシャルソルバーによる木星内部磁気圏電場の太陽風応答の研究

寺田 綱一朗 [1]; 寺田 直樹 [2]; 笠羽 康正 [3]; 北 元 [4]; 垰 千尋 [5]; 中溝 葵 [5]; 吉川 顕正 [6]; Ohtani Shinichi[7]; 土屋 史紀 [8]; 鍵谷 将人 [9]; 坂野井 健 [10]; 村上 豪 [11]; 吉岡 和夫 [12]; 木村 智樹 [13]; 山崎 敦 [14]; 吉川 一朗 [15]
[1] 東北大・理・地物; [2] 東北大・理・地物; [3] 東北大・理; [4] 東北大・理・惑星プラズマ大気; [5] NICT; [6] なし; [7] なし; [8] 東北大・理・惑星プラズマ大気; [9] 東北大・理・惑星プラズマ大気研究センター; [10] 東北大・理; [11] ISAS/JAXA; [12] 東大・理; [13] RIKEN; [14] JAXA・宇宙研; [15] 東大・理・地惑

Study of the solar wind influence on the Jovian inner magnetosphere using an ionospheric potential solver

Koichiro Terada[1]; Naoki Terada[2]; Yasumasa Kasaba[3]; Hajime Kita[4]; Chihiro Tao[5]; Aoi Nakamizo[5]; Akimasa Yoshikawa[6]; Shinichi Ohtani[7]; Fuminori Tsuchiya[8]; Masato Kagitani[9]; Takeshi Sakanoi[10]; Go Murakami[11]; Kazuo Yoshioka[12]; Tomoki Kimura[13]; Atsushi Yamazaki[14]; Ichiro Yoshikawa[15]
[1] Geophysics, Tohoku Univ.; [2] Dept. Geophys., Grad. Sch. Sci., Tohoku Univ.; [3] Tohoku Univ.; [4] Tohoku Univ.; [5] NICT; [6] ICSWSE/Kyushu Univ.; [7] The Johns Hopkins University Applied Physics Laboratory; [8] Planet. Plasma Atmos. Res. Cent., Tohoku Univ.; [9] PPARC, Tohoku Univ; [10] Grad. School of Science, Tohoku Univ.; [11] ISAS/JAXA; [12] The Univ. of Tokyo; [13] RIKEN; [14] ISAS/JAXA; [15] EPS, Univ. of Tokyo

The solar wind hardly influences the plasma convection in the Jovian inner magnetosphere, because the corotation of magnetospheric plasma dominates the convection there. However, the extreme ultraviolet spectroscope (EXCEED) onboard the Hisaki satellite observed that the brightness distribution of the Io plasma torus changed asymmetrically between the dawn and the dusk sides. Furthermore, it was confirmed that this asymmetric change coincided with a rapid increase in the solar wind dynamic pressure. This asymmetric change can be explained by the existence of a dawn-to-dusk electric field of ~3-7 [mV/m] around Io's orbit, and the following processes generated by the solar wind interaction have been suggested as a possible cause of the electric field. First, the solar wind compresses the Jovian magnetosphere. Then, the magnetosphere-ionosphere coupling current system is modified, and the field-aligned current into the high-latitude ionosphere increases. As a result, the ionospheric electric field increases and penetrates to low-latitude regions. It is mapped to the equatorial plane of the magnetosphere along the magnetic field line, and the dawn-to-dusk electric field is created in the vicinity of Io's orbit (~6 R_J) in the inner magnetosphere. Among a series of these processes, the existence of the field-aligned current was observationally confirmed from the divergence of the ring current on the equatorial plane using the Galileo spacecraft data [Khurana, 2001].

We have constructed a 2-D ionospheric potential solver in order to demonstrate this scenario quantitatively. We have investigated how the global distribution of the ionospheric potential changes responding to the input of the field-aligned current using the potential solver. We use the intensity of the total field-aligned current obtained from the Galileo observation [Khurana, 2001] and adopt a Gaussian function for its distribution in a similar way to the Earth's modeling. Also, we have modeled the ionospheric conductivities in two ways; (1) the conductivities are reduced to 10 percent of the Earth's values globally [Tao et al., 2009], (2) the conductivities are calculated from the collision frequencies and the cyclotron frequencies of charged particles in the Jovian upper atmosphere. Although the latter is still under construction, we deduce the distribution of the atmospheric temperature from the latitudinal distribution of the infrared observation by Cassini [Stallard et al., 2015] and the altitude distribution by the Galileo entry probe [Seiff er al., 1997], the ionospheric density distribution from a photochemistry model for hydrocarbon species [Kim and Fox, 1994], the collision frequencies from ion-H_2 and electron-H_2 collisions [Tao, 2009], and the magnetic field from the VIP4 empirical model [Connerney et al., 1998].

We calculate the Jovian electric potential distribution by the aforementioned current and conductivity distributions to obtain the dawn-to-dusk electric field around Io's orbit. In the case (1), the dawn-to-dusk electric field mapped to Io's orbit appears to be of the same order as or larger than the ~3-7 [mV/m] suggested by the Hisaki satellite observation. However, this value is obtained without considering the temporal variation of the solar wind dynamic pressure. In this presentation, we will present results from the cases (1) and (2).

木星内部磁気圏はプラズマ共回転が対流を支配する領域で、この領域のプラズマ対流には太陽風の影響が及びにくいとする考え方が一般的である。しかし最近、Hisaki 衛星搭載の極端紫外線分光器 EXCEED によって、イオプラズマトーラス発光分布が朝側・夕側で非対称に変動することが観測された。さらに、この変動が太陽風の動圧の急激な増加に伴って生じていることも確認された。これら現象から、イオプラズマトーラスの発光分布の非対称な変動はイオ軌道上にかかる~3-7[mV/m] の朝夕電場により生じると見積もられている。朝夕電場の起源として以下の太陽風影響プロセスが示唆されている。まず太陽風が木星磁気圏に衝突して磁気圏を圧縮する。これにより磁気圏-電離圏結合電流系が変調され、高緯度電離圏へ流入する沿磁力線電流が増大する。その結果、沿磁力線電流によって形成された電離圏電場が増大し、低緯度領域へと拡大侵入する。これが磁力線を介して磁気圏赤道面に投影されることで、内部磁気圏深部に位置するイオ軌道近傍 (~6 R_J) に朝夕電場が生成される、というものである。このプロセスの内、沿磁力線電流の存在は Galileo 衛星観測に基づく赤道面上のリングカレントの発散値から間接的に確認されている [Khurana, 2001]。

このシナリオをモデルによって定量評価するため、木星における 2 次元電離圏ポテンシャルソルバーを開発した。こ

れにより、任意の沿磁力線電流分布に対する全球電離圏ポテンシャル分布の導出を試みた。沿磁力線電流量には Galileo 探査機などの観測結果 [Khurana, 2001] を用い、その分布には地球の場合でも採用されているガウス関数を用いた。また、電離圏の電気伝導度分布は、まず (1) 木星電離圏環境への規格化として全球一様に地球の 1/10[Tao et al., 2009] としたもの、ついで (2) 木星超高層領域における荷電粒子の衝突周波数とサイクロトロン周波数から直接計算したもの、の二通りを採用した。後者は現在開発中であり、大気温度分布を Cassini 探査機赤外線観測による緯度方向の分布 [Stallard et al., 2015] と Galileo 探査機エントリープローブ観測による高度方向の分布 [Seiff et al., 1997] から演繹し、電離圏密度分布を炭化水素イオン化学モデル [Kim and Fox, 1994] から求める。また、衝突周波数はイオン-H_2 衝突と電子-H_2 衝突を考慮している [Tao, 2009]。木星固有磁場は経験モデルである VIP4[Connerney et al., 1998] を用いる。

以上の電流・電気伝導度分布を基に木星電場ポテンシャル分布を導出し、朝夕電場強度を求める。(1) では、イオ軌道上での朝夕電場強度は Hisaki 衛星観測が示唆する˜3-7[mV/m] と同オーダーないしやや大きな値が得られた。ただしこの値は太陽風動圧の時間的変動を考慮したものではなく、定常状態を定量的に評価したものである。今学会では、(2) の結果も合わせて報告する。

テスト粒子シミュレーションを用いた500eV-50keV磁気圏電子とEnceladusトーラス中H2O分子の弾性衝突

田所 裕康 [1]; 加藤 雄人 [2]
[1] 武蔵野大学; [2] 東北大・理・地球物理

Simulation of elastic collisions between magnetospheric 500eV-50keV electrons and neutral H2O molecules in the Enceladus torus

Hiroyasu Tadokoro[1]; Yuto Katoh[2]
[1] Musashino University; [2] Dept. Geophys., Grad. Sch. Sci., Tohoku Univ.

Water group neutrals (H_2O, OH, and O) in Saturn's inner magnetosphere play the dominant role in loss of energetic electrons and ions because of abundance of the neutrals [e.g., Paranicas et al., 2007; Sittler et al., 2008]. The observations of injected plasmas in the inner magnetosphere suggest that these particles do not survive very long time due to the neutral cloud originated from Enceladus [e.g., Paranicas et al., 2007; 2008]. Thus, the previous studies suggested that the neutral cloud contributes to loss processes of plasma in the inner magnetosphere. However, little has been reported on a quantitative study of the electron loss process due to electron-neutral collisions.

Tadokoro et al., [2014] examined the variation of 1keV electron pitch angle distribution due to elastic collisions with the dense region of H_2O originated from Enceladus using one-dimensional test-particle simulation. They reported that the electrons of ˜11.4% to the total number of equatoriall electrons at the initial condition are lost in ˜380sec, corresponding to the co-rotating electron flux tube passes the dense H_2O region in the vicinity of Enceladus.

The examination of elastic collisions with other electron energy is required to understand the electron loss process due to elastic collision. We show the loss rates through pitch angle scattering of electrons with 500 eV - 50keV. We compare the loss rate due to the elastic collision close to the plume with that in the neutral torus.

The observation of water-group molecule emission in the Enceladus torus with Haleakala T60

hiromu ono[1]; Takeshi Sakanoi[2]; Masato Kagitani[3]; Kunihiro Kodama[4]
[1] PPARC, Tohoku Univ; [2] Grad. School of Science, Tohoku Univ.; [3] PPARC, Tohoku Univ; [4] Planet. Plasma Atmos. Res. Cent., Tohoku Univ.

We report the result on the observations of Enceladus torus emissions at the atomic oxygen 630.0nm and the water-vapor ion emission at around 615nm(8-0 band) with Haleakala/T60 and a Vispec(Visible Imager and Spectrograph with Coronagrpahy) during the period from 2015/7/13 to 2015/9/18 (first run) and from 2016/5/17 to 2016/7/23 (second run).

The moon Enceladus, revolves round Saturn at 3.9 Saturn Radii(Rs), emits the plume mainly composed of water vapor from cracks in south polar region called 'Tiger Stripe'. This plume cause the neutral particle rich inner magnetosphere of Saturn and the neutral density is ten times greater than the plasma density. However, its time variation and spatial distribution has been discussed by models and simulation studies, and there is few studies based on observation data. We aim to understand the physical processes in the Saturn's inner magnetosphere by observing the Enceladus torus emissions.

Vispec has two kinds of spectroscopy modes with a high-dispersion echelle gratig(R=76000) and with a single-order grating(R=10000) In the first run, We employed the high-dispersion mode with two kind of slits; one is 60[micro-m] width$*$20[mm] length, or 100[micro-m] width$*$20[mm] length, of which correspond to FOVs of 200"$*$2";,200"$*$3', respectively. In the former slit case the slit was located in the east-west direction of Saturn's equatorial plane (E-W slit), and in the latter slit case the slit was located north-south direction(N-S slit). The detector is covering the wavelength of 629-632[nm] with a wavelength dispersion of $5.98*10^{-3}$[nm/pix] with a 2$*$2 binning mode. Exposure time was 20[min] per 1 frame, and we totally obtained 74 frames (38 frames of E-W data, 36 frames of N-S data). Using the N-S silt data(22 frames, total exposure time is 7.3[hour]), we derived the [OI]630.0[nm] at 3.9Rs in the east side of Saturn to be 0.8+-0.5[R] in 1-sigma suggesting that no significant emission was etected. Considering previous observational result from Kodama et al. 2011 [OI]630.0[nm] brightness is significantly reduced from 4.1+-0.7[R] to 0.8+-0.5[R]. We suggest that the cause of variation might be the difference of observation geometry between 2009 and 2015. Since Saturn's Ring-Opening Angle(ROA) is changing year by year. ROA in 2009 and 2015 were 4.5[deg.](nearly horizontal) and 22.4[deg.], respectively. The column number density of atomic oxygen along the line-of-sight direction is smaller with large ROA, and therefore, the apparent intensity would decrease in the 2015. Assuming the same number density of atomic oxygen observed in 2009, we calculated [OI] 630.0nm brightness of 1.2[R] in the same geometry observed in 2015. In addition to changes of observing geometry, variability of Enceladus plume activity may cause the decrease of torus [OI]630nm emission in 2015.

In the second run,we emoloyed the mid-dispersion spectroscopy mode with the former slit used in the first run. The slit was located in the north-south direction at the Enceladus orbital distance (east and west tangential point). The detector is covering the wavelength of 610-630[nm] with a wavelength dispersion of $4.06*^{-2}$[nm/pix] with a 2$*$2 binning mode. Exposure time was same as the first run making 391 frames in total. Based on the simple estimation, an exposure time of 125[min] is required to obtain the emission of water vapor ion(H_2O^+) with S/N=1. We will analyze these data and will discuss about results on water-vapor ion emission intensity as well as about its variabilities on the Enceladus torus.

DIPOL-2による系外惑星の偏光観測

前田 東暁 [1]; 坂野井 健 [2]; 鍵谷 将人 [3]
[1] 東北大・理・地球物理; [2] 東北大・理; [3] 東北大・理・惑星プラズマ大気研究センター

Observation of exoplanets by polarimetry using DIPOL-2

Haruaki Maeda[1]; Takeshi Sakanoi[2]; Masato Kagitani[3]
[1] PPARC,Tohoku Univ.; [2] Grad. School of Science, Tohoku Univ.; [3] PPARC, Tohoku Univ

We present observational results of exoplanets using a double image high precision polarimeter (DIPOL-2, Piirola_et al. 2014) attached Tohoku 60-cm telescope (T60) at Haleakala observatory in Hawaii during January 2015 through July 2016. Light from a primary star reflected or scattered at surface of exoplanets varies periodically with changes in orbital phases of exoplanets. Precise polarimetry of light from the exoplanets in addition to light from the primary star enables us to investigate atmospheric composition and distribution of atmosphere as well as orbital elements of exoplanets even if they do not transit the primary star.

We have investigated maximum degree of linear polarization (DoLP) about well-known 2000 exoplanets in accordance with their orbital elements and planetary radii. Our simple investigation shows HD 189733 b has the tenth largest amplitude of DoLP variation among known exoplanets. Previous observation and modeling study (Berdugina et al., 2008, Berdugina et al., 2011) indicate DoLP of HD 189733 b varies with the amplitude of 1 x 10^{-4}. So we suppose to achieve precise polarimetry with accuracy of 1 x 10^{-5} to examine variation of polarization on exoplanets. DIPOL-2 can achieve photon-noise limited polarimetry in principle though, we focus on development and on validation of procedure deriving polarization from DIPOL-2 measurements.

To achieve precise polarimetry with accuracy better than 10^{-5}, we need to determine intrinsic polarization from the instrumentations including the telescope and to confirm their stability during observing periods. We have made polarimetry of 59 non-polarized stars (< 20 Pc from the Earth) during January 2015 through July 2016 for the purpose of calibrating instrumental polarization. Measured DoLP from non-polarized stars are less than 10^{-4}. The result indicates that the instrumental polarization in addition to small polarization from non-polarized stars is less than 1 x 10^{-4}. We also found there is no seasonal variation on the instrumental polarization exceeding over 1 x 10^{-4}. Based on our analysis method of DIPOL-2 data, accuracy of polarimetry is 2-3 times as much as that expected only from photon-noise assuming the A/D conversation unit of 1 photon/count.

In addition to measurement of non-polarized standards, we made polarimetry of exoplanets, HD 189733 b and tau Boo b during the same observing period. We could not find any periodic variations of polarization exceeding 1 x 10^{-4} . We will also present results from recent observation will be made during August through September, 2016.

今回我々は、ハワイ・ハレアカラの口径 60cm 望遠鏡（T60）の偏光観測装置 DIPOL-2（a double image high precision polarimeter, Piirola_et., al 2014）を用いて行われた、系外惑星の偏光の 2015 年—2016 年の観測成果を報告する。主星を光源とし、惑星大気により散乱反射されて観測者に届く光は、公転に伴い周期的な偏光の変化を生じる。これを主星からの光（無偏光と仮定）と合わせて偏光測定することにより、トランジット天体に限定することなく、惑星の軌道要素、大気組成ならびにその分布についての情報を引き出すことも可能と考えられる。

我々は既知の系外惑星約 2000 個について、軌道要素と質量から想定される惑星直径をもとに、想定される偏光度の最大振幅を見積もった。その結果、HD189733 b は 10 番目に偏光度変化の振幅が大きいと期待される系外惑星である。先行研究の観測報告や、より詳細なモデル計算の結果 (Berdyugina et al., 2008, 2011) では、この振幅は $1*10^{-4}$ であると報告されている。したがって、HD189733 b の振幅を検出する上では 10^{-4} より数倍高精度な偏光観測（目安として 10^{-5} オーダー）を行うが必要である。DIPOL-2 を用いた偏光測定においては、45 度で交差する直線偏光成分を同時に測定することができるため、雲の通過等による減光が生じたとしても、導出される直線偏光の大きさと向き（ストークス Q/I と U/I）には原理的に影響しない。偏光測定の偶然誤差は主に光子雑音に制約されると期待されるため、大口径化の容易な地上観測に適した観測手法であると言える。しかし、過去の研究で偏光観測に成功したのは 1 天体にとどまる。本研究では初段階の目的として、上記の系外惑星の偏光観測のメリットを踏まえ、偏光測定の光子雑音限界を達成する観測・解析方法の確立を目指している。

系外惑星の観測をおこなうための目安となる偏光観測精度 10^{-5} を達成するためには、望遠鏡を含む観測機器固有の偏光（機器偏光）の校正と、その時間安定性の検証が不可欠である。我々は、DIPOL-2 と T60 の機器偏光を明らかにするために、2015 年 1 月から 2016 年 7 月にかけて重複する天体も含み、合計 59 個の無偏光標準星 (地球近傍 20Pc 以内) の観測を行った。解析の結果、測定された無偏光標準星の偏光度は、10^{-4} 以下に収まっていることが分かった。しかしこの値は、機器偏光値、無偏光標準星がわずかにもつと考えられる偏光値、宇宙空間を伝搬する際の影響を受けた偏光値、これらの合計値である。多くの系外惑星を観測する上では、固有偏光の貢献値を決定し、さらに精度を上げる必要がある。また、観測は年間を通じて複数の期間に分けて行われたが、季節による 10^{-4} 以上の機器偏光の変動も無いことが分かった。今後、2016 年 8-9 月に予定されている無偏光標準星の観測を行うことで、系外惑星の偏光変動の検出に必要とされる 10^{-5} の精度で、機器偏光を決定する予定である。無偏光標準星の各データのノイズは光子雑音から推定されるノイズの 2〜3 倍となった。これは、解析時におけるフォトンの取り方による誤差、リードアウトノイズ、天候が影響を及ぼしているなどといった要因に起因するものであると推測される。

無偏光標準星の観測と並行して、2 つの系外惑星（HD189733 b、tau Boo b）の偏光観測も行った。これらの天体につ

いて現状の精度では公転周期での 10^{-4} 以上の変動を見い出すことはできなかった。今回の発表では、以上の結果とそれを踏まえた今後の観測方針について発表する。

ハワイ・ハレアカラ惑星・系外惑星専用望遠鏡2016-2017年成果：東北大-ハワイ大連携T40・T60観測および.8m口径PLANETS計画

坂野井 健[1]; 笠羽 康正[2]; 鍵谷 将人[3]; 中川 広務[4]; 小原 隆博[5]; 岡野 章一[6]; 米田 瑞生[7]; 北 元[8]; 村田 功[9]
[1] 東北大・理; [2] 東北大・理; [3] 東北大・理・惑星プラズマ大気研究センター; [4] 東北大・理・地球物理; [5] 東北大・惑星プラズマセンター; [6] 東北大・理・PPARC; [7] なし; [8] 東北大・理・惑星プラズマ大気; [9] 東北大院・環境

Haleakala T40 and T60 telescopes and the 1.8-m PLANETS project for planetary and exoplanetary observations in 2016-2017

Takeshi Sakanoi[1]; Yasumasa Kasaba[2]; Masato Kagitani[3]; Hiromu Nakagawa[4]; Takahiro Obara[5]; Shoichi Okano[6]; Mizuki Yoneda[7]; Hajime Kita[8]; Isao Murata[9]
[1] Grad. School of Science, Tohoku Univ.; [2] Tohoku Univ.; [3] PPARC, Tohoku Univ; [4] Geophysics, Tohoku Univ.; [5] PPARC, Tohoku University; [6] PPARC, Tohoku Univ.; [7] none; [8] Tohoku Univ.; [9] Environmental Studies, Tohoku Univ.

http://pparc.gp.tohoku.ac.jp/

We report the current status of the T40 and T60 telescope activities including the onboard instruments as well as the updates of 1.8-m aperture telescope PLANETS project at Haleakala dedicated to planetary and exoplanetary observations. Continuous monitoring is essential to understand the planetary atmospheric phenomena, and therefore, own facilities with even small- and mediu sized telescopes and instruments are important. The location of our telescopes, the Haleakala High Altitude Observatories at the summit of Mt. Haleakala is sufficiently high (3050m), and one of the best sites with clear sky, good seeing, and low humidity conditions. Operation is relatively easy because we can access to the airport, major towns, and a good engineering facility, ATRC (Advanced Technology Research Center) of University of Hawaii/Institute for Astronomy within 1-2 hour drive.

On the summit, our group is now operating a 40 cm Schmidt-Cassegrain (T40) and 60 cm Cassegrain (T60) telescopes. The T40 telescope is mainly observing faint atmospheric features such as Io torus, Mercury, Lunar sodium tail, and so on. From fall 2013, ISAS Hisaki/Exceed EUV space telescope run on the orbit. It has uniquely provided long-term Io torus activities for this project, including the identification of Io volcanic enhancement in January-March 2015. The T60 telescope was moved from Iitate Observatory and started the operation from Sep. 2014. This telescope is now observing planetary atmospheres in infrared with newly developed Infrared heterodyne spectrometer (MIRAHI). In addition, high- and medium-resolution grating spectrometers with coronagraph to observe the Io's sulfur ion torus, Io's sodium cloud, and the Enceladus oxygen and water ion torus. Further, the polarization imager called DIPOL-2 is installed to measure the weak polarization of exoplanetary light. These activities are open to any possible collaborators. For example, guest observers visited for Jupiter (Dr. Asada, Kyushu Inst. Univ.), Mercury (Dr. Kameda and colleagues, Rikkyo Univ.) and exoplanets (Dr. Berdyugin, Univ. Turk, Finland, and Dr. Berdyugina, KIS, Germany) observations. Our and guest investigators' observations are also linked to Venus (Akatsuki), Mars (Mars Express, MAVEN) and Jupiter (Juno) in the 2015-2016 observation period.

In addition, we are currently carrying out a new telescope project PLANETS. This is a 1.8m off-axis telescope, which is under the international consortium mainly formed with IfA/UH and KIS (Germany). Although the schedule is delayed by the mirror forming etc., in the earliest case, we will see the first light in the late 2017. To promote these observations, project and instrument developments, T. Sakanoi and M. Yoneda will be stay in IIfA/UH, Maui for next one year, M. Kagitani and H. Nakagawa will frequently visit the observatory, and T. Obara and Y. Kasaba proceed the agreement issue between international consortium for PLANETS.

Any collaboration for science and instrument is very welcome to whom have interest to use our facilities. To encourage the collaboration, Planetary Plasma and Atmospheric Research Center (PPARC) of Tohoku University starts to call for collaborative research programs with funding support. For the applications and guidelines, refer to the PPARC web site at http://pparc.gp.tohoku.ac.jp.

水星磁気圏探査機が目指す科学　－メッセンジャーからベピ・コロンボへ―

村上 豪 [1]; 藤本 正樹 [2]; BepiColombo MMO プロジェクトチーム 早川　基 [3]
[1] ISAS/JAXA; [2] 宇宙研; [3] -

Science goals of Mercury Magnetospheric Orbiter -MESSENGER to BepiColombo-

Go Murakami[1]; Masaki Fujimoto[2]; HAYAKAWA, Hajime BepiColombo MMO Project team[3]
[1] ISAS/JAXA; [2] ISAS, JAXA; [3] -

The first Mercury orbiter MESSENGER successfully entered into its orbit in 2011 and completed its mission in 2015. MESSENGER provided us many surprising discoveries and issues. For example, the magnetometer measurements revealed that the planetary magnetic field has a northward offset by 0.2 Rm. It also found that Mercury's magnetosphere is highly dynamic because of its small magnetic field and proximity of the Sun. Furthermore, high energy electrons up to ˜200 keV were detected inside the magnetosphere and short periodicity (several minutes) of events were observed. The evidence of field-aligned current was also found by the magnetometer observation. These outstanding discoveries, however, still remains as open issues due to some limitations of instruments onboard MESSENGER and its extended elliptical orbit with apherm in southern hemisphere. The next Mercury exploration project BepiColombo will address these open issues. BepiColombo is an ESA-JAXA joint mission to Mercury with the aim to understand the process of planetary formation and evolution as well as to understand similarities and differences between the magnetospheres of Mercury and Earth. The baseline mission consists of two spacecraft, i.e. the Mercury Planetary Orbiter (MPO) and the Mercury Magnetospheric Orbiter (MMO). The two orbiters will be launched in 2018 by an Ariane-5 and arrive at Mercury in 2024. The simultaneous observations by two spacecraft will solve the remaining questions from MESSENGER. JAXA is responsible for the development and operations of MMO, and it is almost ready for launch. Therefore, now we can concentrate on preparing the science operations plans. Here we present a summary of MESSENGER results, remaining issues which should be addressed by BepiColombo, and science operations strategies and plans of MMO.

水星探査機MESSENGERの観測データに基づく水星マグネトポーズ位置の会合周期変化

桂 貴暉 [1]; 藤 浩明 [2]
[1] 京大・理・地物; [2] 京都大学・大学院・理学・地磁気センター

Synodic variation of Mercury's magnetopause from MESSENGER magnetometer observation

Takaaki Katsura[1]; Hiroaki Toh[2]
[1] Solar-Planetary Electromagnetism, Kyoto Univ; [2] DACGSM, Kyoto Univ.

MESSENGER(MErcury Surface, Space Environment, Geochemistry, and Ranging) is the first probe launched into Mercury's polar orbits and observed the planet's electromagnetic environment including its magnetic field over four years since 2011. From this data, the average shape and location of Mercury's magnetopause and bow shock have been determined (Winslow et al., 2013). Furthermore, from the study of the magnetic fields induced at the top of Mercury's core by time-varying magnetospheric fields, the radius of Mercury's core together with its error estimates has been determined (Johnson et al., 2016).

At present, however, the electrical conductivity of Mercury's mantle has not been taken into consideration. And for the period of external magnetic variations, annual variation due to Mercury's high orbital eccentricity alone is considered. Accordingly, the purpose of this research is to estimate the contribution of Mercury's mantle to induction by modeling Mercury as a two-layer spherically symmetric body with different electrical conductivities and taking not only annual variation but synodic variation into consideration.

For simplicity, we exclude cases in which both annual variation and synodic variation are included and so we examine the following four cases : (1)annual variation with core conductivity only,(2)synodic variation with core conductivity only,(3)annual variation by adding mantle conductivity,(4)synodic variation by adding mantle conductivity. Case(1)corresponding to that of Johnson et al.(2016). Comparison of (1)with (2)will tell us how the shallow mantle responds to EM induction by the shorter variation, if the results differ with each other significantly. Since for comparison of(1)and(3), if the electrical conductivity of mantel will not be resulted in negligible,(3)will be a highly accurate model, how the mantle responds to EM induction by longer variation will not be known until calculated. Moreover, if the results of (1)and(4)are in good agreement, it supports the validity of the model presented by the previous research.

We estimate time variation corresponding to synodic period from the location data of Mercury's magnetopause in 3 Mercury years published by Winslow et al.(2013)and report the result.

MESSENGER（MErcury Surface, Space Environment, Geochemistry, and Ranging）は初めて水星の周回軌道に投入された探査機であり、2011年から約4年にわたって磁場をはじめとする電
磁環境観測を行った。このデータに基づき、水星のマグネトポーズとバウショックの平均的な形状と位置が決定された(Winslow et al., 2013)。さらに時間変化する磁気圏磁場によって水星核表面に誘導される磁場の研究から、測地学的な方法とは独立に水星核半径とその誤差が推定された（Johnson et al., 2016）。

しかし、今のところ水星マントルの電気伝導度は無視されている。また外部磁場の変動周期も、水星の離心率が大きいことによって水星が感じる年変化のみが考慮されている。そこで本研究では、水星を異なる電気伝導度を持つ二層の球対称導体としてモデル化し、外部磁場の変動周期として年変化だけでなく、より短周期の会合周期も考慮することで水星マントルの電磁誘導への寄与を推定することを目的とする。

簡単のため年変化と会合周期変化のどちらも考慮する場合は除外すると、可能な変動周期と水星の内部構造の組み合わせとして、（1）年変化・核の電気伝導度のみ、（2）会合周期・核の電気伝導度のみ、（3）年変化・マントルの電気伝導度も考慮、（4）会合周期・マントルの電気伝導度も考慮、の4つの場合分けが考えられる。（1）が Johnson et al.（2016）に対応しており、これと（2）の結果との比較により、水星マントルの寄与を見積もることができる。すなわち，短周期の変化に対しては浅いマントルの電磁誘導効果が現れやすいので、コアの大きさが大きくなったという結果が得られれば、マントルの電気伝導度は無視できない、ということになる。（1）と（3）の比較については、マントルの電気伝導度が無視できないという結果になれば、（3）の方がより精度の良いモデルということになる訳だが、長周期の変動に対してどの程度電磁誘導効果が現れるかは実際に計算してみないとわからない。また（1）と（4）の結果が良く一致していれば、先行研究で提案されたモデルの妥当性を支持することになる。

今回の発表では、Winslow et al.(2013) で公表されている3水星年分の水星マグネトポーズ位
置データから会合周期に伴う時間変化を見積もり、その結果を報告する。

Global configuration and cusp structure of Mercury's magnetosphere

Manabu Yagi[1]; Kanako Seki[2]; Yosuke Matsumoto[3]; Dominique Delcourt[4]; Francois Leblanc[5]
[1] AICS, RIKEN; [2] Dept. Earth & Planetary Sci., Science, Univ. Tokyo; [3] Chiba University; [4] LPP, Ecole Polytechnique, CNRS; [5] LATMOS-IPSL, CNRS

Observations by MESSENGER found that Mercury's magnetosphere is analogous to the Earth's while there are several differences of the two. One of the big differences is a dipole offset which could affect to the global configuration of Mercury's magnetosphere especially making a strong north-south asymmetry. In this study, first we performed several cases of MHD simulation solving a interaction with solar wind plasma and offset dipole of Mercury. Solar wind densities are given nominal(35cm^{-3}) and high(140cm^{-3}) with velocity for 400km/s which is almost average value in the Mercury's orbit. IMF conditions are given ideal one which has only Bz component, and realistic one which comes from Parker Spiral which has strong Bx component at the Mercury's orbit but fluctuations are added in By and Bz components.

When solar wind density is nominal, magnetopause is formed at 1.4R$_M$, and the global structure has weak north-south asymmetry in the MHD simulation. One of the important characteristics is open field line from south pole even in the northward IMF condition without Bx and By components. When solar wind dynamic pressure is high, Mercury's magnetosphere is compressed to the scale of Mercury itself and intrinsic magnetic field cannot sustain the solar wind especially the southward because of the offset. In this case, almost whole area of southward dayside of Mercury is identified as a 'cusp' region, while northward magnetosphere barely keep its structure including cusp. In this case, planetary surface disturbs the magnetospheric convection in the southward, and as the result, north-south asymmetry of magnetosphere as well as similarity to Earth's magnetosphere are strongly violated.

In the realistic IMF case, global configurations of magnetosphere drastically change and become more complicated structures which include north-south and dawn-dusk asymmetry by strong Bx and By components. IMF Bx also affects to the intensity ratio of north and south cusp pressure, and By component 'twist' the cusp region to longitudinal direction. The identification of global structures especially the cusp region is important not only on the understanding of magnetospheric physics itself, but also making a proposal to the observational plan of spacecraft such as Bepi-Colombo.

Advances in planetary magnetospheric simulation with recent supercomputer systems

Keiichiro Fukazawa[1]; Yuto Katoh[2]; Raymond J. Walker[3]
[1] ACCMS, Kyoto Univ.; [2] Dept. Geophys., Grad. Sch. Sci., Tohoku Univ.; [3] IGPP/UCLA

Planetary magnetospheres are very large, while phenomena within them occur on meso- and micro-scales. These scales range from 10s of planetary radii to kilometers. To understand dynamics in these multi-scale systems, numerical simulations need to use the supercomputer systems. We have studied the magnetospheres of Earth, Jupiter and Saturn by using global magnetohydrodynamic (MHD) simulations for a long time, however, we have not yet obtained the phenomena near the limits of the MHD approximation.

Recently we can perform our MHD simulation of Terrestrial magnetosphere with close to the MHD approximation by using the K-computer and obtained multi-scale plasma flow vorticity in the magnetosphere for the both northward and southward IMF. It is also interesting that there are dawn-dusk asymmetries in the formation of vortex.

Furthermore, we can obtain the chance to use supercomputer systems which have latest Xeon, SPARC64, and vector-type CPUs and can do the simulation of Jovian and Kronian magnetospheres with the fine grid spacing. In these simulations, it is possible to provide the magnetic field to the electron hybrid simulation as a background field. Additionally, thanks to these computer resources we can run a lot of parameter survey simulations and compare the results of the magnetosphere with observations from the HISAKI spacecraft. In this study, we will show these simulation results and what we can perform using these supercomputer resources in the future.

Design of an ion mass/isotope spectrometer for observation around planets and moons

Shoichiro Yokota[1]; Yoshifumi Saito[1]
[1] ISAS

In situ low-energy ion measurement in terrestrial or planetary plasma environment has been done with a variety of ion analyzers onboard spacecraft. Detailed studies of plasma characteristics demand measurement of a three-dimensional distribution function with adequate energy and angular resolution, a wide energy range, full coverage of space, and a high sampling rate. When measuring a variety of ions originating from planetary atmospheres, we need to be able to measure the ion composition with high mass resolution. Therefore, mass analyses as well as energy analyses are important for the planetary plasma and atmosphere physics. For three-dimensional energy analysis of low-energy charged particles, the top-hat electrostatic method using spherical deflectors or toroidal deflectors1 has usually been applied because of its large geometric factor and uniform angular response while requiring relatively few resources. On the other hand, composition measurement of space plasmas, especially near the Earth, Mars, Venus, other planets, the Moon, and asteroids is of great interest. Time-of-flight (TOF) analysis for space use had been applied and further developed mainly for observing highly energetic particles. The development of TOF techniques using thin carbon foil, whose secondary electrons generate start signals, made it possible to measure lower-energy ions, when necessary, in combination with the post-acceleration voltages which accelerate incident ions to energy high enough for the ions to pass through carbon foil. Moreover, a TOF technique with a specific electric field, called a linear electric field (LEF), was developed and has been used for measuring space plasmas around the Moon and planets.

We developed an LEF-TOF ion mass analyzer, MAP-PACE-IMA, for Kaguya, with a mass resolution of M/dMˇ20, which has measured ions originating from the lunar exosphere and surface. In addition, MPPE-MSA of M/dMˇ40 has been prepared for the BepiColombo mission, which will observe the plasma environment around the Mercury. We have recently started developing a next-generation mass analyzer of M/dMˇ100 for the isotope analysis of planetary particles, employing nearly the same technique as that for Kaguya and BepiColombo. We present the outline and design results of the mass analyzer.

The Radio and Plasma Wave Investigation (RPWI) for JUICE: Start of Engineering Model Development

Yasumasa Kasaba[1]; Hiroaki Misawa[2]; Fuminori Tsuchiya[3]; Yoshiya Kasahara[4]; Tomohiko Imachi[4]; Tomoki Kimura[5]; Yuto Katoh[6]; Atsushi Kumamoto[7]; Hirotsugu Kojima[8]; Satoshi Yagitani[4]; Keigo Ishisaka[9]; Yoshizumi Miyoshi[10]

[1] Tohoku Univ.; [2] PPARC, Tohoku Univ.; [3] Planet. Plasma Atmos. Res. Cent., Tohoku Univ.; [4] Kanazawa Univ.; [5] RIKEN; [6] Dept. Geophys., Grad. Sch. Sci., Tohoku Univ.; [7] Dept. Geophys, Tohoku Univ.; [8] RISH, Kyoto Univ.; [9] Toyama Pref. Univ.; [10] ISEE, Nagoya Univ.

RPWI [PI: J.-E. Wahlund (IRF-Uppsala, Sweden)] on the ESA JUICE mission to Jupiter (launch: 2022) consists of Langmuir probe and electromagnetic wave measurements. It will provide the basic information of the exospheres, surfaces, and conducting subsurface oceans of Ganymede, Europa and Callisto and their interactions with surrounding Jovian magnetosphere.

RPWI has put special efforts into the design in order to have the following capabilities: (1) First to determine the properties, dynamics and the electrically conducting state of the cold plasma (<100 eV, and possibly dusty) that originates from the ionization of the dense exospheres of the icy Galilean moons, and its effect on these moons icy surfaces; (2) First to determine the electro-dynamic coupling via electric currents, Alfven waves, electric acceleration structures and plasma waves that transfer energy and momentum between different particle populations in Ganymede's magnetosphere as well as in the induced induced fields coupling to their conducting subsurface Oceans; (3) First to determine the state and dynamics of the Jovian magnetosphere, and how this variable and rotating magnetosphere transfer energy and momentum to the space environments around the icy Galilean moons, with special emphasis on the mechanisms of the electro-dynamic coupling in this interaction; (4) First to determine the location of source regions of the radio emissions within the Jovian domain and to determine the properties of those emissions, such as polarization, to characterize the source regions;

We also do possible sciences coordinated with others for the possible access to the subsurface ocean. (5) RPWI first provide the precise density and temperature of cold plasma and electric fields in Jovian system. Exhaust plumes from cracks on icy moons will also be detected, as well as micron sized dust migrating in these plumes and their interactions. It can provide the global conductivity and current estimations of icy satellite ionospheres, which contributes to the estimation of those characteristics of the conductive subsurface oceans below the non-conductive icy crust. (6) RPWI also first provides the highly resolved information of Jovian radiation emitted from Ganymede and Jupiter including lightning activity, by the first 3-axis E-filed measurement. As a byproduct, reflected Jovian emission can be expected from the boundary of crust (ice) and subsurface ocean (conductive water). It could observed by RPWI like the Lunar surface reflection in terrestrial auroral kilometric radiation seen by Kaguya Lunar Radar Sounder. RIME (Radar for Icy Moons Exploration) on JUICE uses 9 MHz radar pulse by 16 m tip-to-tip antenna and tries to detect the ocean under ˜10 km icy crust. Since the frequency of Jovian radiation is wider, from several 100 kHz to several 10s MHz, RPWI can potentially provide complementary information of RIME, including the vertical distributions of conductivity and permittivity in the icy crust.

RPWI sensors consist of 4 Langmuir probes (LP-PWI) for determination of the vector electric field up to 1.6 MHz and cold plasma properties (including active measurements by LP sweeps and mutual impedance sounding) up to 1.6 MHz, a tri-axial search coil magnetometer (SCM) for determination of the vector magnetic field up to 20 kHz, and a tri-dipole antenna system (RWI) for monitoring of radio emissions (80 kHz - 45 MHz). From Japan, we will provide the RWI preamp and its High Frequency receiver with the onboard software, modifying from the BepiColombo PWI and ERG PWE developments. We will also provide Software Wave-Particle Interaction Analyzer (SWPIA) function to RPWI DPU, for the onboard quantitative detection of electromagnetic field - ion interactions, modifying from the ERG SWPIA developments. We are now developping the Engineering Model to be shipped to ESA in Summer 2017. We will summarize the current development points and their relationships to the scientific products.

France-Japan collaborations in development of integrated data archives of Jovian decametric radiation from multiple observatories

Atsushi Kumamoto[1]; Fuminori Tsuchiya[2]; Yasumasa Kasaba[3]; Hiroaki Misawa[4]; Yuto Katoh[5]; Hajime Kita[6]; Keiichiro Fukazawa[7]; Tomoki Kimura[8]; Manabu Yagi[9]; Yoshizumi Miyoshi[10]; Kazumasa Imai[11]; Masafumi Imai[12]; Tomoyuki Nakajo[13]; Chihiro Tao[14]

[1] Dept. Geophys, Tohoku Univ.; [2] Planet. Plasma Atmos. Res. Cent., Tohoku Univ.; [3] Tohoku Univ.; [4] PPARC, Tohoku Univ.; [5] Dept. Geophys., Grad. Sch. Sci., Tohoku Univ.; [6] Tohoku Univ.; [7] ACCMS, Kyoto Univ.; [8] RIKEN; [9] AICS, RIKEN; [10] ISEE, Nagoya Univ.; [11] NIT, Kochi; [12] University of Iowa; [13] Fukui Univ. Tech.; [14] NICT

In order to support the collaborative studies on Jovian and Kronian auroral radio emissions between French and Japanese researchers, JSPS Bilateral Program "Coordinated observational and theoretical researches for Jovian and Kronian auroral radio emissions" has started since April 2016. In this program, we are planning joint research on (1) Jovian auroral radio emissions based on multiple ground-based observations at Nancay, Iitate, etc., (2) Kronian auroral radio emissions based on dataset from Cassini, (3) Comparison with spectroscopic observations based on dataset from Hisaki, and (4) Models (Solar wind, Jovian MTI coupling). Details on research activities are also shown via http://c.gp.tohoku.ac.jp/sakura/.

With support of this program, we are developing meta data archives of Jovian radio emissions in decametric wavelength range (Jovian DAM, 20-40MHz) obtained at Nancay and Iitate observatories. The merit of the ground-based observations is that high sensitivity antenna and high time resolution receiver can be employed without limitations of the equipment mass and downlink data rate, which often becomes issues in spacecraft observations. On the other hand, the demerit of the ground-based observation with single station is coverage: The ground station cannot observe Jovian radio emission while the Jupiter is below the horizon. However, this demerit can be solved by combining datasets from multiple stations in different longitude range. Virtual Observatory (VO) could be a promising solution for such combined data analyses. In preparation of the collaborative ground-based radio wave observation with Juno, which started the in-situ observations of the Jovian polar magnetosphere in this summer, the researchers working on ground-based observations of Jovian radio wave in Europe, US, and Japan started collaborations such as having a new support portal for collaborative planning of ground-based observations. Wideband radio spectrogram data obtained at Iitate observatory since 2004 in CDF format have been provided via Iitate HF radio wave data archive (http://ariel.gp.tohoku.ac.jp/~jupiter/). In addition, we finished setup of a new repository server for VO interface at Tohoku University in 2015 with supports of Paris Observatory team. This server will be the first step for integrated browsing of the Jovian radio wave data from multiple ground stations via VO interface. In addition, we started development of meta data archives for other datasets such as Jovian synchrotron radiations obtained by Iitate Planetary Radio Telescope (IPRT) and spectroscopic observation data from Hisaki. In the presentation, we are going to show the analyses results focusing on the Jovian DAM during volcanic activity in 2015 found by Hisaki as a typical example of use case of the integrated datasets from Nancay and Iitate.

LWA1で観測された木星電波モジュレーションレーンのデータ解析の半自動化について

中山 雄晟 [1]; 今井 一雅 [1]
[1] 高知高専

Semi-automatic data analysis of Jupiter’s decametric modulation lanes observed by LWA1

Yusei Nakayama[1]; Kazumasa Imai[1]
[1] NIT, Kochi

We present a system of semi-automatic data analysis in the study of Jupiter’s decametric emissions observed by the Long Wavelength Array Station 1 (LWA1). The LWA1 provides excellent spectral and temporal resolution of Jupiter’s decametric radio emissions over the bandwidth of 10-40 MHz. The array consists of 256 dual polarization dipole antennas. The modulation lanes in Jupiter’s decametric are groups of sloping parallel strips of alternately increased and decreased intensity in the dynamic spectral plots. We present the developed data analysis software to measure the slope of the modulation lanes by this semi-automatic method.

木星電波の放射機構を解明するために、時間経過による各周波数成分の強度変動を表すダイナミックスペクトラムの解析・研究が進められてきた。この木星電波ダイナミックスペクトラム構造には様々なものがあるが、Lバースト上に現れる斜めの縞状構造であるモジュレーションレーンを調べることによって、木星電波源の構造や位置の情報 [Imai et al., 1992,1997,2002,2006] を得ることが可能となることを示してきた。この方法を、我々はモジュレーションレーン法と呼んでいる。

この木星電波モジュレーションレーンを調べるための観測手段として、世界最高レベルの感度を持つ広帯域低周波電波望遠鏡 (LWA1: Long Wavelength Array Station 1) がある。この LWA1 は、ニューメキシコ大学のグループにより建設された低周波宇宙電波の研究を目的とするアレイアンテナで、256 基の直交した V 字型の広帯域な 2 系統のアクティブ・ダイポールアンテナで構成され、右回りと左回りの偏波観測が可能で、受信したアナログ信号は超高速サンプリングによりディジタル化されデータ処理の後、アーカイブされている。この超高感度の LWA1 システムによって、木星電波モジュレーションレーンの構造の中でも重要なパラメータとなる傾き (Slope）を詳細に調べることが可能となってきた。

我々は、LWA1 で観測されたダイナミックスペクトラム・データをデータ解析言語である IDL のプログラムによって解析を行っている。今回作成したプログラムでは、従来、手計算によって求められてきた木星電波モジュレーションレーンの傾きをインタラクティブに算出することが可能となった。また、Fortran で記述されたシミュレーションプログラムを IDL から呼び出すことで、電波源の位置に対応する Lead Angle、Source Longitude、Cone-half Angle といった電波源を位置などを示すのに重要なパラメータを瞬時に求めることができ、LWA1 で観測されている多くの木星電波モジュレーションデータについて調べることが可能となった。

LWA1 で観測された木星電波モジュレーションレーンは、従来にない広帯域のカーブしたスロープ構造も調べることが可能で、このカーブしたスロープ構造を自動的にフィットさせることにより、今までにない高精度な木星電波モジュレーションレーンのパラメータを求めるプログラムの開発も進めている。これらの新しい手法により、LWA1 で観測された多くの電波源のケースについての解析を行い、統計的な解析からモジュレーションレーン法により木星電波放射機構を解明するために重要な電波放射源の高精度な位置に関する情報を求めることを最終的なゴールとしている。

CubeSatによる木星電波ビーム観測プロジェクトについて

スフツォードル ラグワドルジ [1]; 中山 雄晟 [1]; 藤田 龍之介 [1]; 安藤 瑞基 [2]; エリック・タン カイ・チアング [2]; 今井 一雅 [1]; 平社 信人 [3]; 高田 拓 [4]; 北村 健太郎 [5]
[1] 高知高専; [2] 群馬高専; [3] 群馬高専; [4] 高知高専・電気; [5] 徳山高専

A CubeSat project to observe the beaming of Jupiter's decametric radio emissions

Lkhagvadorj Sukhtsoodol[1]; Yusei Nakayama[1]; Ryunosuke Fujita[1]; Mizuki Ando[2]; Kai Chiang Eric Tan[2]; Kazumasa Imai[1]; Nobuto Hirakoso[3]; Taku Takada[4]; Kentarou Kitamura[5]
[1] NIT, Kochi; [2] NIT, Gunma; [3] NIT,Gunma; [4] Kochi-CT; [5] NIT,Tokuyama.

The development of a micro satellite (CubeSat) to observe Jupiter's radio emissions is underway by the college students and teachers who belong the Kosen Space Consortium. This 2U-size CubeSat is being considered to be launched from the International Space Station (ISS). The duration of the planned observation is estimated to be more than 50 days. During this period we will use fixed frequency receivers to measure the delay time between the CubeSat and ground observatories for the detection of Jovian S-bursts. The delay time determined by a cross-correlation method reveals very important information for determining the beaming model of Jupiter's radio emissions. We show the current status of the development of our CubeSat project including Jupiter's radio data acquisition system with GPS, receiving antenna, and receiver.

木星電波ビーム観測用 CubeSat の開発が、高知高専を中心として行われている。このプロジェクトは、文部科学省の平成 26 年度宇宙航空科学技術推進委託費・実践的若手宇宙人材育成プログラムに採択された「国立高専超小型衛星実現に向けての全国高専連携宇宙人材育成事業」の中の高専スペース連携による CubeSat 開発プロジェクトの一つである。この CubeSat 開発のサイエンスのターゲットとして選ばれた木星電波は、木星からのデカメートル帯（短波帯）での自然電波放射であり、1955 年に発見されて以来、観測・研究が進んでいるが、その放射機構の全貌はまだ明らかとなっていない。この木星電波は、木星のオーロラ現象と密接に関連し、木星磁気圏内のプラズマと磁場との相互作用により発生するもので、地球でも観測が可能である程、その電波放射エネルギーは極めて大きい。この木星電波放射機構を解明するためには、木星電波放射のビーム構造の研究が重要であると考えられている。この木星電波のビーム構造の研究のための観測は、主に地上の観測点で行われており、地上の 2 地点間で木星電波の同時観測を行って、木星電波のミリ秒オーダーの時間変動のある S バースト波形の相関解析から遅延時間が測定されている。しかしながら、遅延時間測定の精度をあげるためには、東西方向の 2 地点間の距離（基線長）を長くする必要があるが、地上の観測点では基線長に限界がある。そこで、この限界を打破するために、衛星と地上の 2 カ所で同時観測を行うことにより、従来にない基線長を確保した観測を行い、測定精度の向上だけでなく観測頻度の向上を目指すことを考えている。

ミッションとしては、オンボードコンピュータ (OBC) として Linux マイコンボードの Raspberry Pi Zero をベースにした木星電波観測用 CubeSat を、国際宇宙ステーション (ISS) より放出し、50 日以上の木星電波観測のミッション期間を想定している。ISS から放出された後、木星電波受信用アンテナとアップリンク・ダウンリンク用アンテナを展開し、搭載した GPS モジュールの正秒パルスを用いて、受信した木星電波のアナログ信号を A/D コンバータによりデジタル信号へ変換し、OBC に一旦観測データを保存した後、相関に必要な観測データを地上局に送信する。最終的には、地上での同時観測データとの相関解析より木星電波 S バーストの到達遅延時間をミリ秒レベルの精度で求める。この到達遅延時間の測定から、木星電波のビーム特性に起因する木星電波のビーム構造が木星磁場と一緒に共回転しているかどうかについての検証を行うことが可能となる。このミッションで重要な木星電波観測用アンテナは、観測周波数が約 20MHz であることから、衛星に搭載するダイポールアンテナの片方の長さが、約 3.7m となる。アンテナには、バイオメタルファイバ (BMF) を使うこと検討しており、蛇腹状に折りたたんで衛星側面に収納し宇宙空間で展開する。木星電波観測は、木星電波 S バーストが出現すると予測される時刻に行われるように、衛星と地上観測のスケジューリングを行う。本発表では、この木星電波観測用の超小型衛星 (2U の CubeSat) の開発状況について、GPS 同期型のデータ収集システム、木星電波観測用アンテナ、受信機を中心に報告する。